HMMR

High-Resolution Multifrequency Microwave Radiometer

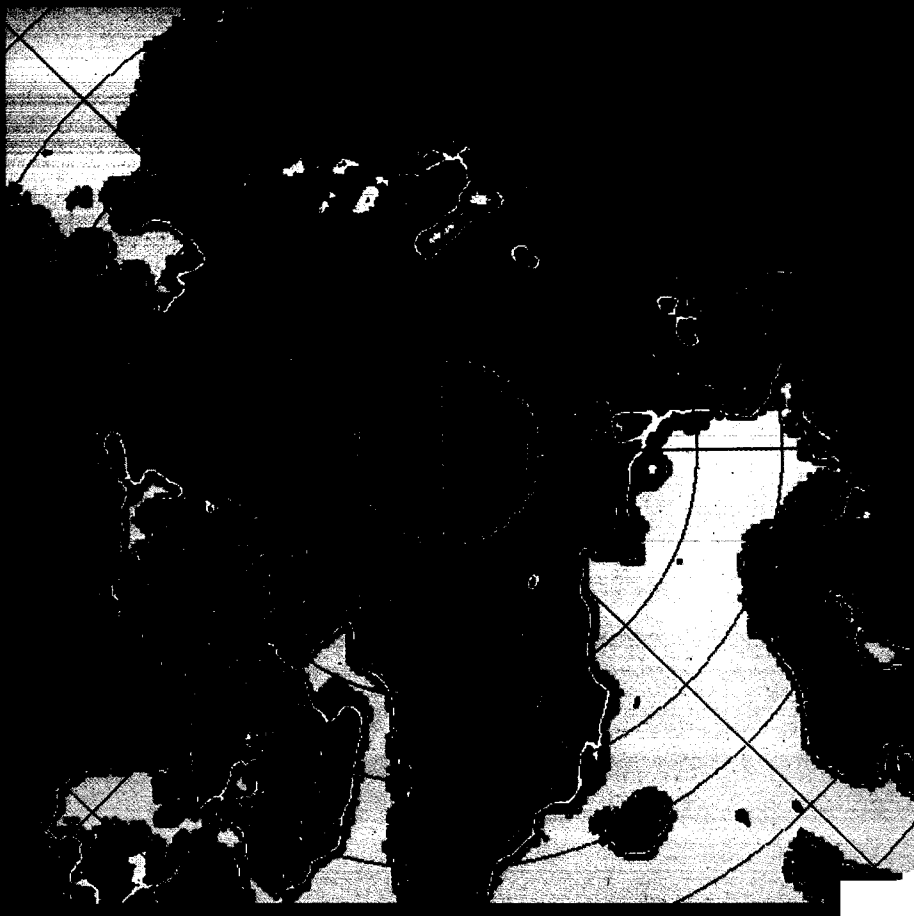

INSTRUMENT PANEL REPORT

HMMR

High-Resolution Multifrequency Microwave Radiometer

EARTH OBSERVING SYSTEM
Volume IIe

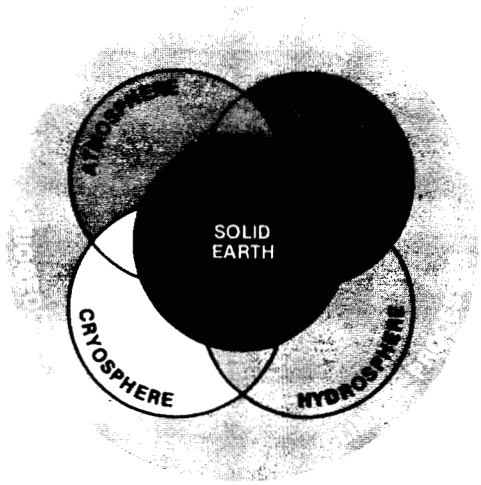

INSTRUMENT PANEL REPORT

National Aeronautics and Space Administration

1987

EARTH OBSERVING SYSTEM REPORTS

Volume I	Science and Mission Requirements Working Group Report
Volume II	From Pattern to Process: The Strategy of the Earth Observing System Science Steering Committee Report
Volume IIa	Data and Information System Data Panel Report
Volume IIb	MODIS Moderate-Resolution Imaging Spectrometer Instrument Panel Report
Volume IIc	HIRIS & SISEX High-Resolution Imaging Spectrometry: Science Opportunities for the 1990s Instrument Panel Report
Volume IId	LASA Lidar Atmospheric Sounder and Altimeter Instrument Panel Report
Volume IIe	HMMR High-Resolution Multifrequency Microwave Radiometer Instrument Panel Report
Volume IIf	SAR Synthetic Aperture Radar Instrument Panel Report
Volume IIg	LAWS Laser Atmospheric Wind Sounder Instrument Panel Report
Volume IIh	Altimetric System Panel Report

HIGH-RESOLUTION MULTIFREQUENCY MICROWAVE RADIOMETER INSTRUMENT PANEL FOR THE EARTH OBSERVING SYSTEM

Robert Murphy, Chairman
David M. Le Vine, Executive Secretary
Frank Barath
Eric Barrett
Robert L. Bernstein
Carolyn A. Clark
Jeff Dozier
Ramesch Kakar
Eni Njoku
Ed Runge
Vincent Salomonson
Calvin T. Swift
Thomas T. Wilheit
Shih Tseng Wu

EXECUTIVE SUMMARY

This report provides recommendations and background for a passive microwave remote sensing system of the future designed to meet the observational needs of Earth scientists in the next decade. This system, called the High-Resolution Multifrequency Microwave Radiometer (HMMR), is to be part of a complement of instruments in polar orbit. Working together, these instruments will form an Earth Observing System (Eos) to provide the information needed to better understand the fundamental, global-scale processes which govern the Earth's environment. The outline of this Earth Observing System is set forth in the report of the Science and Mission Requirements Working Group (Butler *et al.*, 1984), which identified the role of passive microwave observations in the Earth Observing System and gave the label, HMMR, to an otherwise unspecified instrument which would provide these measurements. Subsequently, the HMMR Panel was established under the purview of a follow-on committee, the Eos Science Steering Committee, to define this instrument.

The HMMR Panel was given three major goals. These were:

1. To identify in further detail those measurements which passive observations in the microwave portion of the spectrum could contribute to an Earth Observing System in polar orbit.
2. To establish requirements (e.g., spatial and temporal resolution) for these measurements so that, when combined with the other instruments in the Earth Observing System, they would yield a data set suitable for understanding the fundamental processes governing the Earth's environment.
3. To assess existing and/or planned sensor systems in the light of these requirements, and define any additional sensor hardware needed to meet these observational requirements.

The HMMR Panel approached these objectives in three stages. The first required identifying and prioritizing the information which passive microwave remote sensors could provide from low Earth orbit, and which would promote understanding of the fundamental geophysical processes controlling the environment. The Panel relied heavily on its own expertise and the recommendations of the Science and Mission Requirements Working Group (Butler *et al.*, 1984) in this effort. The hydrologic cycle emerged from this exercise with a high priority as an area where microwave remote sensors would make essential contributions. Among the important observations that passive microwave sensors can contribute to a data set for studying the hydrologic cycle are:

- Soil moisture
- Precipitation
- Snow (coverage/moisture equivalent)
- Atmospheric water vapor
- Evaporation (oceans)
- Evapotranspiration (land)

The last two quantities are derived quantities inferred from direct observations of other variables, and require input from passive microwave, infrared, and other observational tools. Passive measurements in the microwave portion of the spectrum can also provide observational data essential for understanding geophysical processes of the oceans and air-sea interaction. The particular parameters directly observable with a passive microwave instrument are:

- Sea surface temperature
- Sea ice (concentration and properties)
- Surface wind speed

Finally, passive microwave measurements are an important all-weather complement to infrared soundings of the atmosphere and can provide:

- Temperature profiles
- Water vapor profiles
- Total liquid water content

The second step of the Panel's work was to establish requirements for the measurement of these parameters such that the measurements would yield data suitable for understanding the fundamental processes governing the Earth's environment. The requirements call for an imager making measurements at seven frequencies (1.4, 6, 10, 18, 21, 37, and 90 GHz) in the microwave portion of the spectrum, plus multifrequency measurements in the oxygen resonance band (50 to 60 GHz) and at the water resonance line (183 GHz) for making atmospheric temperature and water vapor profiles. Spatial resolution on the order of 10 km or less is desirable with radiometric accuracy of about 1.5 K adequate in most cases. In most cases a revisit time of 2 days is adequate. The exception is atmospheric sounding where more frequent coverage is needed.

The final step in the Panel's work was to define a combination of existing and required hardware to meet these requirements. In this exercise, the Panel relied on a review of past and planned sensor systems and on its own understanding of what could realistically be implemented in space in the next decade. A concept consisting of three separate instruments emerged from the considerations of the Panel. The three instruments are: the AMSU (Advanced Microwave Sounding Unit) presently under development for the National Oceanic and Atmospheric Administration (NOAA), and two new instruments, the

AMSR (Advanced Mechanically Scanned Radiometer), and the ESTAR (Electronically Scanned Thinned Array Radiometer).

The AMSU (Advanced Microwave Sounding Unit)–There are two components of the AMSU instrument (AMSU-A and AMSU-B) which together will provide atmospheric soundings of temperature and water vapor. The AMSU-A will obtain temperature soundings using 12 channels in the oxygen resonance band (50 to 60 GHz), and ancillary channels at 24, 31, and 89 GHz. The AMSU-B will profile water vapor using five channels, one at 89 GHz, one at 157 GHz, and three on the water vapor resonance line at 183 GHz. Spatial resolution is on the order of 50 km for AMSU-A and 15 km for AMSU-B. The Panel concurred that these instruments represent the state of the art in microwave sounding of the atmosphere, and that they will provide soundings sufficient to meet the goals of Eos.

The AMSR (Advanced Mechanically Scanned Radiometer)–The AMSR is a six-frequency, conically-scanned microwave imager. It should include channels at approximately 6, 10, 18, 21, 37, and 90 GHz, each with dual (linear) polarization. Measurements at various combinations of these frequencies and polarization permit data to be obtained on the amount of snow cover over land; the age and areal extent of sea ice; the intensity of precipitation over oceans and land; and the amount of water in the atmosphere (cloud water and total water vapor). In addition, it is possible at the lower frequencies to obtain useful information on sea surface temperature and wind speed at the ocean surface. In order to progress to the next generation of understanding of these phenomena and of the role they play in determining the Earth's environment, a significant improvement in spatial resolution is required. To obtain this resolution, the AMSR will consist of a 4 × 7 meter dish which is rotated to scan the antenna beam at a constant 50° incidence angle. The scan will provide almost an order of magnitude improvement in spatial resolution over existing or planned instruments. The Panel strongly endorsed the Eos science requirements for this higher spatial resolution. The Panel also endorsed the engineering studies, such as were performed as part of the planning for the Naval Ocean Sensing System (NOSS) satellite that show that deployment of a large rotating dish of this size is feasible and could be done in the Eos time frame.

The ESTAR (Electronically Scanned Thinned Array Radiometer)–The ESTAR is a 1.4 GHz imaging radiometer designed specifically to obtain global maps of surface soil moisture, an important input to the hydrologic cycle. Measuring soil moisture from space presents a special challenge because measurements at the low frequency end of the microwave spectrum are needed to reduce the effects of vegetation cover and to increase the depth of penetration into the soil. To obtain the desired spatial resolution (on the order of 10 km) at this end of the spectrum requires an instrument with very large antennas, even in low Earth orbit (LEO). The Panel strongly endorsed Eos requirements for 10 km resolution with a 1- to 3-day revisit time, and sought techniques for obtaining this resolution from space. The ESTAR is a hybrid real aperture and synthetic aperture sensor, which employs an array of long stick antennas to achieve real aperture resolution in the along-track dimension, and uses signal processing to achieve resolution, synthetically, in the crosstrack dimension. Signal processing permits the array to be thinned significantly, resulting in a substantial reduction in the antenna volume needed in space. The Panel considered several alternative approaches and recommended achieving the required resolution by means of antenna aperture synthesis. The ESTAR represents the most novel technology proposed for the HMMR instrument package. However, it is a relatively low-risk innovation, since similar techniques have been used on the ground with impressive success in radio astronomy. Furthermore, the concept used for ESTAR can be applied at other frequencies; consequently, the development of ESTAR could represent a technological breakthrough in spacecraft antenna design leading to practical implementation of large microwave antenna apertures in space for other applications in the future.

The Panel strongly recommends development of the High-Resolution Multifrequency Microwave Radiometer (HMMR). The HMMR will provide data which, in conjunction with the other instruments in the Earth Observing System, will significantly advance our understanding of the fundamental geophysical processes governing the Earth's environment. Microwave sensors in the past have demonstrated the capability of such instrumentation to provide measurements of soil moisture, precipitation, water vapor, sea surface temperature and sea ice, as well as other parameters important for understanding the hydrologic cycle and oceanographic and atmospheric dynamics. The HMMR represents the next logical step in the evolution of microwave instrumentation. It represents a major step forward in spatial resolution, with spatial resolution approaching the scale size of the fundamental geophysical processes driving the Earth's environment.

CONTENTS

LIST OF TABLES

LIST OF FIGURES

ACRONYMS

ADCLS	Automated Data Collection and Location System
AMMS	Advanced Microwave Moisture Sounder
AMSR	Advanced Mechanically Scanned Radiometer
AMSU	Advanced Microwave Sounding Unit
AMTS	Advanced Moisture and Temperature Sounder
AO	Announcement of Opportunity
AVHRR	Advanced Very High Resolution Radiometer
CZCS	Coastal Zone Color Scanner
DMSP	Defense Meterological Satellite Program
DoD	Department of Defense
ENSO	El Niño Southern Oscillation
Eos	Earth Observing System
EPA	Environmental Protection Agency
ERS-1	European Space Agency Remote Sensing Satellite-1
ESMR	Electronically Scanned Microwave Radiometer
ESTAR	Electronically Scanned Thinned Array Radiometer
FDA	Federal Drug Administration
FOV	Field-of-View
GFE	Government-Furnished Equipment
GOES	Geostationary Operational Environment Satellite
GSFC	Goddard Space Flight Center
HIRIS	High-Resolution Imaging Spectrometer
HMMR	High-Resolution Multifrequency Microwave Radiometer
HUD	Housing and Urban Development
IFOV	Instantaneous Field-of-View
IR	Infrared
ISLSCP	International Satellite Land Surface Climatology Project
LAI	Leaf Area Index
LAMMR	Large Aperture Multifrequency Microwave Radiometer
LASA	Lidar Atmospheric Sounder Altimeter
LEO	Low Earth Orbit
LFMR	Low-Frequency Microwave Radiometer
MLS	Microwave Limb Sounder
MODIS	Moderate-Resolution Imaging Spectrometer
MSS	Multispectral Scanner
MSU	Microwave Sounding Unit
NASA	National Aeronautics and Space Administration
NEMS	Nimbus-E Microwave Spectrometer
NOAA	National Oceanographic and Atmospheric Administration
NOSS	Naval Ocean Sensing System

ACRONYMS (continued)

NRC	National Research Council
NROSS	Navy Remote Ocean Sensing System
NWP	Numerical Weather Prediction
OCI	Ocean Color Imager
RFI	Radio Frequency Interference
RMS	Root Mean Square
SAM	Sensing With Active Microwaves
SAR	Synthetic Aperture Radar
SCAMS	Scanning Microwave Spectrometer
SCS	Soil Conservation Service
SISEX	Shuttle Imaging Spectrometer Experiment
SMMR	Scanning Multichannel Microwave Radiometer
SPOT	System Probatoire d'Observation de la Terre
SSM/I	Special Sensor Microwave/Imager
SSM/T	Special Sensor Microwave/Temperature
SST	Sea Surface Temperature
SSU	Stratospheric Sounding Unit
TIMS	Thermal Infrared Multispectral Scanner
TOGA	Tropical Oceans and Global Atmosphere
TOMS	Total Ozone Mapping Spectrometer
TOPEX	The Ocean Topography Experiment
TRMM	Tropical Rain Measuring Mission
UARS	Upper Atmosphere Research Satellite
USACE	United States Army Corps of Engineers
USDA	United States Department of Agriculture
USDI	United States Department of the Interior
VIS	Visible/Infrared Radiometer
VISSR	Visible/Infrared Spin Scanned Radiometer
WOCE	World Ocean Circulation Experiment

I. INTRODUCTION

MICROWAVE REMOTE SENSING

As generally used in reference to remote sensing from space, the microwave portion of the spectrum extends from frequencies near one gigahertz to frequencies of a few hundred gigahertz. In wavelengths this is approximately from 30 centimeters to 0.1 centimeters. This region is bounded at the low end by the UHF band, where noise in the form of television broadcasting and other man-made sources make remote sensing difficult, and at the high end by frequencies (generally referred to as far infrared or submillimeter) at which alternative techniques for detection become practical.

The technology for passive monitoring of radiation in the microwave portion of the spectrum was pioneered in radio astronomy (Ulaby, 1976) and many of the detectors currently used for remote sensing were developed for radio astronomy (e.g., the Dicke radiometer). However, remote sensing of the Earth in the microwave portion of the spectrum is a relatively new application fostered by increased concern for the environment and awareness of the Earth as a geophysical system, by the advent of the satellite which made possible the monitoring of geophysical processes on a global scale, and also because microwave radiation can penetrate clouds to provide the potential for all-weather remote sensing.

The all-weather potential of microwave remote sensing is illustrated in Figure 1, which shows the transmission characteristics of the atmosphere in the microwave portion of the spectrum. Three curves are shown in Figure 1: (1) the total zenith opacity for a dry standard atmosphere; (2) zenith opacity for the same atmosphere with 2 g/cm^2 water vapor added to the atmospheric column; and (3) the same column with an additional 20 mg/cm^2 of liquid water added to represent a typical stratus cloud. The dominant features on the Figure are resonant lines of oxygen between 50 to 70 GHz (which merge into a band at sea level pressures) and at 119 GHz (isolated line) and resonant lines of water vapor at 22 GHz and (a very strong line) at 183 GHz. However, except at the resonant lines the atmosphere is relatively transparent in this portion of the spectrum, and as the Figure illustrates, the presence of a non-raining cloud is only a small effect.

Remote sensing in the microwave portion of the spectrum is traditionally done at frequencies near 1.4, 6, 10, 18, 21, 37, 55, and 90 GHz, and sensors using 157 and 183 GHz are planned. These frequencies have been indicated for reference at the top of Figure 1. They are intentionally chosen among the peaks and valleys of the atmospheric attenuation curve. Measurements near the resonant peaks are used primarily for monitoring atmospheric temperature or water vapor. For example, measurements using a single frequency near the 22 GHz resonance of the water molecule have been used successfully to estimate the total water in a column of the atmosphere (Grody, 1976; Staelin, 1981) and are made as part of remote sensing of other parameters from space to help correct for the effects of atmospheric attenuation. The oxygen resonance lines between 50 to 70 GHz are used to obtain profiles of the temperature of the atmosphere (Staelin, 1981, 1977; Njoku, 1982), and the water resonance at 183 GHz is suited for obtaining profiles of atmospheric water vapor (Njoku, 1982) and sounders to do so are being developed.

Frequencies in the valleys of the attenuation curve are least affected by the atmosphere and are ideally suited for monitoring of the Earth's surface even in the presence of clouds. Measurements have been made of parameters such as sea surface temperature, snow cover, concentration of sea ice, and soil moisture. For example, Figure 2 shows the total concentration of sea ice (top panel) and the concentration of multiyear ice (bottom panel) in the north polar area as obtained from space using microwave measurements at 18 and 37 GHz (Gloersen and Cavalieri, 1986; Cavalieri *et al.*, 1984). Figure 3 is an example which shows the snow covered area of the northern hemisphere as obtained from microwave radiance monitored in space at 37 GHz. Furthermore, this figure has been color coded to show the depth of the snow, a parameter also determined from the microwave data (Chang *et al.*, 1986).

At the long-wavelength end of the microwave spectrum, the radiation emitted or reflected from matter is generally determined by the bulk dielectric

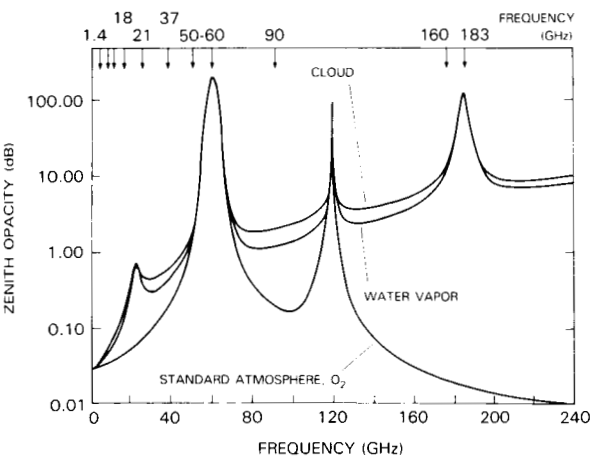

Figure 1. Microwave absorption in the atmosphere. Lower curve – atmospheric opacity due to oxygen. Middle curve – opacity with 20 kg m^{-2} water vapor added to the oxygen. Upper curve – opacity with 0.2 kg m^{-2} stratus cloud added to the oxygen and water vapor.

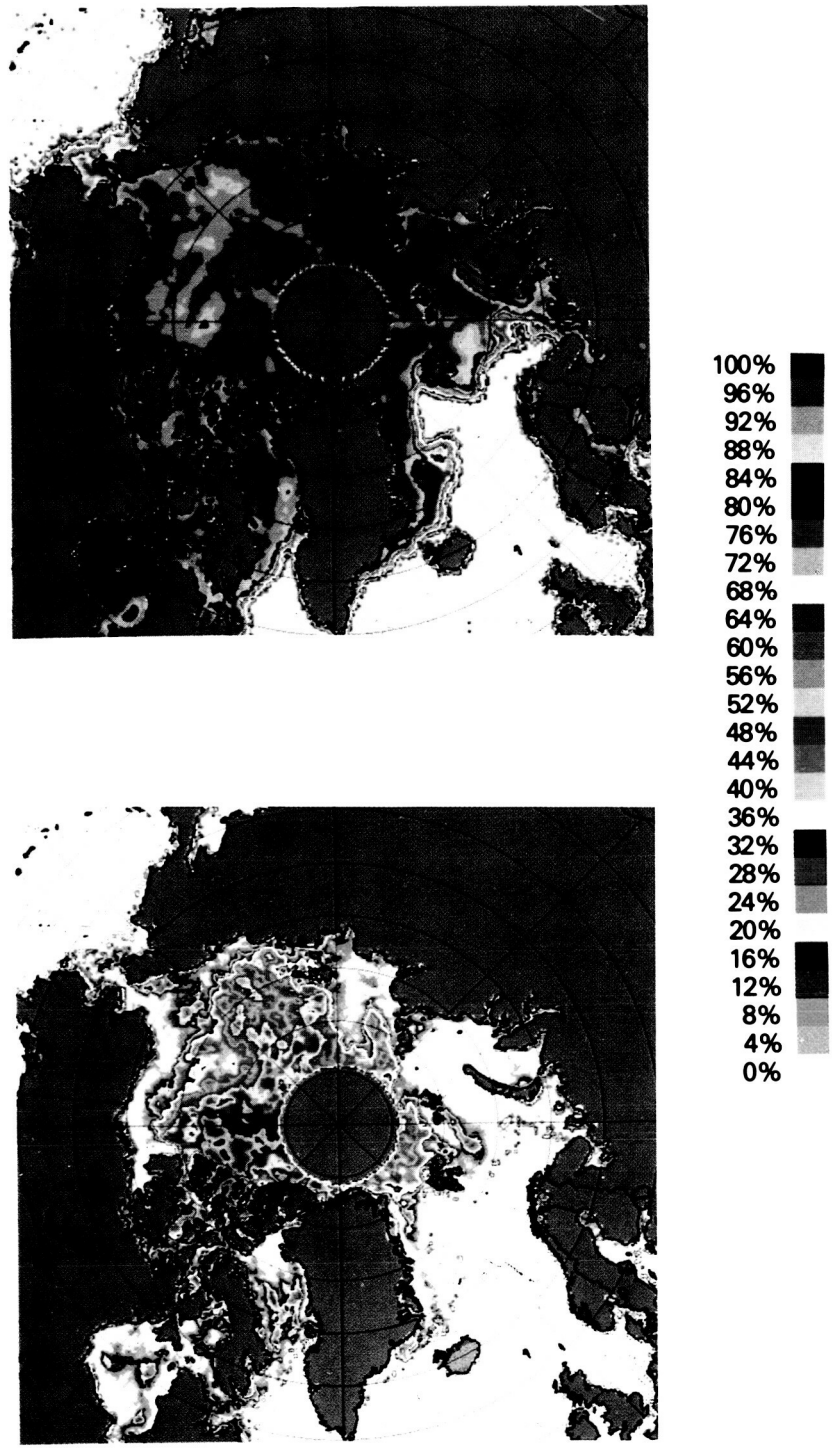

Figure 2. Top: Total sea ice concentration in the north polar area for the period February 3-7, 1979, as calculated from microwave data acquired with the Nimbus-7 SMMR. Bottom: Multiyear sea ice concentration in the same north polar area for the period February 3-7, 1979, as calculated from microwave data acquired with the Nimbus-7 SMMR (from Gloersen and Cavalieri, 1986).

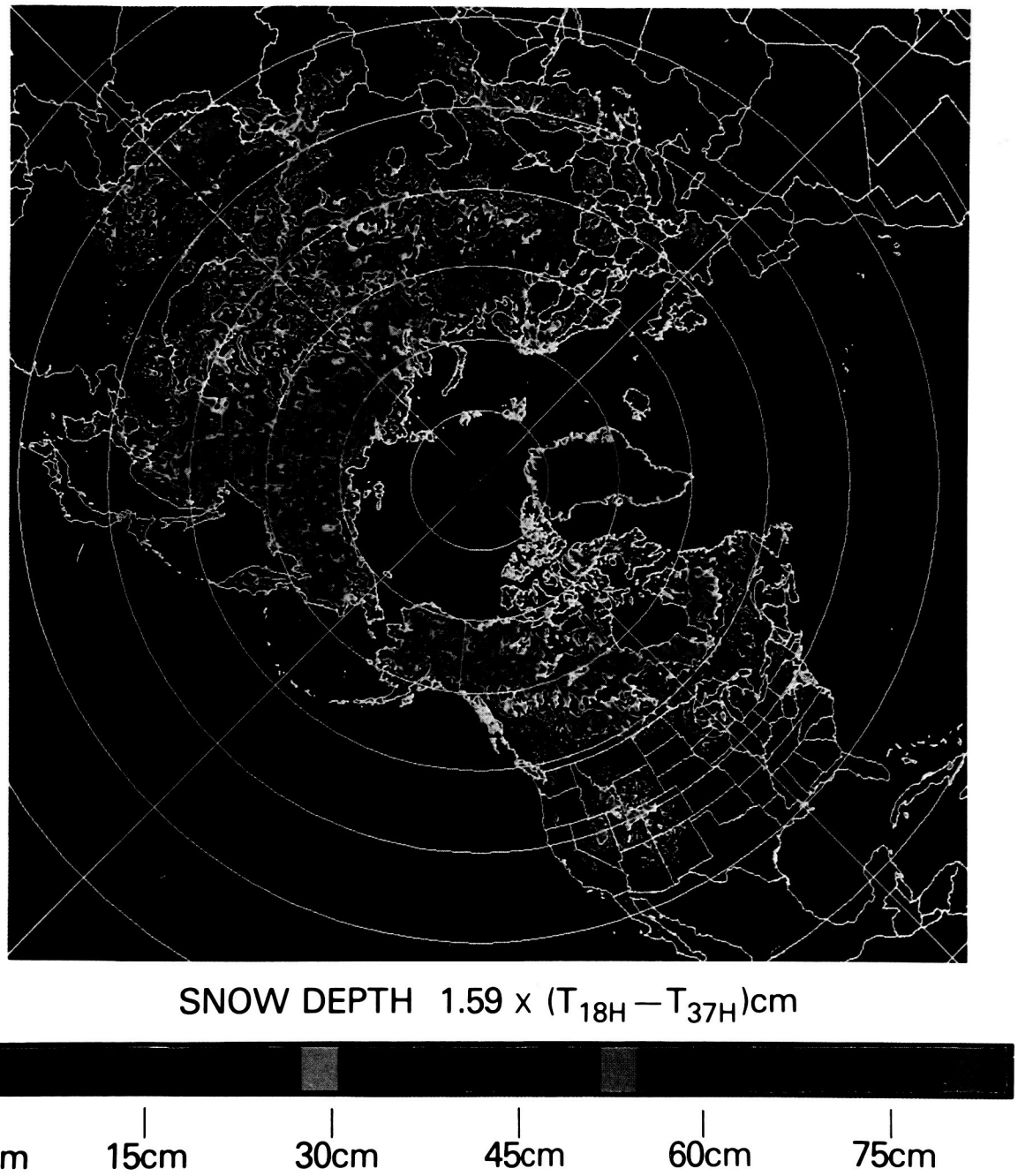

Figure 3. Snow covered area of the northern hemisphere for February, 1983. These data were obtained from the Nimbus-7 SMMR using data at 37 GHz and are color coded to show snow depth (Chang *et. al.*, 1986).

properties of matter and by such properties as the grain size in snow, the size of inclusions in ice, and the shape and size of leaves on trees and other vegetation. Furthermore, microwave radiation at this end of the spectrum penetrates materials such as snow, ice, soil, and vegetation. Consequently, it can be used to monitor average bulk properties of such material and is not limited to surface features or absorption and emission at molecular resonances. Consequently, at this end of the spectrum microwave radiation responds differently to the physical properties of matter than infrared or optical radiation and offers additional information to complement sensing at these very short wavelengths.

Finally, at frequencies in the 10 to 50 GHz range, radiation in the microwave portion of the spectrum penetrates clouds, but is strongly absorbed by rain. This provides the potential for measuring rain from

space (Atlas and Thiele, 1981; Atlas *et al.*, 1984; Wilheit *et al.*, 1977). Frequencies near 18 GHz have shown promise for measuring a wide range of rain rates (Atlas, *et al.*, 1984); however, by combining this observation with measurements at a more attenuating frequency (one near 37 GHz is generally used), one can improve the dynamic range of the measurement by increasing the detectability of the lower rain rates.

Some of the more important parameters which can be measured in the microwave portion of the spectrum together with the frequencies at which these measurements are made are listed in Table 1. The frequencies shown are "generic" in the sense that, except for temperature and pressure soundings where the frequencies are determined by specific molecular resonances, the measurements can generally be made over a broad range of frequencies and engineering considerations will likely determine the specific choice. For example, the emissivity of soil is changed by the presence of water in the soil, making it possible to measure the moisture content of the soil from the emitted thermal radiation (Schmugge, 1978; Cihlar and Ulaby, 1974). By using long wavelength radiation one can mitigate against the competing effects of vegetation cover and surface roughness. Furthermore, long wavelengths penetrate into the soil permitting measurement of the moisture in the upper layer of soil rather than just moisture at the surface. The exact frequency is not particularly important in this application and will be determined by considerations other than soil physics, such as the presence of interference from other radio sources (RFI) and requirements of antenna size (for a given spatial resolution the antenna size increases linearly as frequency decreases). The frequency of 1.4 GHz has received the most attention for measuring soil moisture because it is long enough (21 cm wavelength) to penetrate many crops and into bare soil, and because it corresponds to a quiet band in the spectrum set aside for passive measurements in radio astronomy. A similar situation exists in the case of measurements of sea surface temperature (SST). This is illustrated in Figure 4, which shows the change in brightness temperature of the ocean as a function of changes in temperature, salinity, and surface roughness. The brightness temperature is most sensitive to changes in temperature and least sensitive to competing factors at frequencies near 5 GHz, but higher frequencies could also be suitable especially if the wind speed is known. The precise choice of frequency to be used in a particular sensor system is likely to be determined by other considerations such as the availability of antennas and quiet bands in the spectrum. An instrument currently under development by the Department of Defense (DoD) to monitor sea surface temperature (the Low Frequency Microwave Radiometer, LFMR) will probably operate at 6 and 10 GHz.

Notice in Table 1 the large number of parameters requiring measurement at multiple frequencies. It has

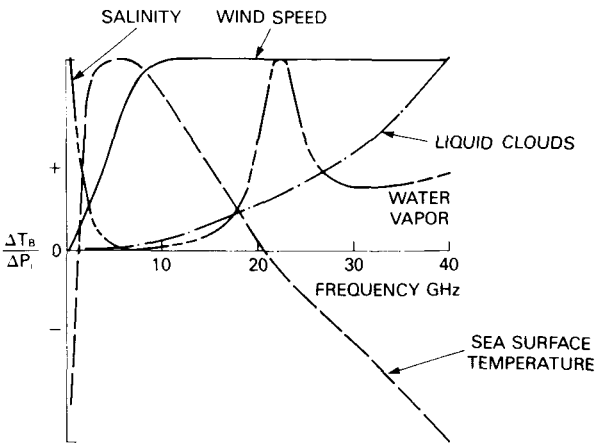

Figure 4. The change in brightness temperature of the ocean as a function of salinity, wind speed, and surface temperature. The relative attenuation due to water vapor and liquid water in clouds is also shown.

become increasingly clear that by choosing measurements at several well-spaced frequencies, many of the competing geophysical phenomena which normally contribute to the radiance can be identified. An example is the measurement of sea ice. Ice has a much different dielectric constant (emissivity) than water and, therefore, can be readily distinguished (Gloersen *et al.*, 1974; Zwally *et al.*, 1983). Because of this, the areal extent of ice can be distinguished at any of a wide range of frequencies, microwave as well as infrared. On the other hand, microwave radiation penetrates ice and scatters from inclusions such as pockets of brine or inhomogeneities. These change with the age of the ice and affect its emissivity. By comparing emissivity at several frequencies (e.g. 18 GHz and 37 GHz) one can distinguish first-year ice from multiyear ice and in some circumstances distinguish other properties of the ice (Svendsen *et al.*, 1983; Cavalieri *et al.*, 1984; Swift *et al.*, 1985). With data from measurements near 90 GHz, it may also be possible to identify the presence of snow cover on the ice. Another application where measurements at multiple frequencies is important is in the retrieval of sea surface temperature (Hollinger and Lo, 1984; Bernstein, 1982). The emissivity of the sea surface is low (on the order of 0.5) and the accuracy demanded for a successful retrieval is stringent (about 1 K). Thus, the influence of competing effects such as wind and waves on the ocean surface (which change the surface emissivity) and the amount of water in the atmosphere (which modifies the radiance at the receiver) must be taken into account. The preferred set of frequencies for sea surface temperature retrieval is 6 GHz, which provides information on temperature; and 10, 18, and 21 GHz, which provide information to correct for the interfering effects of surface winds and attenuation due to water in the

Table 1. Parameters Which are Measured with Microwave Sensors and the Frequencies at Which the Measurements are Made

Physical Observable	Frequency of Observation (GHz)									
	1.4	6	10	18	21	37	50-60	90	160	183
Soil moisture	●	O								
Snow		O	O	●		●		◒		
Precipitation										
Ocean			◒	●	O	◒				
Land				◒		●		●		◒
Sea surface temperature		●	◒	◒	◒	O				
Sea ice										
Extent				●		●		O		
Type		O	◒	●		●		◒		
Wind speed (sea surface)			●	◒	O	O				
Water vapor										
Total (over ocean)				●	●	◒				
Profile					◒	O	◒	O	◒	●
Cloud water (over ocean)					◒	●		◒		
Temperature profile					O	O	●	O		

Key: ● Necessary ◒ Important O Helpful

atmosphere. Even measurements at 37 GHz are used, indirectly, to detect and eliminate cases where rain fills some portion of the field-of-view (FOV).

HERITAGE OF MICROWAVE REMOTE SENSING FROM SPACE

Microwave measurements have been part of the remote sensing program in space from its beginning. This is illustrated in Table 2, which gives a history of microwave radiometers in space.

The instruments listed in Table 2 can be separated into two categories, imagers of surface features or sounders of atmospheric properties such as temperature or water vapor. The Nimbus-E Microwave Spectrometer (NEMS), Scanning Microwave Spectrometer (SCAMS), and Microwave Sounding Unit (MSU) were microwave sounders designed to obtain profiles of atmospheric temperature, although the 22 GHz and 31 GHz channels on the NEMS and SCAMS also provided information on total atmospheric water vapor and some information on features such as rain and snow and ice coverage. The NEMS instrument made measurements with a single nadir pointing antenna beam at three frequencies (53.65, 54.9, and 58.8 GHz) to profile atmospheric temperature. The resolution at nadir was about 180 km. The SCAMS employed the same frequencies as the NEMS but differed in that the antenna was mechanically scanned across track to obtain a wider swath of coverage than obtained with the NEMS. The resolution at nadir was about 145 km. The next generation of sounder, the MSU, which is still in use today, scans across track, has 110 km resolution at nadir, and uses four frequencies (50.3, 53.74, 54.96, and 57.95 GHz) in the

Table 2. History of Microwave Sensors in Space

Year	Spacecraft/ Instrument	1.4	6	10	18	21	37	50-60*	90	160	183	Resolution Nadir (km)**	Frequencies (GHz)
1962	Mariner				X	X						1,300	15.8, 22.2
1968	Cosmos 243	X		X								37	3.5, 8.8
1970	Cosmos 384					X	X					13	
1972	Nimbus-5												
	ESMR				X							25	19.35
	NEMS					X	X	$X^{(3)}$				180	22, 31.4
1973	Skylab												
	S-193			X								16	13.9
	S-194	X										115	
1974	Meteor						X						
1975	Nimbus-6												
	ESMR						X					20 × 43	
	SCAMS					X	X	$X^{(3)}$				150	22, 31
1978	DMSP												
	SSM/T							$X^{(7)}$				175	
1978	Tiros-N												
	MSU							$X^{(4)}$				110	
1978	Nimbus-7												
	SMMR		X	X	X	X	X					18 × 27	(Data at 50 km)
	Seasat												
	SMMR		X	X	X	X	X					22 × 35	
Future	DMSP												
	SSM/I				X	X	X		X			16 × 14	19.3, 22, 85.5
	SSM/T-2								X	X	X	50	150
	NROSS												
	LFMR		X	X								15 × 25	6
	NOAA												
	AMSU-A					X	X	$X^{(12)}$	X			50	24, 31
	AMSU-B								X	X	$X^{(3)}$	15	
	Eos												
	ESTAR	X										10	
	AMSR		X	X	X	X	X		X			1.5	

*Superscript = Number of channels
**At highest frequency

oxygen resonance band to profile temperature. However, the MSU does not include the water-sensitive channels at 21 and 31 GHz present in its predecessors. The Special Sensor Microwave/ Temperature (SSM/T) is also a temperature profiling instrument and is designed for the Defense Meteorological Satellite Program (DMSP). One SSM/T instrument has been in orbit for about 2 years and as many as eight others are projected. These sensors scan across track through nadir with a resolution at nadir of about 200 km. They use seven frequencies (50.5, 53.2, 54.35, 54.9, 58.4, 58.825, and 59.4 GHz) in the oxygen resonance band to profile temperature. The additional frequencies are used to obtain profiles from near the surface to about 30 km, as compared to 20 km for the MSU and its predecessors. The remaining sounder listed in Table 2, the AMSU (Advanced Microwave Sounding Unit), represents a substantial advance in comparison with its predecessors. The AMSU, which is being designed to meet National Oceanographic and Atmospheric Administration (NOAA) operational needs, will consist of two components: the AMSU-A, which is a temperature sounder in the tradition of the SSM/T and MSU, and the AMSU-B, which will obtain profiles of water vapor using measurements near the water resonance line at 183 GHz. The AMSU differs from its predecessors in the increased number of frequencies (channels) used to obtain soundings (12 for the AMSU-A and 3 for the AMSU-B) and in resolution. The increased number of channels will permit soundings from near the surface up to 40 km for the AMSU, compared to only 20 km for the MSU and its predecessors and 30 km for the SSM/T. Also, the antennas to be employed with the AMSU will permit spatial resolution of 50 km or better with a wide

swath coverage. The AMSU is being developed for deployment by NOAA in the late 1980s as an operational sounder beginning with NOAA-K. A water vapor profiler is also being designed for the DMSP. This instrument, a variation on the SSM/T, will measure radiation at the water vapor resonance line (183 GHz) with ancillary channels at 91.5 and 150 GHz. Its resolution on the surface will be about 50 km.

The other category of instruments in Table 2 are devices which primarily respond to and map emission from the Earth's surface. Among the earliest of these is the ESMR (Electronically Scanned Microwave Radiometer). The ESMR employed an 85 × 85 cm phased array antenna which, when pointed at nadir, electronically scanned across track to form images. Two ESMRs have been flown, one aboard Nimbus-5 with the antenna pointed at nadir and operating at 19.3 GHz, and a second flown on Nimbus-6 which was pointed so that the antenna beam was incident at about 50° from normal at the Earth's surface. It operated at 37 GHz. The earlier ESMR had a resolution at nadir of about 25 km and the later one of about 20 × 43 km. The ESMR data has been used to study rain, sea ice, ice sheets, snow coverage, and land features. Two other single-frequency sensors were flown as part of Skylab: the S193 was a 13.9 GHz radiometer which employed a mechanically-scanned parabolic reflector antenna, and the S194 was an experiment to measure soil moisture which employed a nadir-looking phased array at 1.4 GHz. The successor to single-frequency sensors was the SMMR (Scanning Multichannel Microwave Radiometer) which was flown on Nimbus-7 and Seasat. The SMMR was designed to obtain sea surface temperature and wind speed as well as sea ice characteristics, snow and ice extent, and total water vapor and rainfall rate over oceans. It consists of five frequencies, each dual polarized with an antenna system which rotates to obtain a conical scan at a fixed incidence angle of about 50° at the Earth. The SMMR is a multifrequency imaging device which measures at most of the frequencies which had proven useful at the time, and has the advantage of scanning at a fixed incidence angle. The SMMR antenna is about 80 cm in diameter, providing resolution ranging from about 25 km (18 × 27 km) at the highest frequency to nearly 150 km at the lowest frequency. The multifrequency data from this sensor are processed into images with resolution of 50 km or larger.

The Special Sensor Microwave/Imager (SSM/I) and the LFMR are two systems being designed to meet the operational needs of the DoD. Together they cover the same frequencies as the SMMR and have, in addition, a channel at 85.5 GHz (on SSM/I). The SSM/I is similar in principle to the SMMR: it is conically scanned so that its antenna forms a beam with an incidence angle of about 50° at the surface, and it measures at several frequencies (19.35, 22.24, 37.0, and 85.5 GHz) similar to those on SMMR. The antenna used with the SSM/I is 60 × 65 cm, which is slightly smaller than the SMMR antenna. The LFMR is designed primarily to make maps of sea surface temperature. It will operate near 6 and 10 GHz, and to obtain the resolution required by the DoD it will employ an antenna on the order of 6 meters in diameter. Plans for the LFMR include a large deployable mesh antenna to obtain resolutions better than 25 km on the surface, and absolute accuracies of ± 1 K (Hollinger and Lo, 1984).

Multiple-frequency microwave imaging of the Earth's surface has proven successful because, with the increased information provided by simultaneous measurements at different frequencies, one is able to detect additional phenomena and to isolate from a particular measurement the contribution from other surface parameters or intervening atmosphere. However, one of the difficulties of doing multiple-frequency imaging with microwaves is obtaining adequate spatial resolution. In part, this is because large antennas are required at the low-frequency end of the microwave spectrum and because in sensors using a single antenna the resolution is determined by the channel with the lowest frequency. For example, the LFMR requires an antenna about 6 m in diameter to obtain sea surface temperatures with sufficient resolution (10 to 25 km) to meet operational requirements set by the DoD. On the other hand, the spatial resolution required for a particular measurement is determined by the scale size of the geophysical phenomenon to be investigated. The requirements for spatial resolution range from a few kilometers for estimating some parameters of snow and some applications of sea surface temperature measurements, to several tens of kilometers. (The requirements are discussed in sections of this report to follow.) These requirements can be very difficult to meet in the microwave portion of the spectrum. In fact, one of the areas in which progress has not been made in the evolution of microwave remote sensing from space has been in the area of spatial resolution. The spatial resolution obtained with the highest frequencies on present-day sensors is about the same as obtained with the ESMR, flown in 1970. The SSM/I, even at its highest frequency (85.5 GHz), will have resolution little better than ESMR. The next important milestone to be passed in the application of microwave remote sensing from space is to obtain images with spatial resolutions comparable to the scale size of the geophysical phenomena.

ORGANIZATION OF THE REPORT

The objective of the HMMR Panel was to define instrumentation for an Earth Observing System in low Earth orbit which could make the microwave measurements necessary to advance understanding of the global geophysical processes governing the environment. This required defining and assigning priorities to the information which passive microwave

remote sensing can provide from low Earth orbit and determining the resolution required of these measurements so that the data which are obtained will promote understanding of the fundamental processes controlling the environment. The specific microwave measurements identified as important and the requirements for these measurements are described in Chapters II through IV of this report.

The hydrologic cycle emerged from this exercise as the environmental process with the highest priority. Microwave sensors can provide measurements of such elements of the hydrologic cycle as precipitation, soil moisture, snow extent, total water vapor in the atmosphere, and evaporation from the oceans. Over land, microwave sensors in conjunction with other sensors can also help to estimate moisture fluxes from the ground (evaporation and transpiration from plants). In the three sections, Chapters II through IV, a brief review is given of the role microwave remote sensing can play in measuring parameters of environmental importance over land, the oceans, and in the atmosphere, respectively. The focus in these sections is on defining a set of requirements for the microwave measurements so that they will yield a data set to meet future scientific needs and permit significant advance in our understanding of the environment. These requirements are summarized in Chapter V and from them a list of instrument specifications has been deduced (Tables 14 and 15).

In addition to defining measurement requirements and instrument specifications, the Panel sought to determine if there were practical sensor systems which could meet these requirements and which could realistically be implemented in space. In this exercise, the Panel relied on knowledge of past and planned sensor systems and on its own understanding of what could realistically be implemented in space in the next decade. A concept consisting of three separate instruments emerged from the considerations of the Panel. The three instruments are the AMSU (Advanced Microwave Sounding Unit) presently under development for operational atmospheric sounding on NOAA-K, -L, and -M, and two new instruments, the AMSR (Advanced Mechanically Scanned Radiometer), and the ESTAR (Electronically Scanned Thinned Array Radiometer). Details of these instruments are provided in Chapter V. The AMSR is a six-frequency, conically-scanned microwave radiometer conceived to provide measurement of parameters important to the global hydrologic cycle. It includes channels at approximately 6, 10, 18, 21, 37, and 90 GHz each with dual (linear) polarization. The ESTAR is a 1.4 GHz radiometer conceived specifically to obtain global maps of soil moisture, an important element of the hydrologic cycle. The ESTAR is a hybrid real aperture and synthetic aperture sensor. It employs an array of long stick antennas to achieve real aperture resolution in the along-track dimension and uses signal processing to achieve, synthetically, resolution in the crosstrack dimension. The result is a substantial reduction in the antenna volume needed in space.

Some of the parameters can be estimated much more accurately if the measurements that the High-Resolution Multifrequency Microwave Radiometer can provide are made in conjunction with other sensors. This potential synergism between the HMMR and other instruments planned for the Earth Observing System is discussed in Chapter VI. Also in Chapter VI is a description of several microwave instruments which are not part of the Eos but which may be making measurements from space in the future. Reasons why these sensors were not recommended for the Eos are given. Finally a summary is given in Chapter VI of the Tropical Rain Measuring Mission (TRMM) project. This is presented here because of the central role of this type of measurement in developing an algorithm for measuring precipitation from space.

II. SCIENCE OBJECTIVES: LAND

THE HYDROLOGIC CYCLE

Water is one of the key substances in the earth-atmosphere system and it is fundamental to the existence and vitality of life on the planet. Vernadskii (1960) said: "Water occupies a unique position in the history of our planet. No other natural substance can be compared with it insofar as its influence on the course of the most basic geological processes is concerned. All substances on this Earth–whether mineral, rock, or living body–contain some water. All matter on the Earth is affected by water in some way and is either impregnated with it or surrounded by it." The existence of water in all three phases (solid, liquid, and gas) in the environment is one of the most distinctive characteristics separating the Earth from other planets of the solar system. Furthermore, most of the geophysical processes on Earth involve changes between these phases.

Since water is such a key substance, the study of hydrology is closely linked to other Earth science disciplines, such as geophysics, plant ecology, and climatology. The energy and moisture fluxes at the earth-atmosphere boundary and surface conditions such as water content and temperature are some of the variables which couple hydrology and these other disciplines of Earth science. Spaceborne instruments cannot measure these fluxes directly, but they do provide estimates of the state variables such as soil moisture, surface temperature, ground cover characteristics, and snowpack properties from which these quantities can be determined. Physically-based models already exist to calculate integrated fluxes using remotely-sensed data as a major input to the algorithms.

In addition, understanding the general laws governing the distribution of water over the Earth and collecting data on the water balance of the seas and river basins is essential for the rational use and protection of water resources as well as for understanding the physical processes governing the evolution of our planet. Remote sensing of soil moisture and snowpacks helps to monitor the distribution and how it changes. Evapotranspiration, a derived quantity to be determined from directly observable parameters, is a large component of the water balance and its estimation over large areas is also important.

The water cycle is also closely linked to many biogeochemical cycles with implications for plant ecology. For instance, in order to form carbon compounds, plants must transpire water. Wetlands provide the main chemically reducing environments on the Earth, and soil water is essential to many soil chemical reactions. Water is one of the main constraints, along with input energy, on ecological systems. This is illustrated in dryland farming areas in periods of drought where major economic and social changes can be caused by water strategy. The Sahelian zone of Africa is a prime example. Rainfall is also important over the oceans, not only for climate energetics, but because the fresh water on the sea surface alters the surface salinity and its density, and as a result changes the marine circulation and possibly the surface biology.

Also, surface hydrology is very strongly coupled to climatology. For example, evaporation and transpiration are the only source of atmospheric water, and latent and sensible heat fluxes provide much of the energy to drive climate dynamics.

The coupling of the Earth's water cycle to the solid Earth, the atmosphere, and to plant biochemical cycles demonstrates the essential nature of the hydrologic cycle in the Earth System. Figure 5 depicts schematically the relationships among the energy, biogeochemical, and water cycles. The energy and water cycles of the atmosphere are closely linked because energy is needed for latent heat of evaporation, both at the surface and in the atmosphere, and is released on condensation, most notably in precipitating clouds. The source of energy in the system is the sun. Some of the solar energy gets absorbed by the atmosphere directly, and of the portion that reaches the ground, part gets absorbed and the rest gets reflected back into the atmosphere. The atmospheric layers and ground surface also radiate energy (i.e., thermal radiation described for example, by Planck's radiation formula or the Stefan-Boltzmann Law). Non-radiative energy fluxes include sensible heat created by the temperature difference between the surface and the atmospheric boundary layer, and the latent heat flux carried by evaporation.

It is convenient to enter the water cycle with the rainfall, which gets divided into surface runoff, which eventually reaches open water bodies and surface infiltration. Of the latter, some is returned to the atmosphere via evapotranspiration, some goes into short-term soil moisture storage, and the rest goes into the water table. Clearly, the energy and moisture components of the hydrologic cycle are coupled and complex.

Table 3 shows the magnitudes of the storage terms in the world water balance (United Nations Educational, Scientific, and Cultural Organization, 1971). It may be seen that a very high proportion (97.2 percent) of the Earth's water is stored in the oceans and ice sheets, areas with a very long average residence time (>4,000 years). Some of the terms, such as water storage in plants or in the soil and atmosphere, are comparatively very small, but the changes in these provide the major fluxes in the hydrologic cycle and are the fluxes of importance for energy exchanges in the atmosphere and for biological resources. From the Table, one can better begin to appreciate the complexities and magnitudes of the task facing scientists

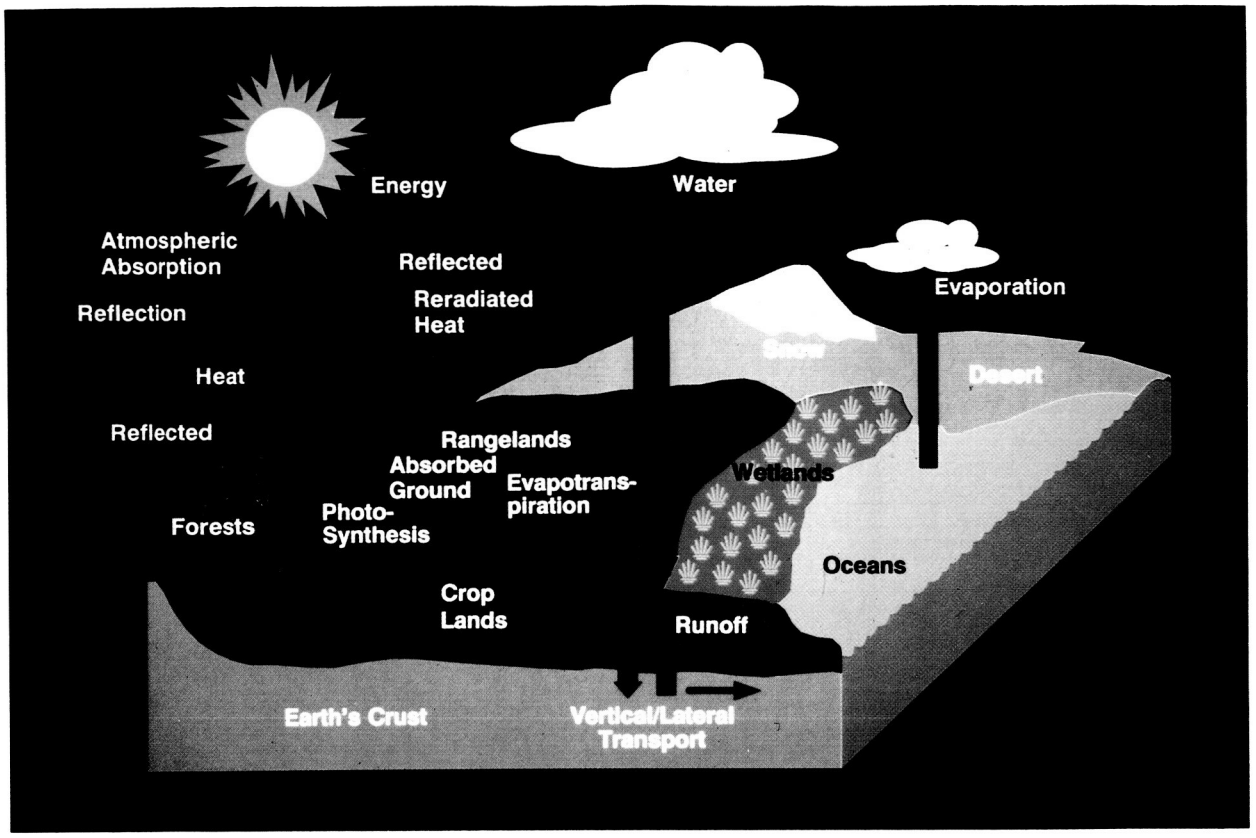

Figure 5. Relationship among the energy, biogeochemical, and water cycles.

Table 3. World Water Balance

Parameter	Volume (km^3)	Equivalent Depth* (m)	Average Residence Time
Atmospheric water	13,000	0.025	8-10 days
Oceans and seas	$1,370 \times 10^6$	2,500	4,000 years
Freshwater lakes and reservoirs	125,000	0.250	
River channels	1,700	0.003	2 weeks
Swamps	3,600	0.007	of the order of years
Biological water	700	0.001	1 week
Moisture in the soil and the unsaturated zone soil moisture	65,000	0.013	2 weeks to 1 year
Ground water	4×10^6	8	days
Frozen water	30×10^6	60	tens of thousands of years

*Computed as though the storage were uniformly distributed over the entire surface of the Earth.

if they wish to observe, model, and understand the hydrologic cycle and its variations over time and space. The problem is complicated by realizing that the readily accessible and dynamic parts of the water cycle in the earth-atmosphere system are a relatively small part of the total. Of the fresh water on the Earth, about 1 part in 10 is in liquid form. Of the liquid portion of this water that is fresh, unfrozen, and available, ground water occupies 99 percent, 1 percent is in the form of water stored in lakes, 0.2 percent is in the form of soil moisture, 0.1 percent is in rivers, and 0.1 percent is atmospheric water. About 0.005 percent exists in plants. In terms of equivalent depth about 1 meter falls annually in the form of precipitation and is evaporated from the surface of the Earth (Dooge, 1973). This precipitation and evaporation represent a latent heat equivalent to about one-fourth of the net energy input from the sun.

Theoretical and numerical studies (simulations) have been used to study the hydrologic cycle and its response to changes in the variable storage terms. The process driving changes in the hydrology of the land surface can best be expressed in terms of conservation equations at the surface for energy and mass (i.e., mass of water). The important terms in the conservation equation for water are the input from precipitation and losses due to run-off, evaporation, and the change in water stored as snow, ice, and soil moisture (e.g., Figure 6). The important terms in the equation for conservation of energy are the input (e.g., from the sun), losses due to radiation from the surface, and fluxes of latent and sensible heat (Figure 5). In the energy balance, the radiation from the soil is generally the least significant term (10 to 30 percent of the net transfer). The fluxes of latent and sensible heat account for 70 to 90 percent of the radiation budget. The proportion of these two varies with time of day and climate, but on the average, they are about the same size. The latent heat flux carries on the average about 40 percent of the radiation budget. Thus, it is important to be able to estimate both the latent and sensible heat flux because of their importance in the energy balance and the latent heat flux alone for its water content.

There have been several studies of the energy and water balance of the Earth (e.g., United Nations Educational, Scientific, and Cultural Organization, 1978; Lvovitch, 1971; Nace, 1970). Numerical simulations of the atmosphere which have provided the framework within which to examine the dynamics of the hydrologic cycle are reviewed by Manabe (1982). These efforts began as early as 1956 with the work of Phillips (1956) and continued through the efforts of Smagorinsky (1963), Mintz (1968), Manabe (1969), and Manabe and Holloway (1975), as well as others.

There has also been other progress which gives insight into the sensitivity of the climate to changes in

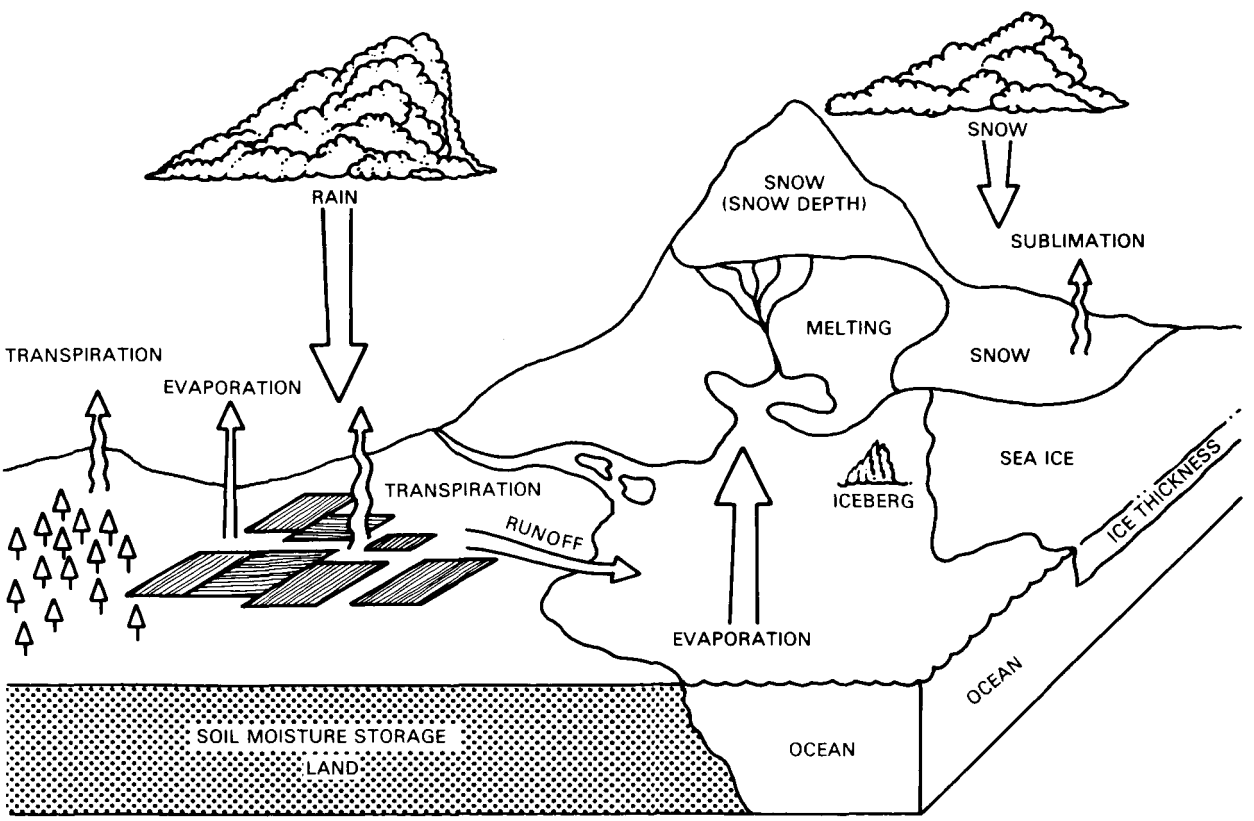

Figure 6. Important processes in the hydrologic cycle (adapted from Smagorinsky, 1982).

conditions at the surface with emphasis on soil moisture, albedo, and evapotranspiration (for examples see Walker and Rowntree, 1977; Rowntree and Bolton, 1978; Rind, 1982; and Shukla and Mintz, 1982).

Mintz (1984) reviewed these results and showed that the distribution of precipitation and dynamic characteristics of the atmospheric circulation and evapotranspiration are clearly sensitive to changes in soil moisture and albedo of the surface. For example, Rowntree and Bolton (1978) showed that precipitation changes over large areas can be the result of changes in the soil moisture over a relatively small region. They modeled an area centered over Western Europe for which the maximum available water that the soil could hold was set equal to 20 gm cm^{-2}, and the ratio of evapotranspiration to potential evapotranspiration was taken as the lesser of unity and [soil water/10 gm cm^{-2}]. Three simulation experiments were made, each for 50 days ending on July 15, in which the only difference was the initial amount of water in the soil at those land points in Europe which lie between 40° and 54°N, and west of 30°E. The initial soil moisture in the three cases was 15 gm cm^{-2} (W), 5 gm cm^{-2} (C) and zero gm cm^{-2} (D).

Figure 7 shows the profiles of the rainfall, along longitude 13°E, for these three cases. Over most of the map the differences in the rainfall are such as can be produced by the natural variability of the atmosphere. But, within and immediately to the north of the region of different initial amounts of soil water, there is a large increase in the rainfall when the initially wet soil case is compared with the initially dry soil case. At the center of the region, the 30-day average rainfall increases from about 1 mm/day to 5 mm/day. Rowntree and Bolton (1983) describe further simulations which showed that the anomalies in soil moisture introduced into the model for Europe caused differences in the precipitation and evapotranspiration to persist for at least 20 to 50 days.

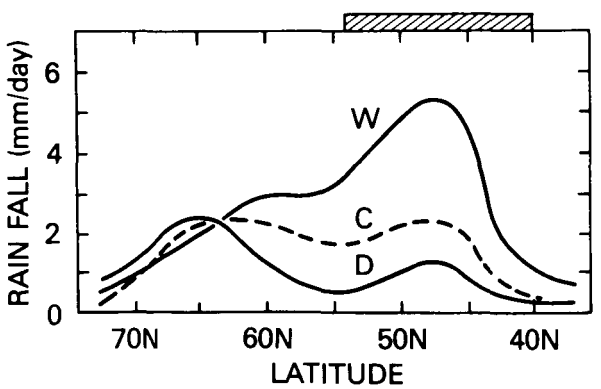

Figure 7. Distribution of precipitation along the 13° meridian, for three cases with different initial values of soil moisture (D = 0 gm cm^{-2}; C = 5 gm cm^{-2}; and W = 15 gm cm^{-2}). The cross hatch at the top indicates the region in which the soil moisture was changed (adapted from Rowntree and Bolton, 1978).

These experiments are for the summer season, when the solar radiation is large and, therefore, the surface radiation balance and the potential evapotranspiration are large. In the winter season, the surface radiation balance and potential evapotranspiration will be smaller and, therefore, the actual evapotranspiration will generally be smaller. Moreover, in the winter season some of the soil water that enters the air will be removed from the continent as cold, dry continental air begins its conversion into warmer, moister air. One would not expect, therefore, that there will be as much precipitation recycling of the soil water in winter as in summer.

Fewer numerical studies have been reported in the literature concerning the effect of changing snow cover on the atmospheric circulation. However, in a closely related experiment, Herman and Johnson (1978) showed that by varying sea-ice cover in the Arctic over the range observed during a 17-year period, not only was the local atmospheric circulation affected, but also significant changes occurred in the middle and subtropical latitudes. Furthermore, since the presence or absence of snow cover can radically change the albedo and the radiation balance, the presence of snow can lead to very significant effects on the evapotranspiration and soil moisture storage over time. Most recently, Walsh *et al.* (1982) have shown that surface temperatures over wide expanses in the eastern and western United States are correlated with snow-covered areas.

Even though many fine studies have been done on the global and regional water balances, there is still much to be done to reduce the uncertainties in the magnitude of the storage parameters for the global water balance, and even more so for continental and regional water balances at time scales shorter than decades (e.g., annually, seasonally). Certainly much remains to be learned about the temporal and spatial variability of evapotranspiration, soil moisture, and precipitation. Over the oceans, in particular, knowledge of the variability in evaporation and precipitation is lacking. The effects of anthropogenic activities on the hydrologic cycle also need to be studied and understood. Deforestation in the tropics, including, in particular, the Amazon basin, drainage of large swamps and marshes to increase river flow in Africa, and the diversion and reversal of the flow of major rivers in Northern Asia are examples of activities ongoing or under consideration that will perturb the hydrologic environment over large areas and on whose effects one can only speculate at present.

The major factor limiting the resolution of questions such as those noted above, is a lack of data of appropriate accuracy, spatial and temporal frequency, and uniformity. Currently available measurements for major components of the hydrologic cycle are very non-uniform in space and time.

Measurements of precipitation and evaporation are very sparse over large expanses of ocean, particularly in the southern hemisphere. Over land, the most common measurements are those of precipation, but even these are unevenly spaced. There is a lack of observations for studies of the hydrologic cycle in the tropics and the southern hemisphere land areas and, in general, over high-altitude areas.

The instrumentation proposed for Eos promises to provide considerable observational advantages compared to existing conventional and remote sensing observing systems. First, passive microwave instrumentation, such as proposed for HMMR, is particularly well-suited for detecting the presence of water; and second, the technology of passive microwave remote sensing is sufficiently advanced to meet the observational requirements needed to design and test global hydrologic models.

The following sections will examine in more detail the current understanding of the physics allowing inversion from microwave signals to estimate hydrologic parameters accurately and will describe the specific relationships of HMMR to the requirements of the scientific community.

REMOTE SENSING OF HYDROLOGIC PARAMETERS

In this section, we review briefly the present state of knowledge about our capability to remotely sense the hydrologically important variables and list science measurement requirements. Both visible/infrared and passive microwave methods are covered, but more emphasis is given to the microwave regime. The general advantages of microwave emission measurements are that, with some exceptions, the signal penetrates from some depth below the surface, whereas reflectance of solar radiation and emission of thermal infrared radiation are determined by the characteristics of a much thinner surface layer; and that the water molecule is resonant and also causes significant changes in the bulk dielectric properties of matter at microwave frequencies, providing the potential for direct measurement of water.

Soil Moisture

Soil moisture is important in both the energy and mass balance approaches to the hydrologic cycle. The magnitude of evaporation from bare soil, plant uptake of soil water for transpiration, and the thermal conductivity and heat capacity of soil all depend on the amount of soil water. Soil moisture also represents a significant storage volume in the land hydrologic cycle.

Visible and Infrared Measurement of Soil Moisture

Visible and infrared techniques have been used for estimation of soil moisture, but both suffer because they can measure soil moisture only in the top few millimeters. They are also restricted to bare soils.

At visible wavelengths, the decrease in soil albedo with increasing moisture can be observed from satellite and empirically correlated with soil moisture. Crist and Cicone (1984) also report a sensitivity of near- and middle-infrared Thematic Mapper data to surface soil moisture, but no quantitative relationships are given.

Thermal infrared remote sensing methods for estimating soil moisture exist using primarily thermal inertia techniques. Van de Griend *et al.* (1985) showed that these thermal infrared data are most related to soil moisture at night, but they also showed that when vegetation cover is present, the sensitivity is very small above the wilting point of the plants. Wetzel *et al.* (1984) used the course of thermal infrared temperature estimates during the morning to estimate soil moisture using radiometers mounted on geostationary spacecraft. Although no comparisons with ground data are available, the method is sensitive to error in estimated surface temperatures because they can alter the morning temperature gradient.

Passive Microwave Measurement of Soil Moisture

The emission of microwave radiation from the soil is heavily dependent on the soil moisture content, because the microwave emissivities of water and of dry soil are very different. However, the signal is attenuated by vegetation covering the soil. This attenuation increases with frequency, so it is desirable to use long-wavelength microwave radiation in order to reduce the attenuation by vegetation. Considerations of vegetation penetration, sampling depths, and technological constraints such as antenna size and potential for RFI have led to the use of 1.4 GHz (L-band) as the most suitable for soil moisture measurements. Microwave emission at this wavelength is most sensitive to soil moisture content variations in the top 2 to 5 cm. Physically-based models of the emission from bare soil have been written (e.g., Wilheit, 1978). One can also account for the effects of surface roughness (Choudhury *et al.*, 1979) and vegetation (Lang and Sidhu, 1983; Lang, 1981). This combined model can be solved numerically to give estimates of the soil moisture content, given some information about the soil type. However, it is probably more practical to use known linear correlations between soil moisture content in the top 5 cm of soil and the emitted radiation for each soil type. The relationship is nearly linear and the explained variance high (Schmugge, 1984; Schmugge *et al.*, 1986), while the number of parameters to be estimated is reduced and computational efficiency is increased.

Passive microwave data at 1.4 GHz (21 cm wavelength) would be very useful for estimating near-surface soil moisture using either of these techniques. This could then be related to moisture status in the subsurface soil columns and to hydraulic parameters

of interest to soil scientists using physically-based soil physics models. The accuracy required of these measurements depends, in part, on the particular application to be made of the data. Requirements for different applications have been collected by the NASA Soil Moisture Working Group and are summarized in the Plan for Integrated Soil Moisture Studies (Rango *et al.*, 1980). Table 4 summarizes requirements for soil moisture data for agricultural applications and Table 5 is a summary of requirements of hydrologists for soil moisture measurements (Rango *et al.*, 1980). Using information presented by the Soil Moisture Working Group (Rango *et al.*, 1980), the Staelin Committee (Staelin and Rosenkranz, 1978), and the Eos Science and Mission Requirements Working Group (Butler *et al.*, 1984, Vol. I and Appendix), the soil scientists on the HMMR Panel concurred that five moisture levels should provide adequate information initially and that observations should be made globally at least once every 3 days with a spatial resolution of 10 km, if possible, but 25 km would be adequate. The 10 km resolution is based on estimates of the size of precipitation cells, the forcing function for soil moisture. The rationale for the lower spatial resolution (25 km) is that the soil moisture, because it is stored in the soil, is averaged as the precipitation event moves through the area. Additional data on the water content of vegetation, either from visible/near-infrared data or from 6 GHz microwave data, could be useful for inferring vegetation attenuation to correct the microwave measurement.

At L-band frequencies (1.4 GHz), the brightness temperature of soil (T_B) depends, in addition to moisture content, on soil temperature, surface roughness, and soil type and vegetation cover. In the presence of this geophysical measurement "noise," and in light of the moisture signal dynamic range (~ 100 K), an instrument brightness temperature sensitivity of 1.5 K rms is adequate and well within the present technological capability. The primary goal in the system design, therefore, should be to reduce the geophysical noise. This may be achieved by including polarization measurements, measurements at more than one frequency, measurements by other sensors (infrared and visible wavelengths or radar), and appropriate spatial and temporal sampling.

Polarization measurements are useful, since at large off-nadir view angles (>40°) low polarization difference (i.e., a small difference between vertical and horizontal brightness temperatures) is associated with increased surface roughness and vegetation. Near nadir, however, there is little sensitivity to roughness.

Table 6 summarizes the requirements for a passive microwave sensor to provide these measurements of soil moisture, and other sensors which will help with the retrieval of soil moisture from the microwave data are discussed in the following section.

Correlative Measurements for Microwave Measurement of Soil Moisture

Visible and near-infrared data, as would be provided by MODIS (Moderate-Resolution Imaging

Table 4. Soil Moisture Information and Data Requirements at Different Crop Production Stages

Crop Production Stage	Accuracy Level*	Frequency (Days)	Resolution (km^2)	Depth
Planning (acreage and yield predictions)	3-5	7-20	1-15	Profile
Ground preparation and planting	1-3	5	0.5-1	Surface layer
Germination	3	5	1-10	Surface layer
Growth and Development				
Nutrient supply	3	7-10	1-10	Profile
Water management				
Irrigation	5	3	0.5	Profile
Drainage	3	3-5	1-10	Profile
Pest management	5	3	0.5	Surface layer
Maturing-yield estimate	3-5	3-10	0.5-1	Profile
Harvest	3	3-7	0.5	Surface layer

*General accuracy of high, medium, or low = 1; gradation between accuracy level 1 and 5 = 2-4; and ±4% accuracy by volume measurement = 5.

Table 5. Needs of Soil Moisture and Data Requirements in Hydrology

Soil Moisture Applications and Identified Users	Accuracy Level*	Frequency (Days)	Resolution (km^2)
Runoff Potential:			
Federal Users: NOAA-NWS, USACE, SCS design engineers, WPRS, HUD Flood Insurance Program	1**	3-7	5-25
State Users: Highway Departments and Water Resources Centers			
County and City Governments			
Private Power Companies			
Erosion Losses:			
Federal Users: Design Departments of USACE, USDI, and USDA-SCS	3	3	5-25
County Organizations of Governments	5	3	0.5
Farmers' Organizations	3	3	1
Reservoir Management:			
Federal Users: USACE, WPRS	1	3-7	5-25
State and Local Users: Water Resources Centers	3	3-7	0.5
Private power companies, regional planners, recreation industries	3	3-7	0.5
Infiltration for Trafficability and Structure Design:			
Federal Users: USACE, USDA-SCS	5	3	0.5
State Users: Drainage Districts, Planners	5	3	0.5
Private irrigation design engineers, mining engineers, developers	5	3	0.1
Water Quality:			
Pesticide and Nutrient Losses:			
Federal Users: EPA, FDA, USDA-SCS	5	3	0.1
State Users: Water Resources Centers	3-5	3	0.1-0.5
Private irrigators, farm organizations, feed lot operators, hydrologic engineers, planners and developers	1-3	3-7	5

*General accuracy of high, medium, or low = 1; gradation between level 1 and 5 = 2-4; ±2% accuracy by volume measurement = 5.
**Data refer only to the users on the respective line in the table

Table 6. Summary of Measurement Requirements (Soil Moisture)

	Ideal	Adequate
Frequency	1.4, 6 GHz	1.4 GHz
Spatial resolution	10 km	25 km
Radiometric accuracy	1.5 K	1.5 K
Radiometric sensitivity	1.0 K	1.0 K
Revisit time	1-3 days	3 days

Spectrometer) or HIRIS (High-Resolution Imaging Spectrometer), can also be used to indicate the presence of vegetation, and may be easier to implement than an off-nadir, conical-scanning radiometer system that would be required for microwave polarization measurements. Thus, a single-polarization, crosstrack scanning radiometer (scan angle <30°) is considered more appropriate at this time.

In addition to providing a vegetation "index" measurement, thermal infrared sensors can provide a skin temperature measurement that may be used to determine a more accurate emissivity from the microwave brightness temperature. The MODIS instrument on Eos could provide the appropriate infrared measurements. It is necessary to have an infrared sensor on the same space platform to obtain coincidence of spatial and temporal sampling with the microwave data.

Additional knowledge of soil type and land usage would be useful in determining soil moisture more accurately. Fortunately, these characteristics are often well known from soil surveys and land classification maps, or can be derived from a time-history of indirect measurements since the characteristics do not change rapidly with time.

Evapotranspiration

Evapotranspiration is the combined loss of water through the process of evaporation and transpiration. Evaporation occurs from water surfaces and bare soil while transpiration occurs from the canopy cover.

The crucial role of evapotranspiration at regional or global hydrologic scales is only recently understood. Climatic simulations with global models now demonstrate that precipitation is sensitive to regional evapotranspiration magnitudes (e.g., Charney, 1977). Moreover, evapotranspiration rates vary interannually because of differing air mass characteristics, and are subject to human modification through vegetation change.

Van Bavel and Hillel (1976) described how the rate of evaporation from soil depends on the soil moisture content. During the first stage when the surface is wet, the rate is limited only by the availability of energy at the surface. As the surface dries, the rate decreases and is controlled by the transfer of water to the surface. The length of time between energy-limited and moisture-limited evaporation depends on the surface soil moisture and the energy available to the surface. Therefore, the rate of evaporation from the soil depends on the soil moisture content.

Transpiration from a canopy depends on the soil moisture available in the volume of soil occupied by active roots, the type of canopy, and the energy input to the system. Transpiration itself is not directly measurable by remote sensing. However, transpiration may be estimated using conventional techniques such as the combination equation (Monteith, 1965) or by energy balance techniques which use remotely-sensed data as input. *In situ* measurements are available of open water evaporation from evaporation pans, but few data of actual evaporation or transpiration are taken except for experimental purposes or for very long time periods to establish water balances. Conventional methods and most remotely-sensed methods make use of the energy balance information about the soil surface (Shuttleworth, 1983).

A possible measurement scheme might proceed as follows. The equation for evapotranspiration from a vegetated or bare surface is

$$\text{L.E.} = \frac{\frac{pc_p}{\gamma}\left[e^*_s(T_s) - e_a\right]}{r_a(u) + r_s(\theta, R_s)} \quad \text{for vegetation}$$

$$= \frac{\frac{pc_p}{\gamma}\left[h(\theta)\, e^*_s(T_s) - e_a\right]}{r_a(u) + r_{soil}(\theta)} \quad \text{for bare soil}$$

where θ is soil moisture, L is the latent heat of vaporization, and E is moisture flux; R_s is the incoming shortwave radiation; T_s is the surface temperature, e^*_s is the saturated vapor pressure at

the surface and e_a is the vapor pressure at some level in the atmospheric boundary layer; r_a is the aerodynamic resistance, which depends on wind speed u, and r_s the stomatal resistance, which depends on soil moisture content; r_{soil} is the moisture-dependent surface resistance, h is the surface relative humidity, p is the air density, c_p the sensible heat of air, and γ the psychrometric constant.

Of these variables, soil moisture θ and surface temperature T_s are directly measurable by remote sensing using 1.4 GHz microwave and the 3.5 to 4.0 μm, 8 to 9 μm, or 10 to 12 μm thermal infrared data. Visible and near-infrared reflectance measurements may be used to estimate vegetation type, and photosynthesis rate, from which the stomatal resistance r_s can be estimated.

There are still some undetermined values. Incoming solar radiation R_s can be estimated from Geostationary Operational Environment Satellite (GOES) data by statistical methods (Tarpley, 1979) or can be measured at surface field stations. Wind speed u, aerodynamic resistance r_a, and humidity e_a are also needed at the surface. They can be estimated (for example, r_a can be roughly estimated from land cover classification, and climatological or approximate values for u and e_a can be used to set bounds) and data from planned Eos sensors such as MODIS and LASA (Lidar Atmospheric Sounder and Altimeter) plus *in situ* measurements can be used to improve the estimates.

It is also possible to estimate the evaporation using a mass balance approach by estimating the lower boundary flux from the top soil layer and observing the changes of soil moisture content in the surface layer over time. Remaining variations are assumed to be due to evaporation and transpiration. Recent work by Arya *et al.* (1983) and Prevot *et al.* (1984) reported results using this method.

From the HMMR point of view, the root zone soil moisture and evapotranspiration parameters should be treated together, because the microwave observable surface soil moisture is not sufficient to satisfy all requirements and because the depth of the root zone is larger than the sampling depth of the signal. Evapotranspiration is the major depletion mechanism for the root zone soil moisture reservoir. Thus, determination of one leads to the estimation of the other. Estimation of the evapotranspiration magnitude can be done by using either energy balance or mass balance approaches.

Precipitation

Rainfall is important because it is the primary input into the hydrologic cycle and its role in the dynamics of the Earth's atmosphere is enormous. However, it is difficult to monitor satisfactorily by conventional (*in situ*) means because of its highly variable space and time distributions and because of the practical and economic problems of maintaining rain-gauge and surface radar networks over many types of surfaces, including oceans, areas of high relief, high latitutes, deserts, etc. Consequently, rainfall data are inadequate for hydrologic science and operations, weather forecasting, and climate studies over most of the globe (Atlas and Thiele, 1981). They are inadequate particularly for near real-time operations, which need a speedy and regular flow of data, and for research, especially when sets of relatively dense and homogeneous observations are necessary. Spaceborne remote sensing can help resolve these problems and figures to be a major component of any global-scale precipitation monitoring system.

Already satellite remote sensing has begun to play an important part in the parameterization of the rainfall input into the hydrologic cycle (Atlas and Thiele, 1981; Barrett and Martin, 1981). Many different techniques have been developed and tested for such purposes. These include:

- Visible and infrared techniques, which derive rainfall estimates from satellite imagery through models which relate the indirect evidence of rainfall derived from cloud analyses to either ground calibration data, and/or to physical expectations based on cycles of cloud growth and dissipation.
- Microwave techniques, which have yielded rainfall estimates from the physically more direct evidence of radiation emanating from the active rain areas themselves, embedded within the clouds.

Visible and Infrared Measurement of Precipitation

Of the visible and infrared techniques, *life-history methods* (based on geostationary satellite data) have given useful results over both land and sea surfaces in the tropics where convective activity is dominant. Elsewhere, *cloud indexing* techniques have been necessary to provide rainfall estimates from areas not covered with geostationary imagery, or which are dominated by stratiform (frontal) rain-cloud systems. Few such studies have been carried out over oceans, due partly to the greater problems of calibration and verification, but more fundamentally to the low scientific priority attached to such activities until recently. Unfortunately, visible/infrared techniques do not cope well with the finer details of the meso- and local-scale instantaneous rainfall distributions prevalent within the tropics, and which are so significant for the initialization of weather forecasting models, for air-sea and tropical-extratropical interactions, and for a variety of applications in overland hydrology. Neither do visible/infrared techniques function adequately even for present scientific and operational applications outside the tropics, primarily because of the difficulties of defining rain/no rain boundaries, assessing low-intensity rainfall, and evaluating very high-intensity rain events when the

cloud system is stratiform or mixed stratiform and cumuliform.

Passive Microwave Measurement of Precipitation

Microwave techniques hold great promise for improved satellite observations of precipitation because microwave observations are little affected by clouds and are directly related to the hydrometeors themselves. Passive microwave measurements of rain fall into two regimes, *emission/absorption* and *scattering*. In the former regime one observes rainfall through the emission of thermal energy (e.g., Wilheit *et al.*, 1982). A cold background is required in order to make such observations, so it is only practical when viewing over the oceans, which are highly reflective at microwave frequencies. The liquid raindrops themselves are the dominant contributors to this absorption and emission, providing a direct physical relationship between the rainfall and the observed microwave radiances. In the scattering regime, the rainfall is observed via the scattering within the rain column, which reflects the cold cosmic background towards the satellite (e.g., Spencer *et al.*, 1983). This process allows the observation of rainfall over any background, but since the scattering is primarily from the frozen hydrometeors aloft rather than from the raindrops, the relationship to rain rate is less direct than in the emission/absorption regime. Generally, at frequencies below the 22 GHz water vapor line, emission/absorption is the dominant process, and at frequencies above the 60 GHz oxygen complex, scattering dominates. Between 22 and 60 GHz either can be dominant according to the specific situation.

Figure 8 depicts a model used in relating observed brightness temperature (radiances) to rain rates and will be used here to illustrate some of the issues involved in extracting rainfall from microwave brightness temperature. We assume a layer of rain drops described by a Marshall-Palmer (1948) drop size distribution from the surface to the freezing level (0 degree isotherm). The surface may be either land or ocean. The atmospheric lapse rate is assumed to be 6.5 deg/km and we assume 80 percent relative humidity at the surface that increases linearly to 100 percent at the freezing level and above, so that the atmospheric water vapor and the surface temperature are tied to the freezing level parameter in the calculation. Above the freezing level a variable thickness of frozen hydrometeors is assumed. We use the same Marshall-Palmer distribution for the ice spheres as for the rain layer, but a better description of the ice layer remains an open research issue. This model is thus left with three free parameters: freezing level (rain layer thickness), ice layer thickness, and the rain rate which is determined by parameters of the Marshall-Palmer distribution.

At frequencies below 22 GHz, the details of the ice layer are not important, because the absorption-dominated signal is not affected by the presence of some of the less absorptive ice. However, at higher microwave frequencies (above 30 GHz), ice is far less absorptive than water, and the scattering-dominated signal is sensitive to the thickness of the ice layer. The importance of including an ice layer is illustrated by observations such as those taken with the 92 GHz channel of the AMMS (Advanced Microwave Moisture Sounder) on the NASA RB-57 aircraft over severe thunderstorms near Tampa, Florida, in 1979 (Wilheit, 1986). Brightness temperatures as low as 150 K were observed there and are also commonly observed in cumuliform precipitation. Observations

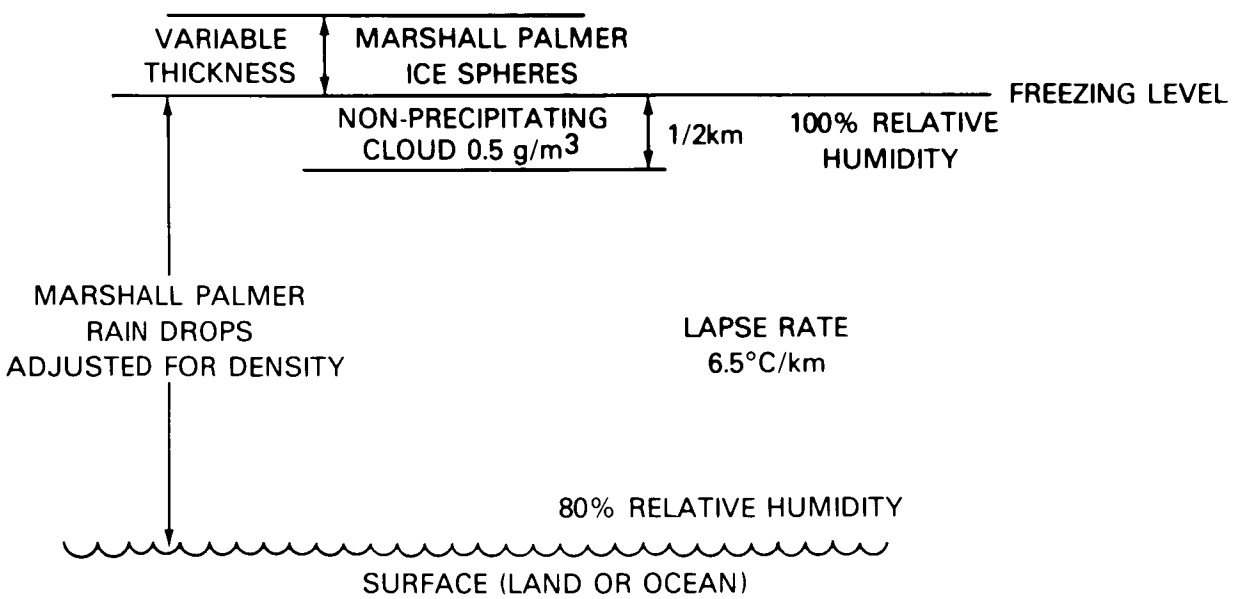

Figure 8. The model used to relate observed values of brightness temperature to rain rate in an emission/absorption model.

of this sort cannot be explained without including an ice layer in the model.

This is illustrated in Figure 9, which shows the effects of the ice layer on the model calculation of brightness temperature for a hypothetical sensor at 92 GHz (Wilheit *et al*, 1982). The brightness temperatures are expressed as a function of rain rate at the bottom and as a function of sphere diameter (and density) at the top of the graph. (The same Marshall-Palmer distribution has been used for the rain drops and the ice spheres.) First of all, notice that without the ice layer, the model does not predict brightness temperatures less than 250 K. However, with ice layers as thin as 0.5 km it is possible to get much lower brightness temperatures. Low brightness temperatures are obtained for particles with diameters of only a few hundred microns and densities of a few tenths of a gram per cubic meter. Ice particles of this size are generally associated with the rain drop formation process. These particles will precipitate through the freezing level, melt, and hit the surface as rain. However, the ice particles associated with cirrus clouds are much too small to cause any great effect. Thus the extremely low brightness temperatures observed in convective rainfall are probably caused by frozen hydrometeors.

Although the observations of this scattering effect have been confined to 92 and 183 GHz, the phenomenon is present in some measure at lower frequencies; and Spencer *et al.* (1983) have exploited this fact to develop an empirical rain-rate algorithm for use over land using Scanning Multichannel Microwave Radiometer (SMMR) data from the Nimbus-7 satellite. The performance of the algorithm is quite reasonable. When compared with radar data obtained by digitizing the film records from WSR-57 radars and averaging over 20 km squares, they found that the algorithm would explain 62 percent of the variance. The rain information is obtained primarily from the SMMR data in the 37 GHz vertically polarized channel and many of the remaining channels are used for corrections.

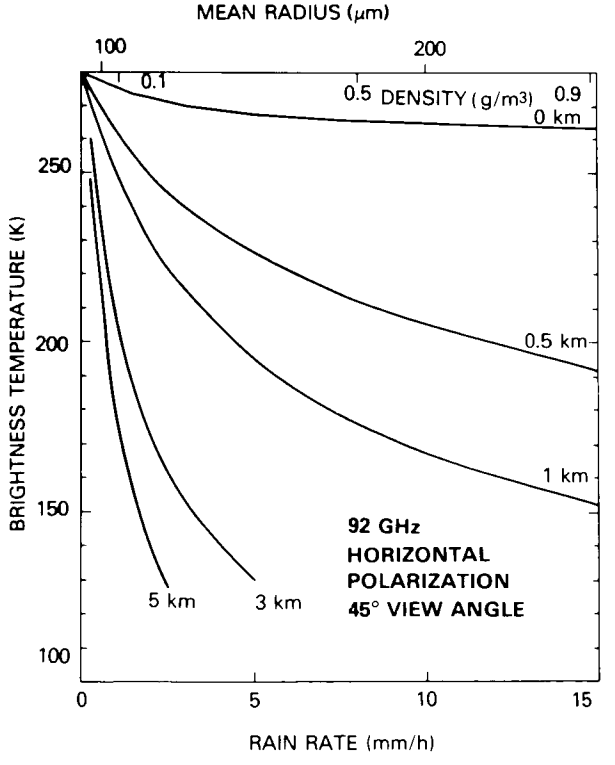

Figure 9. Brightness temperature calculations at 92 GHz for various thicknesses of the ice layer.

Although the relationship between brightness temperature and rain rate is generally well understood (Atlas and Thiele, 1981; Wilheit *et al.*, 1977), there are details of the models employed which need to be considered. The rain layer thickness is the foremost of these. The assumption of a liquid rain layer extending from the surface is clearly inadequate in warm rain situations, where the drops form without an ice phase. This is especially important because the global importance of warm rain is not now known. Rao *et al.* (1976) questioned this rain layer thickness assumption in high latitude winter situations. They found that using the climatological freezing level resulted in absurdly large calculated rain rates and corrected the model by never assuming a freezing level below 3 km regardless of season or location. Since wintertime rain is more likely to be associated with warmer atmospheres than the seasonal average, one might also question the use of the climatological freezing level for rain situations.

The effect of water vapor on the brightness temperature is another source of error in the determination of rain intensity. The water vapor is determined from the freezing level in the model but this introduces error. One solution would be to have a channel near the water vapor line (e.g., 21 GHz) in the sensor system and correct for the water vapor contribution to the brightness temperature.

Current models also include a non-precipitating cloud of arbitrary density. These small (<50 μm diameter) droplets absorb in direct proportion to their mass but generally much less than a corresponding mass distributed in precipitation-sized (>50 μm) particles. Therefore, the cloud contributes only a few degrees to the brightness temperature in the model calculations, but if the assumption is grossly wrong this could be a larger source of error. Multifrequency observations possibly could alleviate this problem, and additional experiments are needed to obtain estimates of the severity of the problem.

The modeling in the scattering dominated mode is not nearly so well advanced. The ice is modeled as an ensemble of spheres, but the shapes of the ice particles actually found in a rainstorm are much more varied. It is generally assumed that for particles that are very small compared to the wavelength of the observation, the scattering is well approximated by

an "equivalent" sphere, but the actual electromagnetic solution is intractable for all but a very few shapes. Moreover, the distribution of ice particles for a given rain rate, which is assumed in the model described above to be the same Marshall-Palmer distribution as for the rain drops, is in fact really completely unknown and may not even be uniquely related to the rainfall at all.

Finally, there are some additional problems peculiar to measuring rainfall which are the result of the high spatial and temporal variability of rain. In particular, the large spatial variability of rain causes an error peculiar to microwave techniques because high spatial resolution is difficult to achieve in microwave sensors due to the antenna aperture required. The transfer function between rain rate and brightness temperature is highly nonlinear. Because of this nonlinearity, if there is any inhomogeneity in the field-of-view, direct application of the transfer function will result in an underestimate of the rain rate. This results in a significant bias in the measurements when a great many observations are averaged. Estimates varied as to how much of a problem this was in 25 km ESMR data; there were no extensive studies to estimate and correct for this bias. Nevertheless, the Rao *et al.* (1976) atlas and the Adler and Rodgers (1977) tropical storm study produced quantitatively reasonable results with no correction for partial filling of the antenna beam with rain. One would conclude that at the 25 km resolution of ESMR the so-called "beam filling" problem is serious but not crippling. The SMMR and SSM/I resolutions (60 km at 19 GHz) are a different matter; there have been no studies but the problem would be expected to be extremely serious and to require careful study and correction. To alleviate this problem, and reduce it to manageable proportions, the resolution should be of the order of the correlation length of rain (10 km or less).

Another problem is that rain rate is the parameter being estimated, whereas the desired quantity is generally an integrated rainfall over some period of time. Any remote rainfall measurement scheme will, therefore, depend on sampling of the rain with its associated uncertainties. Statistically, the solution can be shown to be reasonable for many applications with a properly designed measurement strategy (e.g., Appendix B).

A final problem is that in some circumstances there is a large diurnal cycle in rainfall. This causes a large potential error in any sun-synchronous measurement approach.

Measurement Requirements

To summarize, microwave radiation responds directly to hydrometeors and remote sensing with microwaves offers the potential for significantly improving our knowledge of the global distribution of rainfall. To be practical, such a system should have the following characteristics:

- *Frequency*—Several frequencies, including 18, 21, 37, and 90 GHz with dual polarization to sort out the ice layer thickness problems
- *Spatial Resolution*—Sufficiently high to detect even the smaller meso- to local-scale rain cell structures (10 to 20 km range)
- *Temporal Resolution*—Enough temporal resolution for the dynamics and distribution of these smaller scale rainfall events to be studied

A specific list of the requirements for a passive microwave remote sensor for measuring precipitation is given in Table 7.

Obtaining adequate temporal resolution (i.e., the amount of time between measurements) presents a problem from low Earth orbit. However, statistical studies suggest that even revisit times of up to 3 days can provide accurate estimates of the mean monthly rainfall once a large data base is obtained (see Appendix B). A more severe problem is the bias introduced in sun-synchronous or polar orbits. A knowledge of the diurnal variability of rain is needed to determine the magnitude of and to correct for such biases.

Active microwave sensors (radar) also have the potential for providing accurate measurements of rain from space, and probably a combination of active and passive sensors would be ideal for this

Table 7. Summary of Measurement Requirements (Precipitation)

	Ideal	Adequate
Frequency	18, 21, 37, 90 GHz	18, 21, 37, 90 GHz
Spatial resolution	1 km	10 km
Radiometric accuracy	2.0 K	2.0 K
Radiometric sensitivity	2.0 K	2.0 K
Sampling interval	1 day	3 days

measurement problem (Atlas *et al.*, 1982). Just having a radar to determine the height of the precipitation column would significantly improve the passive measurement.

Snow Properties

Snow has two major roles in the hydrologic cycle: (1) snowmelt is the principal source of water for runoff and soil moisture recharge at high latitudes and at high altitudes; and (2) snow cover influences the global climate, and even small areas in the mid-latitude mountains may be sensitive indicators of climate change. Both the mass and energy balance equations are influenced by snow. It represents a large component in the water (mass) balance equation because it is the largest single source of fresh water on the Earth. Its difference in albedo from other materials and its lower thermal conductivity and lower temperature make it important to the energy balance as well.

Most of the water supply in the western U.S. has its source in snowmelt, as is also the case for major areas of Europe, Asia, South America, and Australia. The variation in the amount of snowfall and the rate of snowmelt affect development and scheduling of hydroelectric power generation facilities, management of irrigation, crop planting selection and strategy, management of agricultural commodities, and protection from floods.

The snow cover extent affects the Earth's radiation balance, because snow typically has high albedo (>0.8) whereas soil, vegetation, and water typically have low albedo (<0.2). The presence or absence of snow alters the energy balance and surface temperature, thereby affecting atmospheric circulation, global water supply, and food production. The interannual variability of the areal extent of snow in the northern hemisphere is greater than that of any other land cover. Because of the propensity of snow to be moved by wind after it falls, and because fall velocities of snow are lower than for rain, the spatial variation in the depth and water equivalent of snowfall is greater than for rainfall, especially in mountainous regions. Moreover, the rate of melt varies. The acid precipitation problem is magnified in the snow cover. Soluble impurities are leached by the first meltwater, and as a result the ionic concentration in the first melt can be much higher than in the snowpack as a whole (Colbeck, 1981).

In observations of snow cover, two parameters are widely used in forecasting schemes: snow water equivalent (the depth of water produced if the snow were to melt) and snow-covered area. In addition, three other parameters are important for climate studies and could be used in more sophisticated runoff forecasting methods that are likely in the future: snow wetness, albedo, and temperature.

Current methods for forecasting snowmelt runoff in the U.S. use snow water equivalence measurements made manually at selected snow courses, supplemented by satellite estimates of snow-covered area from Landsat, the NOAA polar-orbiting meteorological satellites, and GOES. For global climate studies, snow cover and albedo data from the NOAA and DMSP satellites are used.

The spatial scale at which snow data are needed is similar to that of soil moisture *in similar topography*. In the U.S., however, there is no pressing need to measure soil moisture in rugged terrain, but much of the snow resource exists in mountainous areas. In the plains, a spatial resolution of 10 km is adequate, but in mountainous areas 1 km probably is necessary. The way in which topographic variation within a resolution element influences the signal is unknown.

Visible and Infrared Measurements of Snow

Snow-covered area can be mapped in the visible wavelengths at spatial resolutions from 30 m to 4 km and temporal resolutions from daily to monthly. It can be monitored from Landsat, NOAA meteorological satellites, DMSP, or GOES because snow has a higher albedo than other land covers. Only clouds are as bright as snow, but snow and clouds can be discriminated in the 1.55 to 1.75 μm wavelength bands on the Landsat Thematic Mapper and the DMSP satellites (Valovcin, 1976; Crane and Anderson, 1984; Dozier, 1984). In addition, this band is to be added to the NOAA polar-orbiting meteorological satellites. The near-infrared bands of Landsat and the NOAA meteorological satellites can distinguish new snow from that which has been melted (Dozier *et al.*, 1981).

Snow water equivalence cannot be measured at visible or infrared wavelengths, unless the depth is shallow. In visible wavelengths, springtime snow becomes effectively semi-infinite at about 50 cm depth (Warren, 1982). McGinnis *et al.* (1975) have correlated NOAA meteorological satellite measurements with snow depth from a few storms in the southeastern U.S., and Dozier *et al.* (1981) have used the NOAA satellite to estimate snow water equivalence over lakes in the Canadian Arctic.

Snow water equivalence has been estimated from Landsat data by residual methods, whereby satellite images from successive overpasses are compared to runoff data (Rango and Martinec, 1979).

Snow albedo can be estimated from visible and near-infrared data. Visible wavelength measurements can reveal the extent to which snow albedo is reduced by contamination, and near-infrared reflectance is sensitive to grain size (Warren and Wiscombe, 1980; Wiscombe and Warren, 1980; Dozier, 1984).

Microwave Remote Sensing of Snow Properties

There are two major shortcomings in our present use of satellite visible and infrared data to investigate the Earth's snow cover: (1) our measurements of snow water equivalence, the most crucial variable in

snow hydrology, are often faulty because, in part, depth cannot be measured from satellite in the visible or infrared; and (2) because rapid snowmelt can sometimes occur in cloudy weather, it is important to be able to measure snow-covered area in all weather.

Microwave measurements from satellite could help to remedy both problems, as well as provide information on snow wetness. Albedo and surface temperatures can be obtained with measurements in the visible and infrared and probably will be adequate even if knowledge is restricted to clear conditions.

Foster *et al.* (1984) summarize the capability of microwave remote sensing of snow properties. Snow cover extent is the easiest parameter to measure from orbit. Microwave data allow snow cover extent to be monitored through clouds. Because dry snow has such low emissivity at microwave frequencies, snow boundaries can usually be delineated at 18 GHz or 37 GHz. However, the microwave signature of melting snow may resemble that of bare ground, and concurrent measurements of snow extent from satellite visible data may be helpful to resolve the boundary in such cases. Alternatively, the snow boundary can be observed at night after the snow has refrozen.

Measurement of snow water equivalence from microwave emission is in its infancy, but development of a successful method would be a significant achievement in hydrology. For snow of a given grain size, microwave emission decreases as the water equivalence increases, but an increase in grain size also causes emission to decrease (see Figure 10). Moreover, the influence of grain shape and snowpack stratigraphy are unknown. When snow is wet, emission increases substantially, as does the optical depth of the snowpack. For dry snow, however, a method can probably be developed using a multifrequency, dual polarized sensor. The higher frequencies (18 and 37 GHz) would be useful for shallower snow, while 5 to 10 GHz would be useful for deeper snow. Multiple frequencies are necessary to cover the range of snow water equivalences expected. Increases in microwave emission with the presence of liquid water in the snowpack are especially noticeable at 18 and 37 GHz.

Continuing research can be expected to improve the information which can be extracted from microwave remote sensing of snow. Among the more important research issues are: (1) The dielectric constant of ice is not well measured at many of the frequencies useful for remote sensing. For example, there are no reliable measurements between 24 and 240 GHz and different sets of apparently reliable measurements between 2.7 and 24 GHz are in conflict (Warren, 1984); (2) Microwave emission from snow depends on other attributes beside depth and water equivalence. These apparently include grain size and shape, stratigraphy, and density. We know that depth and microwave emission are inversely related, but we do not know enough to model emission given specification of snowpack properties; (3) The microwave signal can tell us when snow is wet, but our understanding is not enough to allow a quantitative estimate of wetness (i.e., the free water content of the snow). The wetness fraction influences the microwave signal, but in some frequency ranges the shape of the liquid water inclusions is also important. We have very little idea of typical distributions of these shapes.

Table 8 summarizes our current knowledge about the snow properties which can be measured by remote

Table 8. Summary of Snow Parameters and Measurements

Parameters	Instrumentation	Technological Development State
Snow cover extent	Microwave at 18 or 37 GHz	Demonstrated feasibility
Snow water equivalent	Microwave at 1.4, 6, 10, 18, and 37 GHz dual polarization	Demonstrated feasibility to obtain relative values for shallow, dry snow; research needed for deeper snowpacks and to assess influence of snow properties
Snow wetness	18 or 37 GHz	Feasible up to ~5% water content
Albedo	Optical 0.6, 0.9, and 1.6 μm	Demonstrated feasibility
Temperature	3.7 and 11 μm	Demonstrated feasibility

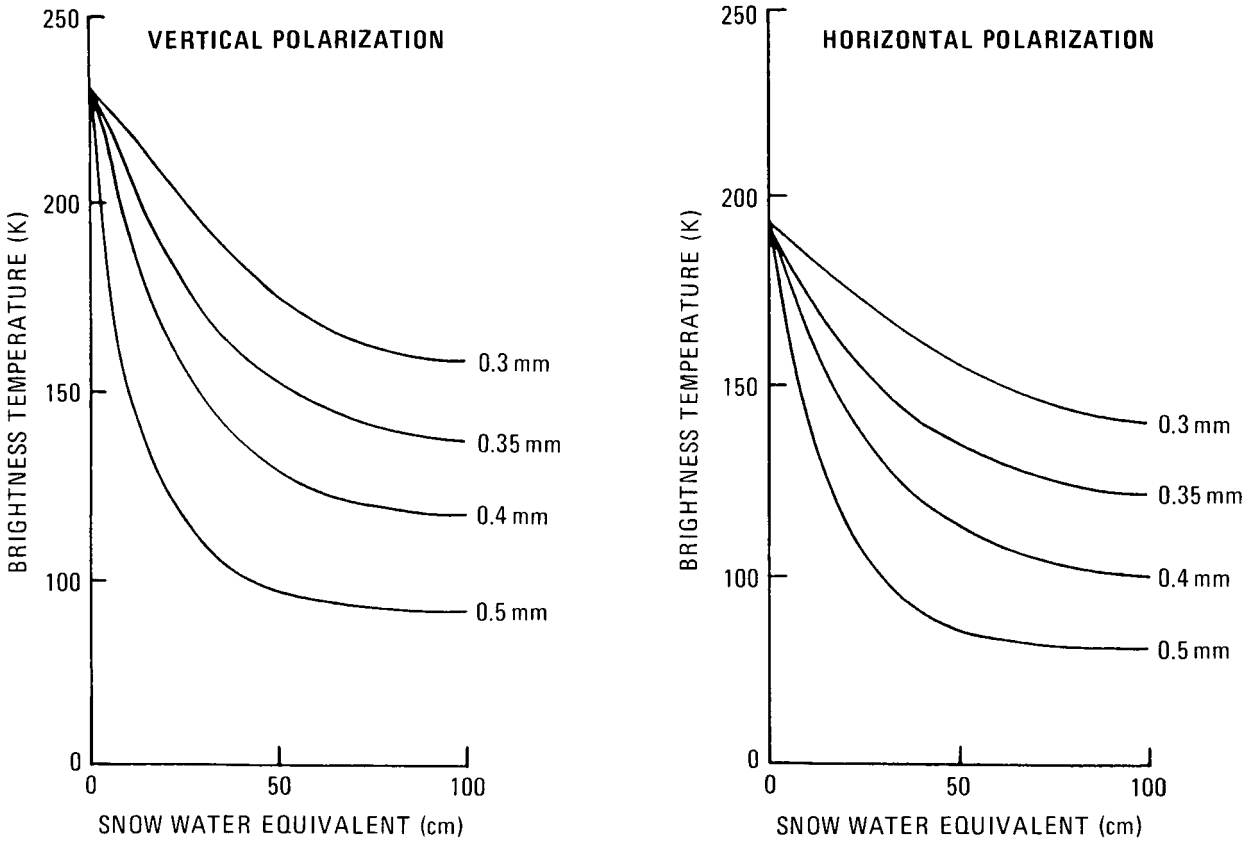

Figure 10. Calculated 37 GHz brightness temperature versus snow water equivalent for dry snow over unfrozen soil (incidence angle = 50°) using a microscopic scattering model at various mean snow grain sizes.

sensing, and Table 9 summarizes the requirements which a passive microwave system should meet to provide this information.

Runoff

This parameter is very difficult to estimate directly using remotely-sensed data, and is usually measured by conventional river gauging. However, the mass balance equation can be used to give estimates of runoff using rainfall-runoff models. Changes in precipitation, evaporation, and soil moisture status can be input into runoff estimation models to augment existing stream gauge data. Soil moisture status is a requirement here for physically-based modeling, because the infiltration rate into soil and the soil hydraulic properties are closely related to soil moisture status. Blanchard and O'Neill (1983), using a time series of microwave data immediately after a saturating rain-storm, were able to estimate saturated hydraulic conductivity and thus differentiate the properties of sand and clay in soil. This relationship between sand, clay, and hydraulic conductivity has recently been explored in detail using conventional data by Cosby *et al.* (1984).

Table 9. Summary of Measurement Requirements (Snow)

	Ideal	Adequate
Frequency	1.4, 6, 10, 18, 37, 91 GHz	10, 18, 37, 91 GHz
Spatial resolution	1 km	10 km
Radiometric accuracy	2.0 K	2.0 K
Radiometric sensitivity	2.0 K	2.0 K
Revisit time	0.5 days	3 days

III. SCIENCE OBJECTIVES: OCEAN

PHYSICAL OCEANOGRAPHY

Background

Because of the high heat capacity and circulation of the oceans, it has often been stated that the oceans are the flywheel of the heat engine which determines the weather and climate of the Earth. In any case, the role of the oceans in determining the weather and climate of the Earth is an important one, and we are only beginning to understand the dynamic processes that participate. The decisions to initiate the Tropical Ocean and Global Atmosphere (TOGA) research program and the World Ocean Circulation Experiment (WOCE) reflect the central role of the oceans in global change. The results of the observations and research on the recent Southern Oscillation-El Niño Event (ENSO) clearly show the importance of atmosphere-ocean couplings. They also have shown the great potential of remote sensing as a tool of inquiry in climatological and oceanographic research.

Passive microwave measurements with the Electronically Scanned Microwave Radiometer (ESMR) on Nimbus-5 and the Scanning Multifrequency Microwave Radiometer (SMMR) on Nimbus-7 and Seasat, showed the importance of microwave measurements of sea surface radiance, from which one can infer sea surface temperature, surface wind speed, and other variables.

These data also demonstrated the need for resolution substantially better than obtained with the SMMR. The retrieval of sea surface temperature from microwave radiance measurements is severely affected by the presence of land in the radiometer antenna beam. Land surfaces are much warmer (have a much larger brightness temperature) than the ocean surface near 6 GHz where measurements of sea surface temperature are made. In the case of the SMMR, radiation from land strong enough to corrupt the measurement was picked up through antenna sidelobes when the sensor (footprint) was within several hundred kilometers of land surface. As a result, large areas of the oceans of great climatological and dynamic importance could not be covered. Regions affected included the important western boundary current and most upwelling areas and wind driven coastal currents as well. A microwave radiometer with a finer spatial resolution and better antenna design would represent a significant improvement in sea surface temperature determination from space. The data would be useful in the TOGA and the WOCE experiments, as well as for general oceanographic research applications.

A microwave radiometer is also capable of providing the measurements needed to estimate heat fluxes from the ocean (e.g. Liu, 1985). Locally, the heat flux changes atmospheric and oceanic density stratification and modifies winds and currents. On a large scale, differential heating drives atmospheric circulation which in turn drives ocean currents and redistributes the heat. The radiances observed by a microwave radiometer can be used to derive coincident estimates of surface wind speed, sea surface temperature, atmospheric water vapor, and (potentially) rain rate. These are the parameters needed to deduce the latent heat flux due to evaporation from the ocean, the largest time varying component of the ocean-atmosphere heat exchange on seasonal and interannual time scales.

Specifically, diabatic heating of the atmosphere is mainly due to the release of latent heat when water vapor condenses. Therefore, the atmospheric heat budget can be approximated by the atmospheric water budget:

$$\partial w/\partial t = \vec{U} \cdot \nabla w + E - P$$

where the terms (from left to right) are the time rate of change of columnar water vapor (w), the advection of water vapor ($\vec{U} \cdot \nabla w$), and the evaporation (E) and precipitation (P) rates. Multiplying each term with the latent heat of vaporization (L) will result in the atmospheric heat balance equation. A microwave radiometer can measure $\partial w/\partial t$, ∇w, and P, and E can be deduced from measurable quantities such as temperature and humidity at the surface. So with an estimate of the effective wind vector $\vec{U}$, the global atmospheric heat balance can be studied. On the other hand, if either $\vec{U}$ or P is measured, the other parameter will be determined as the residual in the water budget equation. The former provides information on circulation pattern and the latter on diabatic heating of the atmosphere.

The heat budget of the upper ocean can be approximated by:

$$\partial T/\partial t + \vec{V} \cdot \nabla T + WT_c/R = (R - LE)/\rho ch$$

where ρ is the density of water, c is its heat capacity and h is the height of the mixed layer. After multiplying both sides by ρ, c, and h, the terms are (from left to right) the time rate of change of heat content, the horizontal advection of heat, the vertical advection of heat from below (W is the velocity of water flowing in from below and T_c is its temperature) and on the right hand side is the net flux of heat at the surface. In the latter, the sensible heat and longwave radiation component have been assumed to be small compared with the latent heat (LE) and shortwave radiation (R). A microwave radiometer can measure $\partial T/\partial t$ and ∇T directly and can provide measurements from which LE can be calculated. R can be computed from cloud parameters. The other terms have to be inferred from other measurements

such as measurements of surface wind stress which can be obtained with a microwave scatterometer.

From the preceding discussion, it is clear that a microwave radiometer can play a major role in furthering our understanding of the atmospheric and oceanic heat balance. In turn, one has to understand the heat budgets of the atmosphere and oceans in order to understand atmospheric and ocean circulation. Finally, from an understanding of the circulation, one can begin to understand climate variability.

In addition to providing the basic measurements needed to understand the heat budgets of the atmosphere-ocean system, microwave radiometers can yield data in cloud-covered as well as cloud-free regions. Measurements can be done under a wide range of atmospheric conditions, permitting data sets to be obtained with uniform sampling, uninterrupted by changes in local weather conditions. Furthermore, measurements can be obtained in adverse weather, an important factor, since many surface phenomena of interest are coupled with relatively adverse weather conditions. An example is the change in local climate that was apparently coupled with the recent El Niño off the west coast of South America.

Observational Requirements

In remote sensing, as in most other things, balance and compromise are essential: balancing what one would like against what is realistic. For example, in the case of ocean dynamics, surface winds and currents have certain natural scales which should be resolved by an ideal system. Thus, in mid-latitudes, synoptic storms have spatial scales of several thousand kilometers, and time scales of several days. An ideal sensor system would measure the surface wind with space/time resolutions of about one-tenth these scales, i.e., a few hundred kilometers and a few hours. However, the curl of the wind vector, as well as wind stress, is important for driving ocean circulation. The curl is concentrated in atmospheric frontal regions. Consequently, a few tens of kilometers spatial resolution may in fact be required.

Similar considerations apply for the determination of sea surface geostrophic currents. The dominant surface geostrophic currents are those of the major flows such as the Gulf Stream, Kuroshio, etc., and their associated meandering and eddying currents. A typical Gulf Stream eddy has a diameter of about 150 km, and tends to slowly drift westward at about 5 km/day, thus taking 30 days to move its own diameter. Invoking again the 10:1 rule of thumb for resolution, one would like to have a system with a resolution of 15 km and revisit every 3 days. In the case of sea surface temperature, the same scales apply, yielding a space/time resolution requirement of 15 km and 3 days. This resolution is quite similar to that set forth by the U.S. Navy. The Navy requirement is usually stated as 10 km desired, 25 km acceptable (Hollinger and Lo, 1984). The spatial resolution needed to derive a useful global sea surface temperature data set is probably near 10 km. The sharpest gradients in sea surface temperature fields can exceed 10 K/km; however, this is rare and a 10 km resolution should be satisfactory.

Gulf Stream shear waves can be as short as 50 km and have a period of 12 hours. Their amplitude is less than 10 km, and it is doubtful that they could be resolved with the preceding resolution. However, larger scale waves, with amplitudes of 10s of km and periods of 2 days or more, could be resolved with spatial resolution of 10 km and sampling of once per day. Phenomena of this type are the cyclogenesis processes that take place near Taiwan in the Kuroshio and near Cape Hatteras in the Gulf Stream. The reactions of major oceanic currents to air-sea interaction events involving cyclogenesis may therefore be accessible for research with data of this space/time resolution.

Another especially important phenomenon that can be observed at this space/time resolution is the motion of patterns of high winds, such as those created by polar low pressure systems in the atmosphere and by tropical storms at low latitudes. The extent, speed, and intensity of this atmospheric forcing of the ocean is important information for realistic modeling of air-sea interaction, and the feedback from the ocean on these atmospheric systems is also significant. A passive microwave instrument would serve as an important data source for assessment and research on such air-sea interaction processes. Early identification of polar lows and cyclones at mid- and low-latitudes would also be made more likely.

Summary of Measurement Requirements

The minimum usable spatial resolution of any remote sensing measurement is sometimes hard to define. In the case of SMMR, the resolution of the sea surface temperature measurement was approximately 150 km, yet impressive global temperature maps have appeared in the literature. On the other side of the coin, a logical question concerns the ideal scale of resolution needed for research. To this end, the Panel reviewed digitized infrared-derived images of sea surface temperature as the resolution was degraded in successive stages. When the resolution was better than 5 km, eddy patterns became distinct and consequently useful for modeling purposes. Such fine scale of resolution requires an antenna on the order of 12 m in diameter at 6 GHz. The engineering job is further compounded by the fact that brightness temperature must be measured to an accuracy of better than 0.5 K. Meeting both of these requirements is a challenging task, indeed. Clearly, the choice of requirements involves a choice between what is ideal, given as a limitation only our ability to use the scientific data, and what is adequate to provide new information of a fundamental nature but more in line with technological feasibility. With this in mind, the

requirements in physical oceanography for passive microwave sensor are listed in Table 10.

The measurement at 18 GHz in the "ideal" column has been included because of the sensitivity of this channel to surface wind speed.

SEA AND GLACIAL ICE

Scientific Background

The surface of the Earth at high latitudes is unique because it is generally covered with an extensive blanket of snow and ice. This highly reflective covering prevents the heat of the sun from warming the glaciated land and insulates the ocean by inhibiting the loss of thermal radiation to the atmosphere. Because of this property of the ice and snow blanket for moderating the energy exchange at the surface, changes in this cover can have an important effect on climate. For example, increases in the ice cover could raise the Earth's albedo causing less of the sun's energy to be absorbed by the Earth. At present, the ice sheets are but slowly changing, and although the areal extent of sea ice undergoes dramatic seasonal variations, on the average it is also approximately in equilibrium (Zwally *et al.*, 1983; Parkinson *et al.*, 1986). However, the climatic record as preserved in ocean sediments and in ice cores indicates that the present equilibrium is unstable and that the recent history of the Earth has been punctuated by major advances and retreats of the ice. Evidence from ice cores collected in Greenland and Antarctica suggest that the last glacial cycle, which lasted almost 100,000 years, ended abruptly about 15,000 years ago for reasons not yet explained. Because the complex interplay between ocean, atmosphere, and ice that triggered this change in climate is not understood, neither is the scenario that might lead to another readvance of the ice (Mosely-Thompson *et al.*, 1985).

The natural cycle of ice ages is now further complicated by man's activities. Burning of fossil fuels and deforestation of the land are contributing to a steady increase in atmospheric CO_2. Given that CO_2 can trap heat within the atmosphere, a global warming has been predicted that could seriously alter the present extent and configuration of the polar ice cover. Because the high surface albedo at the poles reduces the amount of radiative energy penetrating the surface, a climatic change causing a reduction in the ice cover can lead in turn to further warming as solar radiation heats the previously ice-covered land and ocean surfaces. Indeed, climate models indicate that such a warming will be significantly amplified in the polar regions. Eventually, sufficient warming can affect even the great ice sheets, causing them to shrink with an accompanying rise in sea level (Department of Energy, 1984). Therefore, a fundamental question confronting polar research programs is to determine whether the world's ice masses are growing or shrinking (Barry, 1983).

The importance in improving our understanding of the polar regions is relevant not only because of their impact on world climate, but also because of the increasing commercial and strategic significance of the Arctic. Operational activities to exploit the mineral wealth of the Arctic, to harvest fish from arctic seas, and to maintain a crucial military capability all encounter a common hazard-sea ice. The margin of the floating ice can shift tens of kilometers per day, impacting navigation, and similar motions of ice floes within the ice pack present a formidable threat to offshore structures. Moreover, because the ice margin is an area of nutrient-rich water upwelled from the deep ocean, an accurate knowledge of ice edge conditions is needed for a thorough understanding of the food chain in the Arctic. The fundamental observables needed to support these programs are the extent and concentration of the ice.

Given as the goal of a measuring system, establishing bench marks against which the effects of climatic change can be measured, enhancing our understanding of the influence of the polar oceans on global circulation, and also providing support of operational programs at high latitudes, then the parameters which this system needs to observe are the concentration and age of sea ice, the size and distribution of polynyas in the consolidated ice pack, motion of the

Table 10. Summary of Measurement Requirements (Oceans)

	Ideal	Adequate
Frequency	6, 10, 18 GHz	6, 10 GHz
Spatial resolution	1-5 km	10-25 km
Radiometric accuracy	1.0 K	1.0 K
Radiometric sensitivity	0.1 K	0.5 K
Revisit time	1 day	3 days

ice pack, surface temperature, and the accumulation and surface melting on the ice sheets. Because the geophysical processes that influence these parameters vary in spatial extent and duration, the scale and repeat cycle required at the observations similarly is variable. Furthermore, the observational requirements for the ice sheets and sea ice are quite different. Because of the slow growth rates of the ice sheets, careful measurements undertaken at intervals of years are adequate. On the other hand, observations every few days are needed to monitor sea ice. Also, the physical properties of sea ice, which is brine rich and highly conductive, are radically different from glacier ice, which is nearly free of impurities. For example, the conductivity of ice sheets is so small that microwaves penetrate several meters to permit observation of subsurface characteristics. On the other hand, the conductivity of recently frozen sea ice is so high (because salt is present) that electromagnetic waves only penetrate the first few millimeters of the surface. Also, salt leaches out of sea ice with elapsed time, so that old sea ice exhibits different properties than new sea ice.

Eventually, a compliment of visible, infrared, and microwave sensors will be needed to provide all the information required in the cryosphere; however, microwave sensors have proven to be the most useful instruments to date for collecting information from space over the Earth's poles. The reasons for this success are: (1) microwave instruments are little affected by the clouds and fog which frequently shroud the polar regions; (2) they are unaffected by the polar night which inhibits the use of optical instruments; and (3) the large difference between the microwave emissivity of water and ice makes discrimination between them relatively easy.

Observational Requirements

Remote Sensing of Ice Sheets

Ice sheets flow under the force of gravity, spreading and thinning in a manner dictated by the physical properties of ice, the bedrock topography, and the surface mass balance rate. Of these parameters, perhaps the surface balance is the least well-known quantity over the large ice sheets. In the Antarctic, uncertainty in the total annual snow accumulation has thwarted attempts to compute convincingly the total mass budget of either the East or West Antarctic ice sheets. In Greenland, calculations are further complicated because melting at low elevations on the ice sheet is probably the principal form of ablation and to date there are no reliable means for measuring the melt rate on the ice sheet.

Microwave observations have the potential for greatly refining our estimates of the surface balance. The microwave emissivity of a snow surface is sensitive to the grain size and its distribution with depth, which is determined mainly by snow accumulation rates and snow temperature. Preliminary ice-sheet accumulation maps have been derived based on an empirical relationship between observed emissivity and the few measured accumulation rates, but additional research is needed to refine this relationship and to take fuller account of snow surface temperatures. (It has been suggested that brightness temperatures collected at a few GHz, frequencies which are relatively insensitive to scattering in the snow, could be used to determine average temperature in the upper 10 m of the ice sheet.) In regions where extensive accumulation rate measurements have been made, significant variations in surface balance were observed over distances on the order of kilometers suggesting that areal coverage of the ice sheet at a scale of 10 km would be desirable for surface balance maps.

Because the microwave emissivity of snow increases markedly with wetness, the change in emissivity due to the onset of surface melting is large and easy to detect. Consequently, microwave observations could be used as key indicators of the yearly onset and extent of melting. Variations in melt characteristics from year to year could be a herald of changing environment. In this vein, an intriguing possibility for investigating the climate of the recent past is suggested by new work (Swift *et al.*, 1985), showing that combined radiometer and scatterometer measurements can be used to map the distribution of buried ice lenses. The buried lenses are features formed by melting and refreezing in previous years, so the comparison of present melt extent with maps of ice lens distributions could be used to investigate recent climatic trends. Also, surface melting is the principal ablation mechanism on the flanks of the Greenland ice sheet and maps accurate to several kilometers would be valuable in studies of the local environment. Summer melt on the surface of the Antarctic ice sheet generally freezes in place, so a knowledge of the spatial extent (tens of kilometers) and temporal variation (on a daily basis in summer) would be a proxy indicator of surface temperature.

An adequate measurement of accumulation and ablation rates requires data at about 1 km resolution with an accuracy of 1 to 5 cm per year, and data on surface melting is also required with about 1 km spatial resolution with an update each day in the summer. The requirements for a passive microwave sensor to help provide this information are given in Table 11.

Remote Sensing of Sea Ice

Two measurements are crucial to understanding the role of sea ice in the climate system. The first is the extent and concentration of the polar sea ice cover and the second is the distribution of sea ice thickness. The importance of the variation of ice thickness across the Arctic to both the dynamics and thermodynamics of the region has been noted in recent studies (Hibler, 1980; Maykut, 1982). This is especially true of energy exchanges at the surface during

Table 11. Summary of Measurement Requirements (Sheet Ice)

	Ideal	Adequate
Frequency	10, 18, 37, 90 GHz	18, 37 GHz
Spatial resolution (spot size: one spot every 10 km)	1 km	1 km
Accuracy	2 K	2 K
Revisit time		
Surface melt	1 day	3 days
Accumulation rate	1 day	3 days

winter. Rates of ice growth, heat loss from the ocean to the atmosphere, and salt rejection to the underlying ocean can be up to two orders of magnitude larger over refreezing leads and polynyas, and up to an order of magnitude larger over 50 cm ice than over thick, perennial sea ice (Maykut, 1978; 1982). Our understanding of the role of sea ice in the climate system depends on our ability to determine both the distribution of open water and sea ice, and also the distribution of ice thickness within the arctic ice pack. This capability is central to addressing the fundamental problems of heat and mass balance of the Arctic.

Satellite data from visible, infrared, and microwave sensors provide information on the global distribution of sea ice and its seasonal variation; however, the microwave radiometer has emerged as the sensor of primary importance for identifying many ice parameters. In contrast to visible and infrared measurements, microwave imagery allows nighttime as well as daytime coverage and is not obscured by clouds. Although the passive microwave observations are generally at a much coarser resolution (limited to about 30 km with existing sensors), they do provide complete polar coverage with as little as 1 day of data, and a quantitative determination of sea ice concentration can be obtained even though individual floes and leads are not resolved (Swift and Cavalieri, 1985).

The potential inherent in microwave observations of sea ice is due to the sharp contrast between the microwave emissivities of sea ice and open water. At 1.55 cm (19.35 GHz), the wavelength of the single channel Nimbus-5 ESMR instrument, sea ice has emissivities ranging from 0.84 to 0.95, roughly twice the emissivity (approximately 0.44) for open water. Consequently, if there is a mixture of sea ice and open water within a given 30 km resolution cell, the composite emissivity for that resolution cell lies between these limits. This allows the brightness temperatures recorded by the microwave instruments to be converted to approximate sea ice concentrations. Estimated accuracy is approximately ± 15 percent in regions with predominantly first-year ice (Zwally *et al.*, 1983). Accuracy is less in regions with a mixture of ice types, since brine drainage through the ice during the summer melt results in a generally lower microwave emissivity for multiyear ice than for first-year ice.

Measurements of the areal distribution of sea ice, or sea ice concentration, have been made quite successfully with passive microwave imagers (Zwally *et al.*, 1983; Parkinson *et al.*, 1986). However, determining ice thickness has been more difficult. Ice thickness cannot be measured directly with passive microwave instruments, although it can be inferred from the age of the ice because changes which occur with ice age, such as the leaching of salt, affect the microwave signature. Algorithms using the multichannel microwave data of the type obtained with the Nimbus-7 SMMR have been developed to obtain quantitative estimates of first year ice (ice of thickness up to 2 m) and multiyear ice (ice with thickness greater than 2 m) with success (Svendsen *et al.*, 1983; Cavalieri *et al.*, 1984; Swift *et al.*, 1985; Swift and Cavalieri, 1985; Comiso, 1986). However, variations in the signature of various species of multiyear ice, and the inability to discriminate unambiguously among multiyear ice types, remain a serious limitation.

Multichannel microwave instruments not only have the potential of measuring ice concentration and thickness, but also of allowing determination of such additional variables as ice temperature, snow cover, and surface melting. The Scanning Multichannel Microwave Radiometer (SMMR) on the Nimbus-7 satellite has 10 channels of microwave information, and algorithms to extract various sea ice parameters from the SMMR data have been developed and tested by groups in Norway, Canada, and the United States (Svendsen *et al.*, 1983; Norsex Group, 1983; Cavalieri *et al.*, 1984). A major restriction of the Nimbus-7 SMMR data for studies of the Central Arctic has

been that the satellite's orbit prevents data collection poleward of 84°, in contrast to the global data collection of the Nimbus-5 ESMR. But, even with the limited data sets available, passive microwave remote sensing has already made substantial contributions to our knowledge of sea ice and its variations. The current status of satellite passive microwave remote sensing for sea ice research has recently been reviewed (Untersteiner *et al.*, 1984; Cavalieri and Zwally, 1985; Swift and Cavalieri, 1985).

For sea ice, the parameters which need to be measured are location of the sea-ice boundary, concentration of ice, ice type, albedo, and the state of surface melting. The spatial requirements for these measurements exhibit a dual threshold. One set of useful observations is achieved at a spatial scale of 25 km, which corresponds to the diurnal change in the gross extent of the ice boundary. The enhanced capabilities, which require resolutions of 1 to 10 km, represent the scale needed to monitor convergence and divergence processes that affect ice mass balance, hence the total production that determines heat exchange into the atmosphere. These requirements have been summarized in Table 12.

Table 12. Summary of Measurement Requirements (Sea Ice)

	Ideal	Adequate
Frequency	10, 18, 37, 90 GHz	18, 37, 90 GHz
Spatial resolution		
Ice boundary	5-25 km	25 km
Concentration	1-10 km	25 km
Type	1-10 km	25 km
Albedo	1-10 km	10 km
Surface melt	1-10 km	10 km
Radiometric accuracy	2.0 K	2.0 K
Radiometric sensitivity	2.0 K	2.0 K
Revisit time	1 day	3 days

IV. SCIENCE OBJECTIVES: ATMOSPHERE

BACKGROUND

Temperature variation with height is a characteristic feature of the Earth's atmosphere. A common way of describing the atmosphere in terms of layers and shells is based upon this temperature variation. The lowest of these layers is called the troposphere. It averages from 6 to 18 km in depth, depending on latitude and weather conditions, and is deepest over the equator and shallowest over the poles. It contains 80 percent or so of the total gaseous mass of the atmosphere and virtually all the water vapor and aerosols. It is also the zone where weather phenomena and atmospheric turbulence are most marked. This layer is characterized by a general decrease of temperature with height at a mean rate of about 6.5 K/km, and the whole zone is capped in most places by a temperature inversion level and in others by a zone which is isothermal with height. The troposphere thus remains to a large extent self-contained, because the inversion acts as a "lid" which effectively limits convection.

The ongoing studies of the troposphere are focused on the development of an improved understanding of the physical processes important in determining the circulation of the atmosphere on all scales, ranging from the mesoscale to the global scale, and an improved capability to predict its evolution on a wide variety of temporal and spatial scales. The current tropospheric knowledge base for global and regional understanding and prediction is one that has evolved over the last half-century, accelerating in accuracy and scope over the past decade or so. The enhanced prediction accuracy, which has been attained in recent years, can be explained primarily as the result of improved three-dimensional (3-D) temperature input (from satellites) and wind information (satellite cloud-tracked and aircraft-measured), as well as improved numerical weather prediction (NWP) models. The range of useful prediction by models has increased from 4 to 7 or 8 days, and 4-day forecasts are now roughly of the same accuracy as 2-day forecasts were 20 years ago.

To further advance our current understanding of the nature of tropospheric processes, a combination of observational objectives and advances in theory and modeling must be realized. Progress will be most rapid if observations and theory advance concurrently, and it is within such an integrated program that space-based measurements must be utilized to be effective. With this in mind, the primary scientific objectives for the observation of the troposphere from space over the next 10 to 15 years may be set forth with the help of a recent National Research Council (NRC) publication (1985). In order of priority these objectives are as follows:

1. (a) To obtain global data sets for atmospheric and surface parameters needed for the study and understanding of the internal and boundary forcing processes that maintain the atmospheric circulation. (b) To obtain temporally continuous global data sets of sufficient spatial density and accuracy to determine the large-scale structure of the troposphere.
2. To obtain special high-resolution data sets to answer fundamental scientific questions concerning the generation, maintenance, propagation, and decay of mesoscale atmospheric phenomena.

The required data sets are for: (1) surface and atmospheric wind, atmospheric temperature and humidity, wind stress over the oceans, and land and sea surface temperature; (2) precipitation and closely related surface characteristics such as soil moisture, snow and ice cover, and vegetative biomass; (3) surface radiation and albedo, and radiation at the top of the atmosphere; (4) cloud characteristics including type, amount, height, temperature, liquid water content, and radiative properties; and (5) sea level pressure.

Microwave radiometric observations from space can provide data on atmospheric temperature and humidity, sea surface temperature, snow and ice cover, soil moisture, precipitation, vegetative biomass, and cloud liquid water content. All of these parameters, except atmospheric temperature and humidity and cloud liquid water content, have been dealt with in other parts of this report.

The measurement of atmospheric temperature and humidity, along with wind and sea level pressure, represent the core measurements required to define the dynamic and thermal states of the troposphere. To determine the global atmospheric structure for large-scale dynamical systems and for weather forecasting, observations of temperature and humidity are needed in three dimensions and at frequent intervals. Measurements of the 3-D distribution of temperature and humidity in the atmosphere are already part of the ongoing World Weather Watch program (endorsed and overseen by the World Meteorological Organization), but there are notable gaps over the oceans, and further improvements in reliability and accuracy are desirable. Optimal measurement systems are likely to make use of both microwave and infrared radiometers. The NWP models can be expected to asymptomatically approach horizontal and vertical resolutions of nearly 100 km and 1 km, respectively, in the quest for improving the accuracy of medium range (1- to 14-day) forecasts. Economic factors and cost/benefit considerations make these

estimates valid within a factor of two. Data resolution requirements are strongly related to model resolutions but are somewhat less stringent. In terms of atmospheric temperature and humidity measurement requirements, until the turn of this century global data coverage with horizontal and vertical resolutions of 200 and 2 km, respectively, seemed adequate. The National Research Council publication cited above recommends resolutions of 10 km in the horizontal and 1 km in the vertical. It further recommends that the measurement accuracies should be ± 1 K for temperature and ± 1 g/kg or ± 10 percent for specific humidity. The temporal resolution is established by the time scales associated with atmospheric variability on these synoptic spatial scales; a minimum sampling interval of 12 hours is necessary in the case of atmospheric temperature and humidity. For mesoscale studies, the minimum necessary sampling interval and the horizontal and vertical scales of the measurements decrease significantly. Although the required data density (in both time and space) varies with the specific phenomenon of interest, most field studies require data about every hour on a horizontal scale of 20 km and a vertical scale of 500 m. Even though these high resolution measurements are done most effectively with ground-based remote sensing systems, a detailed knowledge of the synoptic-scale flow is essential, in virtually all mesoscale studies, to understand the complete scale-interaction problem.

Measurements of surface atmospheric temperature and humidity are needed in conjunction with the wind speed in order to estimate the surface fluxes of sensible and latent heat. Surface temperatures appear also to be obtainable using combinations of infrared and microwave sounders. The accuracy desired is 1 K for air-sea temperature differences or 10 W/m^2 in the fluxes over 100-km spatial scales. Sea surface temperature, in addition to being an important parameter in estimating surface energy fluxes, is in a more general sense a vital indicator of the oceanic mixed-layer heat storage. As such, it is frequently necessary to specify sea surface temperature as the lower boundary condition over the oceans for atmospheric models. Again, the measurement accuracy desired is 1 K at a 100 km resolution (or better in regions of oceanic fronts) over a period of 5 days, although with a daily sampling frequency.

Clouds play a major role in the radiation balance of the Earth atmosphere system. Definitive climate studies will not be possible until cloud properties are more realistically incorporated in numerical global circulation models. Clouds are also important in many ways for mesoscale weather systems. The evolution of convective clouds and their interaction with their environment is one of the central problems of mesoscale meteorology. A second major problem is precipitation and the processes that determine its spatial and temporal distribution. Even thin layers of nonprecipitating clouds affect many mesoscale phenomena through their effect on the surface energy budget. Cloud liquid water content is an important cloud parameter that can be effectively measured by microwave radiometric methods. The NRC publication cited earlier recommends that the cloud liquid water content be measured globally with a horizontal resolution of 200 km and a mean accuracy of 25 percent.

MEASUREMENT PHYSICS

The brightness temperature, T_B, seen by a microwave radiometer looking down on the Earth, can be written in the following succinct form (Schaerer and Wilheit, 1979; Meeks and Lilley, 1963):

$$T_B(\nu) = \int T(h)\, K(\nu,h)\, dh + A$$

where the Rayleigh-Jeans approximation has been used and where T(h) is the profile of the physical temperature of the atmosphere with height, h; where ν is frequency of the measurement; A represents additional terms which are essentially independent of the temperature profile; and $K(\nu,h)$ are kernels called the temperature weighting functions. The $K(\nu,h)$ depend on the resonance near which the measurement is made but generally peak at a particular altitude, which depends on the frequency at which the measurement is made. By making measurements at several different frequencies, a set of equations is obtained which can then be inverted to obtain the temperature profile, T(h). A somewhat similar procedure can be used to obtain profiles of the atmospheric constituents such as water vapor, except that in this case the weighting functions tend to be dependent on the parameter (e.g., water vapor) to be measured. However, algorithms for obtaining water vapor can be obtained using perturbation techniques (e.g., Schaerer and Wilheit, 1979).

Profiling atmospheric temperature and water vapor at resonances in the microwave portion of the spectrum has the advantage that microwave radiation penetrates most forms of clouds so that profiling can be done on an all-weather basis. Microwave remote sensing also has the advantage, especially for measurements over oceans, that the surface is very cold (a good reflector). This enhances the signal-to-noise ratio and permits profiles to be obtained very near the surface where, especially in the case of water vapor, the most important information about the parameter is found. The disadvantage of profiling at microwave frequencies as compared to infrared systems is that one obtains poorer spatial resolution on the surface for a given size antenna aperture. Microwave systems with resolutions approaching 15 km are now practical from low Earth orbit.

MEASUREMENT REQUIREMENTS

The performance required of a passive microwave sounder of the atmosphere to meet future needs for atmospheric temperature and humidity profiles is

listed in Table 13. Notice that in order to obtain accurate measurements, corrections must be made for opacity due to moisture in the atmosphere and attenuation and scattering due to ice and rain. Ancillary channels near 21, 37, and 90 GHz can be used for this purpose for temperature soundings and additional channels at 90 and 160 GHz are helpful for profiling water vapor.

Table 13. Summary of Measurement Requirements (Atmosphere)

	Ideal	Adequate
Temperature Profiles		
Frequency	50-60* GHz	50-60 GHz
Resolution (horizontal)	10 km	100 km
Resolution (vertical)	500 m	2 km
Accuracy	±1 K	±1 K
Radiometric sensitivity	0.3 K	0.3 K
Radiometric accuracy	1.0 K	1.0 K
Temporal resolution	1 per hour	2 per day
Humidity Profiles		
Frequency	183** GHz	183 GHz
Resolution (horizontal)	10 km	100 km
Resolution (vertical)	500 m	2 km
Accuracy	±10% (±1 g/kg)	±10% (±1 g/kg)
Radiometric sensitivity	0.8 K	0.8 K
Radiometric accuracy	2.0 K	2.0 K
Temporal resolution	1 per hour	2 per day

*Plus ancillary channels at 21, 37, and 90 GHz for atmospheric corrections
**Plus ancillary channels at 90 and 160 GHz for atmospheric corrections

V. THE HMMR INSTRUMENT

INTRODUCTION

The preceding chapters have described the most important measurements which a microwave radiometer would contribute to the Earth Observing System. A passive microwave sensor would further the understanding of the hydrologic cycle by providing data on soil moisture, precipitation, evaporation, and snow cover; it would provide important information about the troposphere by providing profiles of atmospheric temperature and water vapor in cloudy regions where gaps are found in existing infrared soundings; a microwave radiometer could provide maps of sea surface temperature and would provide much of the information about sea ice needed to understand its dynamics and its effect on energy exchange processes in the polar regions; finally, a microwave sensor can provide the information on total water vapor needed to determine atmospheric opacity and correct the measurements of other instruments for the effects of atmospheric attenuation.

The preceding chapters have also identified the requirements that measurements of these quantities must meet if a data set is to be obtained which is adequate to advance our understanding of the environment. These requirements are summarized in Table 14. The Table shows the frequencies at which microwave measurements are needed to observe each parameter, the spatial resolution with which the data must be collected, and the accuracy required of the radiometer. The rationale for these requirements has been set forth in the preceding chapters.

From this list of measurement requirements, the Panel has deduced a set of specifications for the HMMR instrument. These specifications are given in Table 15. The specifications represent a compromise between future needs for scientific data under ideal circumstances and the Panel's assessment of what can feasibly be built and put into space within the next decade. The specifications are a set of realistic engineering design requirements. A radiometer system which meets these specifications would provide data of sufficiently high quality to significantly improve our understanding of the Earth's environment, and in many cases, the data will approach the scale size of the fundamental geophysical processes which drive the Earth's environment.

The consensus of the Panel was that the most effective approach to meet the requirements set forth above was to divide HMMR into three independent but related instruments, each performing a specific subset of the necessary observations. This approach permits a cost-effective, gradual phasing into operation of the complete HMMR capability and makes maximum use of existing developments. The three instruments and their primary measurements are:

- The Electronically Scanned Thinned Array Radiometer (ESTAR)
  - Soil moisture
- The Advanced Mechanically Scanned Radiometer (AMSR)
  - Precipitation

Table 14. Summary of Measurement Requirements

Parameter	Frequency (GHz)									Radiometer (K)		Spatial Resolution (km)	
	1.4	6	10	18	21	37	50-60	90	183	Accuracy	Sensitivity	Ideal	Adequate
Soil moisture	X									1.5	1.0	1	10
Precipitation			X	X		X		X		2.0	2.0	1	10
Sea ice			X	X		X		X		2.0	2.0	1-10	25
Snow				X		X		X		2.0	2.0	1	10
Sea surface temperature		X	X	X	X					1.0	0.5	1-10	10-50
Total water vapor				X	X	X				2.0	0.5	10	100
Water vapor profile					X	X		X	X	2.0	0.8	10	100
Temperature profile					X	X	X	X		1.5	0.3	10	100

Table 15. HMMR Requirements

Frequency (GHz)	Spatial Resolution (km)	Accuracy (K)	Sensitivity (K)
1.4	10	1.5	1.0
6	25	0.3	0.5
10	15	0.3	0.1
18	8	1.5	1.0
21	8	1.5	1.0
37	4	1.5	1.0
50-60	<100	1.0	0.5
90	2	1.5	1.0
183	<100	2.0	1.0

  - Snow cover
  - Sea ice
  - Water vapor (total)
  - Sea surface temperature and wind speed
- The Advanced Microwave Sounding Unit (AMSU)
  - Temperature profiles
  - Water vapor profiles

Instrument Characteristics Summary

The key HMMR instrument characteristics are summarized in Table 16. The tabulated values for ESTAR are based on preliminary conceptual studies; for AMSR they were obtained from detailed implementation proposals prepared for the NOSS Large Aperture Multifrequency Microwave Radiometer (LAMMR) by Aerojet Electrosystems Company (report #6069, February, 1980) and by General Electric Space Division (February, 1980), and for AMSU the specifications were taken from the contract written with Aerojet Electrosystems Company for its development.

Instrument Selection Rationale

Selection of the HMMR instruments was based on consideration of the following factors:

- Science and Mission Requirements for Eos, as described in Butler *et al.* (1984)
- Applicability of instruments already under development (SSM/I, SSM/T, AMSU)
- Inheritance from successfully flown instruments (SMMR, ESMR, NEMS, SCAMS)
- Inheritance from instrument concepts developed in some depth (LAMMR)
- Applicability of state of the art concepts, such as electronically steered phased arrays and thinned arrays, and hardware such as large space structures and integrated microwave receivers, where necessary to meet the requirements in a practical manner

The complex of three HMMR instruments which followed from consideration of the above factors has the following features:

- Each instrument is capable of making at least one definitive measurement (i.e., has demonstrated superiority over other types of remote sensors). These capabilities are summarized in Table 17.
- One of the three instruments is nearing implementation (AMSU). This would allow low-cost duplicates to be procured immediately with high cost-effectiveness and low risk.
- One of the instruments, AMSR, is functionally a direct descendant of the Nimbus/Seasat SMMR. It has been studied in depth as part of planning for the NOSS program and is technically a relatively low risk.
- One of the instruments, ESTAR, although utilizing novel concepts requiring development, appears to be the most cost-effective manner of obtaining the very challenging soil moisture measurement. Development of this instrument

Table 16. HMMR Measurement Characteristics

Parameter	ESTAR	AMSR	AMSU-A	AMSU-B
Frequencies (GHz)	1.4	6, 10, 18, 21, 37, 90	23.8, 31.4 50-60 (12 Ch), 89	89, 157, 183 (3 Ch)
Wavelengths (mm)	212	50, 28, 16, 14, 8.2, 3.3	12.6, 9.6 5.5 (12 Ch), 3.4	3.4, 1.8, 1.6 (3 Ch)
Antenna size (m)	18×18	4×7	0.15, 0.28	0.28
IFOV (km)	10	25 to 2	50	15
Swath (km)	1,400	1,400	1,500	1,500
ΔT (K)	1.0	0.4–1.7	0.25–1.3	1.0–1.2
Data rate (kbps)	5	50	5	5
Instrument size (m)	18×18×0.5	6×8×4	1.5×1×1	0.7×0.7×0.5
Power (W)	200	250	115	60
Weight (Kg)	350	350	64	30

Table 17. HMMR Measurement Capability

Parameter	ESTAR	AMSR	AMSU-A	AMSU-B
Hydrologic Cycle				
Evaporation (land)*	B	B		B
Evaporation (ocean)*		A		B
Soil moisture	A			
Sea surface temperature		B		
Snow		A		B
Precipitation (ocean)		A		
Precipitation (land)		A		B
Oceanic Science				
Ocean dynamics		C		
Sea ice		A		
Tropospheric Science				
Temperature profile			A	
Water vapor (total)		A	A	A
Water vapor (profile)				A
Cloud water		B	B	

Code: A = Definitive Measurement
B = Significant Measurement
C = Contributing Measurement

*Evaporation is an inferred quantity. It requires measurement of supporting geophysical parameters by HMMR and other Eos instruments.

will also provide the experience necessary for development of larger, more sophisticated instruments for other applications in the future.

It is to be noted that the HMMR concept, as described here, is functionally optimized to meet the scientific measurement requirements (Table 14) and represents a technically sound potential implementation. In the case of ESTAR and AMSR, other possible implementations meeting the requirements and yielding similar performance characteristics are possible and deserve to be studied.

ELECTRONICALLY SCANNED THINNED ARRAY RADIOMETER

The spatial resolution of a filled aperture antenna is proportional to the ratio of the operating wavelength to the antenna diameter. The measurement of soil moisture requires a long electromagnetic wavelength (21 cm), hence a large antenna to achieve the desired spatial resolution of 10 km. From an orbiting altitude of 700 km the required antenna is approximately 18 meters by 18 meters. Even if one were to construct an antenna of this size in space, mechanical scanning is not attractive due to the mass of the moving structure. Another approach is a "pushbroom" mode, whereby multiple receivers and a feed network are used to illuminate several crosstrack pixels simultaneously. A four-beam microwave pushbroom concept has been demonstrated from an aircraft using four identical receivers with a multiple beam antenna; however, it is a technical challenge to construct such a system using several hundred identical receivers as would be necessary for application in space. The problem is further complicated by the large swath widths required to obtain global coverage (about 1,400 km with presently planned orbits).

In order to achieve high resolution L-band measurements in space at reasonable cost, the Panel examined the possibility of employing the concept of aperture synthesis as successfully developed in radio astronomy.

Aperture synthesis involves coherently measuring the signal from pairs of antennas at many different spacings. The concept is illustrated in Figure 11. Imagine two antennas L meters apart receiving radiation from a portion of the Earth with a surface temperature, T(x), which is to be measured. The voltages out of each antenna are coherently multiplied together (i.e., both phase and amplitude information are preserved) and the product is averaged. A device which makes such a measurement is called a correlating interferometer (Kraus, 1966) and the signal which is the output of the interferometer is called the spatial correlation function of the antenna voltages. It is readily shown (e.g., Le Vine and Good, 1983; Swenson and Mathur, 1968) that the correlation function is proportional to the spectrum (i.e., Fourier transform) of the temperature profile T(x) evaluated

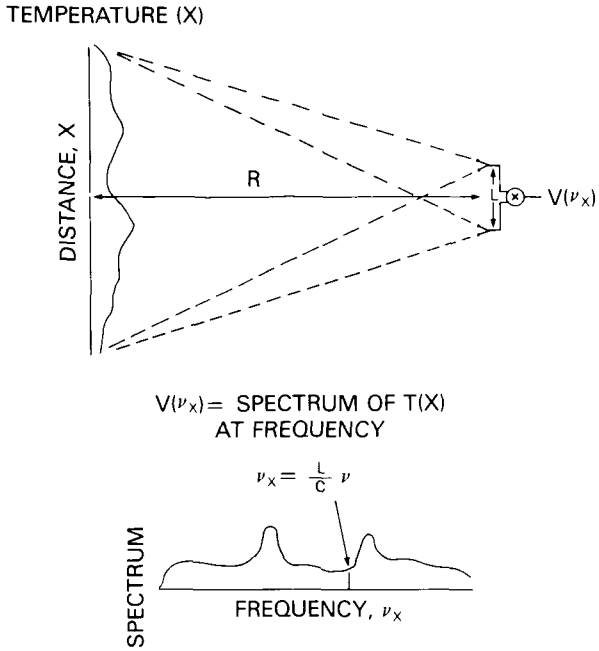

Figure 11. The principles of aperture synthesis. T(x) is the temperature profile on the surface and $V(\nu_x)$ is the correlation of the antenna voltages when the antennas are spaced L meters apart, corresponding to a spatial frequency ν_x.

at a particular frequency $\nu_x = L\,\nu_0/c$, where L is the distance between antennas, c is the speed of light in vacuum, and ν_0 is the nominal frequency at which the measurement is made. Since ν_x depends on the spacing between antennas, the spectrum of T(x) can be measured at many points, ν_x, simply by repeating the measurement with different L. In principle, one could make measurements at many different antenna baselines, L, and obtain a map of the spectrum. Then, the temperature profile itself, T(x), could be obtained by Fourier transforming the spectrum. The important point for aperture synthesis is that the resolution obtained in the image formed after Fourier transforming is determined by how well the spectrum has been sampled (i.e., by the number and spacing of the sample points, ν_x) and not by the size of the antennas used in the measurement. In principle, one could use very small antennas to obtain a wide field-of-view, and by making many measurements closely-spaced in spatial frequency space obtain a map of T(x) with very high spatial resolution.

Aperture synthesis has been successfully implemented on the Earth by radio astronomers for making high resolution maps of radio sources (Brouw, 1975; Hewish, 1965). The Very Large Array in Socorro, New Mexico, is an example (e.g. Napier *et al.*, 1983). A variation of aperture synthesis for viewing the Earth from space has been proposed by Schanda (1979); Carl Wiley and co-workers at Hughes Aircraft Company have demonstrated other variations which may be suitable for implementation in space; and Le Vine and Good (1983) have shown

how the theoretical issues of viewing a large extended source (the Earth) from relatively nearby can be successfully overcome. However, in order for aperture synthesis to be practical from low Earth orbit, it is necessary to form images with good spatial resolution and high sensitivity in the relatively short times permitted for observation by satellite motion. This led the Panel to a hybrid concept in which long stick antennas are used to form a real aperture in the along-track dimension, and aperture synthesis is used to obtain resolution in the crosstrack dimension. This hybrid would result in an order of magnitude reduction in the antenna needed in space to make soil moisture measurements.

Figure 12 illustrates this hybrid system. It consists of an array of long (stick) antennas each with a real aperture (fan beam pattern) oriented to give resolution in the direction of satellite motion. In the other dimension (across-track), resolution is obtained with aperture synthesis by connecting pairs of the stick antennas together to form a collection of correlating interferometers. The number and placement of the sticks is determined by the sampling in the frequency domain needed to obtain the desired synthesized antenna pattern. Arrangements which employ the minimum number of antennas to obtain a desired sampling in the frequency domain are generally referred to as minimum redundancy thinned arrays (e.g. Moffet, 1968).

The hybrid shown in Figure 12 can make images with sufficient sensitivity to measure changes in soil moisture in the short time permitted by motion of the satellite. A configuration of this type is being proposed for the L-band radiometer to measure soil moisture as part of HMMR. To obtain an idea of how such a system would perform, a preliminary design has been made assuming a system in orbit at 700 km and operating at 1.4 GHz with stick antennas 18 m long. Such a system would have a resolution at nadir of 10 km, a swath width of 1,400 km, and a sensitivity of 0.7 K. Table 18 lists the parameters of the system and the formulas used to evaluate its performance. Notice that the sensitivity ΔT in the Table is the fluctuation in brightness temperature in the final image (i.e., after all signal processing is complete). Also, in the equation for sensitivity, "A" is the effective area (18 m $\times$ 18 m in the system above) of a real aperture antenna with the same spatial resolution as obtained with the synthesized antenna, "a" is the area of the individual real aperture antennas employed in the array, and "n" is the number of antennas in the array. This formula is the same as that employed in radio astronomy (e.g., Napier *et al.*, 1983).

The 32 stick antennas employed in the system can be arranged to be equivalent to 256 antennas uniformly spaced in the array (e.g., using the algorithms of Moffet (1968) or Leech (1956)).

Each antenna is deployed with coincident element fan beams projected crosstrack to the velocity vector

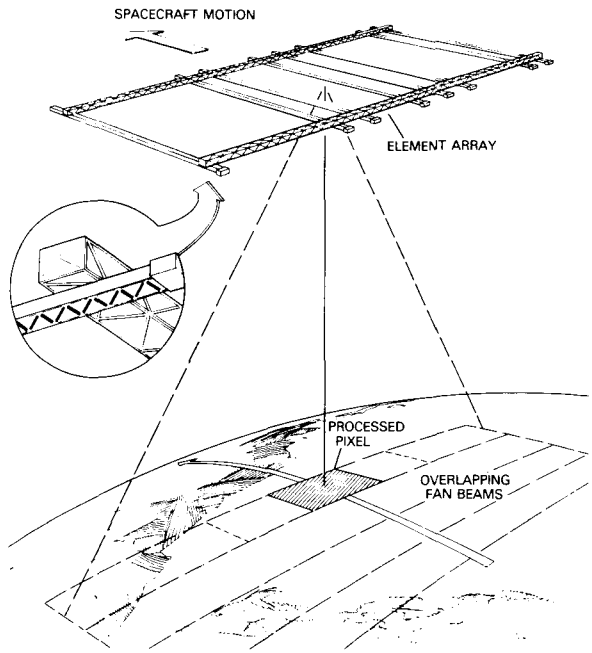

Figure 12. The ESTAR concept. The long stick antennas are aligned in the direction of motion to give real aperture resolution along the satellite ground track. Resolution across-track is obtained synthetically through signal processing.

of the satellite as shown in Figure 12. The ESTAR consists of these antenna sticks and an associated matrix of correlating receivers. The system above has been designed to operate within the radio astronomy band centered at about 1.4 GHz (21 cm) and would have a minimum spacing between antenna elements of approximately one-half wavelength.

Table 18. ESTAR Specifications and Performance

Specifications:

Wavelength (λ)	21.23 cm
Antenna length (D)	18 m
Antenna width (d)	10 cm
Orbit altitude (H)	700 km
Satellite speed (V)	7.5 km/s
Receiver bandwidth (B)	20 MHz
System noise temperature (T)	300 K
Number of antennas (n)	32
Integration time (t)	0.5

Performance:

Resolution (10 km)	1.2 (λ/D) H
Swath width* (1,400 km)	(λ/d) H
Sensitivity (0.7 K)	(T/$\sqrt{Bt}$) (A/na)

*Determined by the beam of each real antenna aperture.

The detailed physical characteristics of the ESTAR, such as power and weight, require further study. Research is needed to determine the optimum configurations for implementing the array and to determine techniques for calibration of the radiometer. This is new technology which has never been applied to Earth viewing; consequently, construction of a small prototype instrument for testing from an aircraft should be seriously considered.

It is expected that calibration of the ESTAR will proceed very much as calibration is performed for synthesis arrays in radio astronomy. Reference sources on board the spacecraft will be needed for an absolute calibration, as well as schemes for ensuring phase consistency of the local oscillators at the various mixers. The ocean will provide a potential reference source at this frequency (1.4 GHz) to aid in calibration, and sharp boundaries (e.g., ocean-land boundaries) can be used to help "focus" the image. In a synthesis array, processing can be done after the measurement by weighing the measurements at the different spacings. Trade-offs can be made between processing algorithms and antenna placement. This provides both a potential flexibility in the placement of the elements in the array (e.g., to accommodate spacecraft configuring) and as a tool to improve the image once the antenna placements have been made.

ADVANCED MECHANICALLY SCANNED RADIOMETER

The AMSR is envisioned as an instrument which combines the advantages of multifrequency microwave remote sensing with sufficiently high spatial resolution to provide measurements approaching the geophysical scale of the observable. The AMSR is envisioned to include channels at approximately 6, 10, 18, 21, 37, and 90 GHz, each with dual (linear) polarization. Measurements at various combinations of these frequencies permit data to be obtained on the amount of precipitation over oceans (18 and 37 GHz) and possibly over land (18, 37, and 90 GHz); on the amount of snow cover over land (37 and 90 GHz); on the areal extent and characteristics of sea ice (10, 18, 37, and 90 GHz); on the total amount of water (cloud water and water vapor) in the atmosphere (21 GHz); and finally, at the lower frequencies (6 and 10 GHz), information to be obtained on sea surface temperature and wind speed at the ocean surface. The primary geophysical measurements and the resolution to be provided by AMSR are given in Table 19.

Among the alternative means of implementing the system of radiometers required to make the measurements described above, the HMMR Panel selected a concept in which a large solid antenna dish is conically scanned to obtain wide swath coverage. By tilting the antenna and rotating it about the vertical, the footprint of the antenna beam is made to describe a circle on the surface (Figure 13). The motion of the spacecraft displaces successive circles, and by proper choice of the scan rate for a given incidence angle, antenna size, and satellite velocity, one can align the circles to obtain complete coverage of the swath below the spacecraft. In order to keep the scan rate reasonable, multiple beams are employed at the higher frequencies. This concept has the advantage that the antenna feed system can be rotated with the main reflector preserving polarization purity and making calibration easier. Also, using a solid antenna dish reduces noise and improves sensitivity.

This concept has been thoroughly examined during a series of design reviews for the Large Aperture Multifrequency Microwave Radiometer (LAMMR) during planning for a Seasat follow-on mission (NOSS). The engineering studies by Aerojet Electrosystems Co. (1980) and General Electric (1980) indicated that a system such as the above is feasible with antennas as large as can be fitted into the shuttle cargo bay and with rotation rates approaching one per second. The following specifications are based on these design studies.

The AMSR will consist of a 4 × 7 m dish which is rotated to obtain a conical scan with the antenna beam pointing at 50° incidence angle. The scan rate is 60 rpm, which provides contiguous coverage of a 1,400 km wide swath with resolution ranging from 20 km at 6 GHz to 1.5 km at 90 GHz from an altitude of 700 km. Because the antenna footprints are much smaller at 37 and 90 GHz than at the lower frequencies, radiometers at these frequencies will use multiple feeds to obtain contiguous scans at this rotation rate. (The option of using multiple feeds at the lower frequencies is a way of reducing the rotation rate and should be examined as a way of potentially reducing the cost.) The feed assembly is designed to rotate with

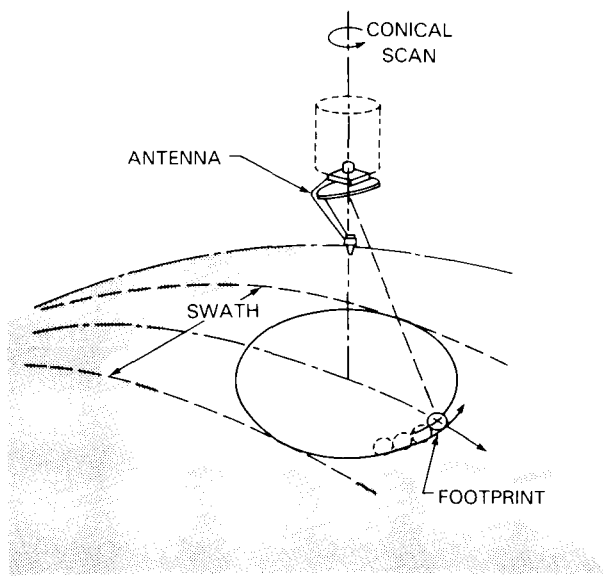

Figure 13. The AMSR will conically scan with the antenna pointing at 50° from the normal and rotating at 60 rpm.

Table 19. AMSR (Advanced Mechanically Scanned Radiometer)

Sensor Parameters						
Frequency (GHz)	6	10	18	21	37	90
Spatial resolution (km)	18	10	6	5	3	1.5
Sensitivity (K)	0.15	0.8	1.5	1.5	0.5	1.0
Geophysical Parameters						
Precipitation (land)			◒		●	●
Precipitation (ocean)		◒	●	O	◒	
Snow cover	O	O	●		●	◒
Sea ice (extent, type)	O	◒	●		●	◒
Sea surface temperature	●	◒	◒	◒	O	
Wind speed (ocean)		●	◒	O	O	
Atmospheric water (total)			●	●	◒	

At the top this Table lists the six frequencies at which the AMSR makes measurements and the spatial resolution and sensitivity of these measurements. Listed below are the major geophysical parameters which can be deduced from these measurements. The Table indicates data which is important for determining each parameter using the following code: ● = Critical; ◒ = Important; O = Helpful.

the dish to maintain polarization purity and to improve beam efficiency and make calibration easier. The radiometers are to be total power radiometers with predetection band widths greater than 100 MHz.

Table 20 lists the performance characteristics of the radiometers and Figure 14 is a schematic of a representative receiver channel. Figure 15 is a schematic of the antenna-feed system, as deployed in space, and Figure 16 shows how the system would be stowed for shuttle launch and then opened into a focal point feed system once in orbit. The entire system would weigh approximately 700 pounds and require an average of about 250 watts of power. The data rate, assuming that all the above measurements are made simultaneously, is still less than 50 kbits/sec.

Engineering studies have verified that rotating this large structure at these high rates is structurally feasible. Even larger antennas could conceivably be handled; however, the antenna size is presently limited by the shuttle cargo bay capacity. A deployable aperture (e.g., an unfurlable umbrella) would permit larger apertures but would increase costs and would likely compromise the quality of the data because of the impact of losses in the mesh on sensitivity and calibration.

The specific concept recommended for AMSR has been motivated in part by consideration for the calibration of the instrument. Among the relevant features are: (1) independent receivers to be used with each channel (polarization and frequency) and, (2) the entire antenna-receiver assembly is to rotate as a unit. The latter maintains the polarization purity of the system because the receiver-antenna geometry never changes. The polarization purity is further enhanced by the rotation because each channel always views the ground at the same angle of incidence as well as with the same polarization relative to the ground. These choices are motivated by experience gained with the SMMR, a microwave imager currently still in orbit. These system requirements should eliminate the calibration difficulties encountered with the SMMR. A similar system (rotating antenna-receiver assembly) is being implemented in the design for the SSM/I.

ADVANCED MICROWAVE SOUNDING UNIT

The AMSU is a 20 channel microwave radiometer system designed to measure profiles of atmospheric temperature and humidity. The channels selected for the AMSU system are shown in Figure 17 relative to the spectral characteristics of the atmosphere in the microwave region. The AMSU is being designed to be used aboard the NOAA series of spacecraft and for engineering considerations is being implemented as two separate subsystems AMSU-A (channels 1 to 15) and AMSU-B (channels 16 to 20).

Table 20. AMSR Performance

Frequency (GHz)	6	10	18	21	37	90
Polarization	V and H*	V and H	V and H	V and H	V and H	V and H
Radiometric accuracy (K)	0.5	1.0	1.5	1.5	1.5	2.0
Sensitivity, ΔT (K)	0.15	0.8	1.5	1.5	0.5	1.0
Dynamic range (K)	3-350	3-350	3-350	3-3,500	3-350	3-350
Integration time (ms)	3.0	1.6	1.6	1.6	1.6	1.6
Bandwidth (GHz)	0.2	0.1	0.1	0.1	0.5	1.0
3db Beamwidth (degrees)	0.9	0.5	0.3	0.25	0.15	0.08
Spatial resolution (km) (spot size diameter determined by 3db beam)	18.0	10.0	6.0	5.0	3.0	1.5

*V = vertical; H = horizontal.

The channels have been chosen to obtain accurate profiles of temperature and humidity (water vapor). Channels 3 to 14, which are situated on the low frequency side of the oxygen resonance band (50 to 60 GHz), are used for atmospheric temperature sounding. Successive channels in this band are situated at frequencies with increasing opacity (attenuation through the atmosphere) and therefore respond to radiation from increasing altitudes. Temperature profiling is possible because the mixing ratio of oxygen in the atmosphere is relatively constant and the line shape changes with pressure. Channel 1 is located on the first (weak) water vapor resonance line. It is used to obtain estimates of total water vapor in the atmosphere. (Water vapor is the primary source of atmospheric attenuation in the non-resonant regions of the microwave spectrum (Figure 17) and the total water vapor is used to correct measurements for effects of the intervening atmosphere.) Channel 2 is at 31 GHz in the valley between the oxygen and water vapor resonances. Microwave radiation at this frequency is absorbed strongly by precipitation, and this channel is used to indicate the presence of rain in the field-of-view of the sensor over oceans. Channel 15

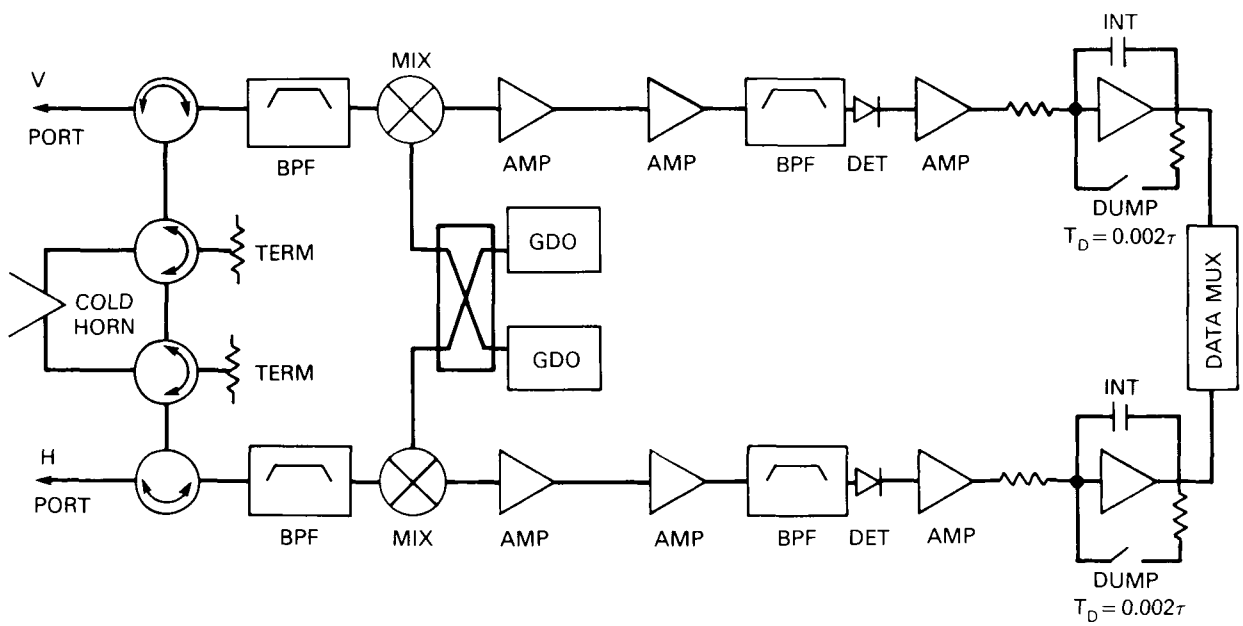

Figure 14. Schematic of the receiver of a typical channel of the AMSR.

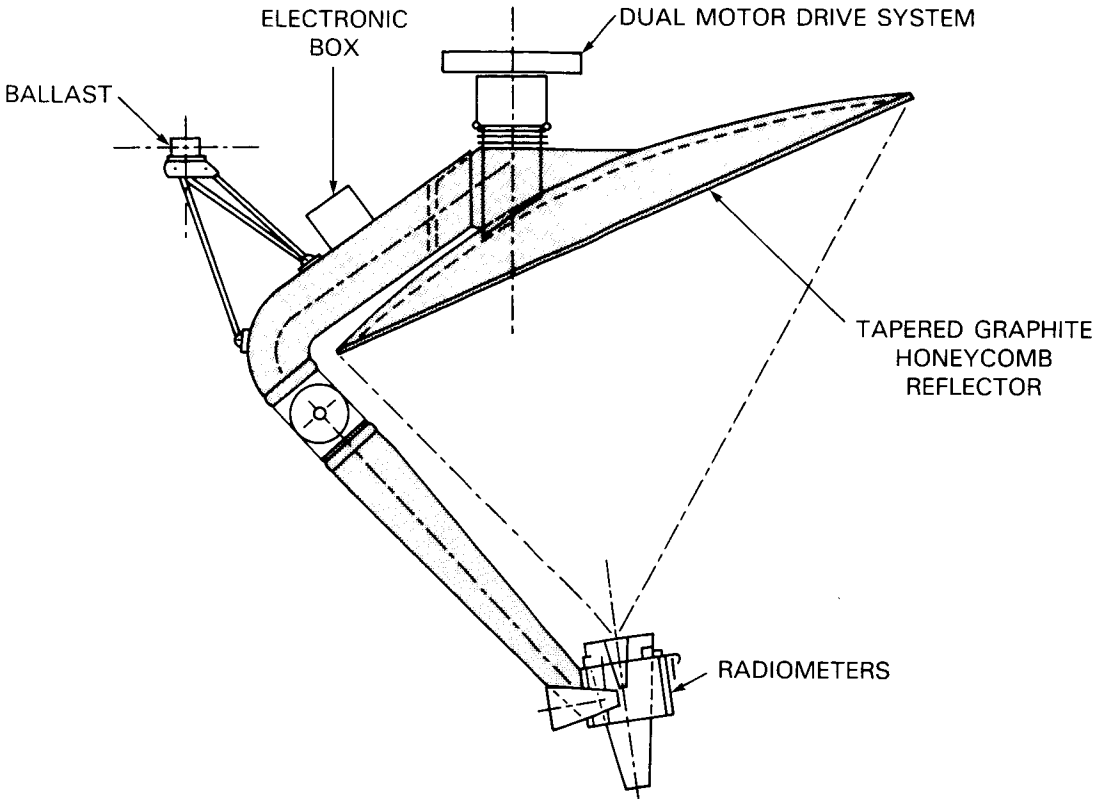

Figure 15. The AMSR as it would look deployed in space.

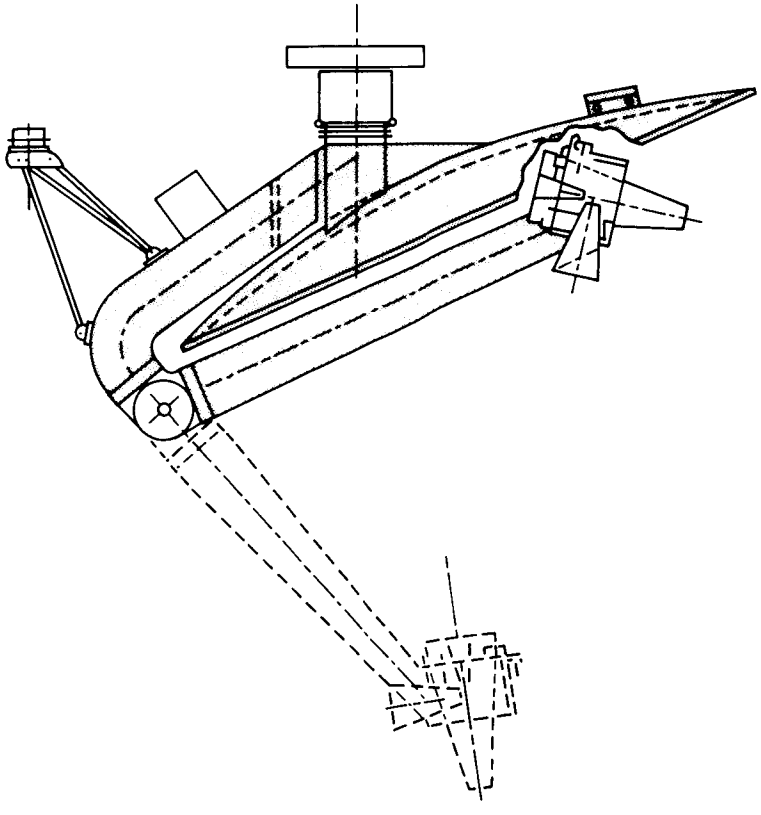

Figure 16. The AMSR in the stowed position for launch by the shuttle.

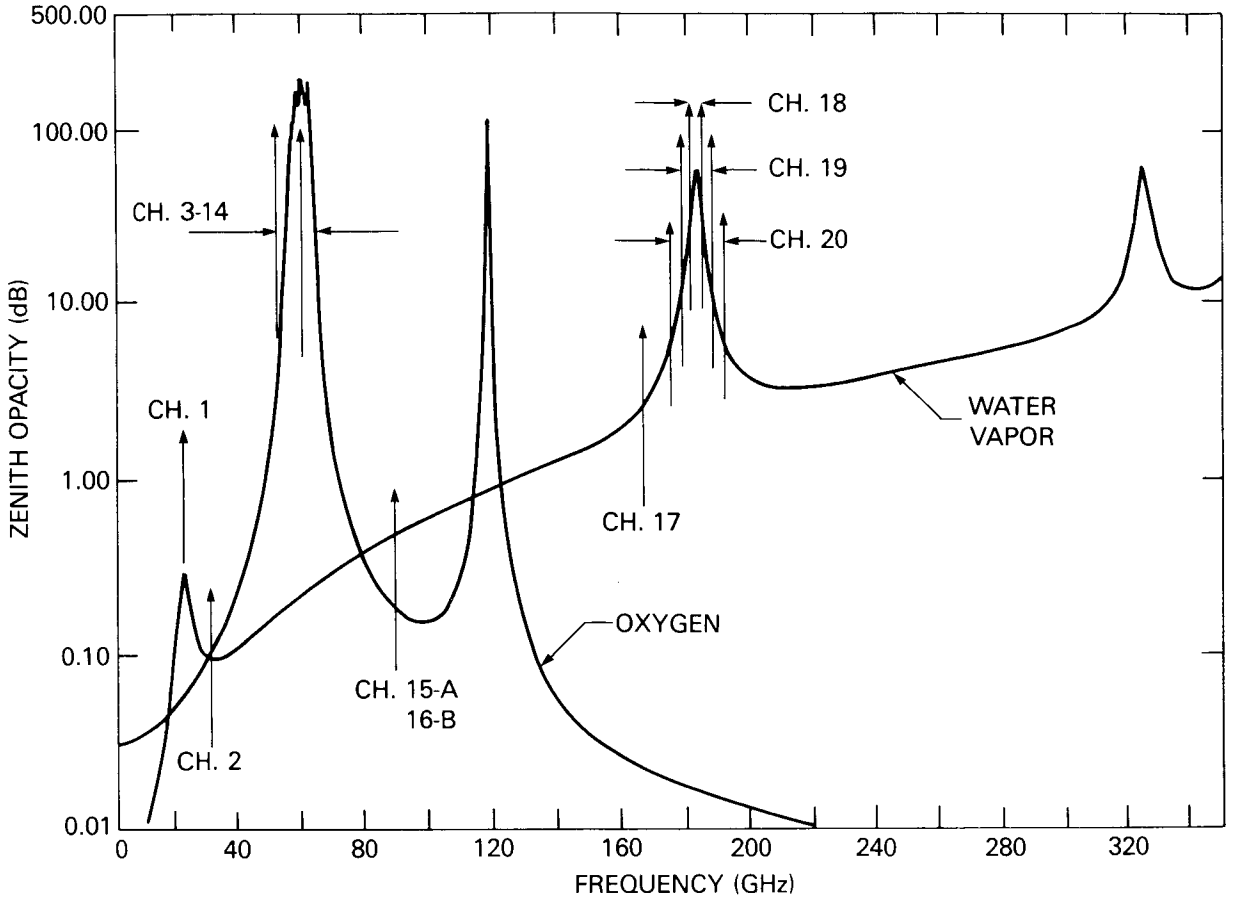

Figure 17. Oxygen and water vapor lines and AMSU channel frequencies.

(AMSU-A) and channel 16 (AMSU-B) are both at 89 GHz and are also used to indicate precipitation. At 89 GHz microwave radiation scatters from ice particles (frozen hydrometeors) in the atmosphere and can be used to indicate rain (Spencer *et al.*, 1983). Channels 18 to 20 are spread symmetrically down both sides of the strong water vapor resonance line at 183 GHz, and channel 17 is located far off the resonance line at 157 GHz. Channels 17 to 20 with input from channel 16 and channels 1 and 2 from AMSU-A are used to obtain profiles of atmospheric humidity (water vapor).

The unique advantage of the Advanced Microwave Sounding Unit over other (i.e., infrared) sounders is its ability to penetrate most types of cloud cover and, therefore, to obtain soundings in meteorologically active regions. Because of the additional channels, it also will be able to sound at higher altitudes and with better resolution near the tropopause than its microwave predecessors.

AMSU-A

The AMSU-A is the module of the Advanced Microwave Sounding Unit designed primarily to obtain profiles of atmospheric temperature (channels 1 to 15). It will obtain temperature soundings from the surface up to an altitude of 40 km with accuracies of about 1 to 1.5 K except near the surface. The ancillary channels of the AMSU-A (channels 1, 2, and 15) can also be used to sense total water vapor in the atmosphere (channel 1), precipitation over oceans (channels 2 and 15), and provide some information on sea-ice type and coverage (channels 2 and 15).

The AMSU-A antennas will scan across-track and have a beam width of 3.3° (half power points) at each frequency. The scan will cover about 50° on both sides of the suborbital track, a swath wide enough to yield global coverage every 12 hours with two satellites in polar orbit. The time per scan line is 8 seconds, providing full coverage along the ground track with 30 contiguous resolution cells per scan line and a resolution (at nadir) of about 50 km (assuming an altitude of 825 km).

In order to obtain the combination of high spatial resolution and large swath width required of AMSU-A, radiometers with high sensitivity and good calibration accuracy are required. Total power radiometers will be used with in-flight calibrations (through-the-antenna) once every scan line. The in-flight calibration circuit consists of a surface at ambient temperature (warm load) and the cosmic background (cold

load). In addition to careful pre-flight calibration, the systematic error will be reduced by end-to-end calibration using co-located radiosondes for the tropospheric channels. Comparison of zonal mean radiances with measurements from other space instruments and co-located rocket measurements, plus interchannel consistency checks of in-flight calibration, will be carried out to verify calibration accuracy of the stratospheric channels.

Table 21 is a summary of the performance characteristics required of AMSU-A listing frequency, bandwidth, temperature sensitivity, etc. The polarization of the measured radiation is determined by the receiving antenna. For engineering reasons, the polarization vector is allowed to rotate with the antenna during the scan. The polarization angle is equal to the complement of the scan angle as measured from nadir.

Channels 1 to 9, except for channel 8, contain one pass band each. Channel 8 was split into two bands to avoid the weak oxygen line, 25^-. Channels 4 to 9 (except 8) are situated on the "valley" points between two oxygen lines where the opacity as a function of frequency is a local minimum. These frequencies provide the smallest broadening of the channel weighing function halfpower widths. Channels 10 to 14 are tropospheric channels, ranging from 20 to 40 km in altitude, whose pass bands are situated symmetrically about the "valley" point between oxygen lines 13^- and 11^- with increasing opacity up both sides of these lines. Hence, each channel senses a layer of atmosphere at increasingly higher altitudes. The multiplicity of pass bands of these channels serves to improve the signal-to-noise ratio of the measurement and is needed because the line widths are relatively narrow.

Because of the relatively wide spread in frequencies and because a uniform beam width of 3.3° is required for every channel, the AMSU-A may require three separate reflector antennas, one with a projected aperture diameter of 28 cm for channels 1 and 2, and two others with apertures of 15 cm for the remainder of the channels.

The AMSU-A instrument will consist of two modules approximately 76 × 61 × 30 cm and 91 × 43 × 70 cm in size, weighing 64 kg and requiring 115 watts of power.

AMSU-B

The AMSU-B is the module of the Advanced Microwave Sounding Unit designed to obtain profiles of atmospheric humidity. It will obtain humidity soundings up to 40 km altitude with accuracies estimated to be 5 to 15 percent of saturation.

The humidity channels (16 to 20) all will have a beam width of 1.1°, which at an altitude of 825 km will yield a resolution of 15 km at nadir. The scan is across-track and ±50° to either side of nadir. This yields global coverage every 12 hours with two satellites in polar orbit. The time per scan line is 2.67 seconds, which will provide full coverage of the swath with 90 contiguous resolution cells per scan line. As in the case of AMSU-A, total power radiometers will

Table 21. AMSU-A

Channel Number	Center Frequency (GHz)	Number of Pass Bands	Maximum Bandwidth (MHz)	Center Frequency Stability (MHz)	Temperature Sensitivity (K)	Absolute Calibration Accuracy (K)
1	23.9	1	270	10.0	0.30	2.0
2	31.4	1	180	10.0	0.30	2.0
3	50.3	1	180	10.0	0.40	1.5
4	52.8	1	400	5.0	0.25	1.5
5	53.596 ± 0.115	2	170	5.0	0.25	1.5
6	54.4	1	400	5.0	0.25	1.5
7	54.94	1	400	5.0	0.25	1.5
8	55.5	1	330	10.0	0.25	1.5
9	57.29	1	330	0.5	0.25	1.5
10	57.29 ± 0.217	2	78	0.5	0.40	1.5
11	57.29 ± 0.322 57.29 ± 0.048	4	36	0.5	0.40	1.5
12	57.29 ± 0.322 57.29 ± 0.022	4	16	0.5	0.60	1.5
13	57.29 ± 0.322 57.29 ± 0.010	4	8	0.5	0.80	1.5
14	57.29 ± 0.322 57.29 ± 0.004	4	3	0.5	1.20	1.5
15	89.0	1	6,000	50.0	0.50	2.0

be used with calibration procedures similar to those used for AMSU-A. Table 22 summarizes the essential characteristics and performance required of AMSU-B. Notice that channel 16 of AMSU-B has the same frequency as channel 15 of AMSU-A. The difference between the two channels is the beam width which is much larger in the case of AMSU-A. As in the case of AMSU-A, the polarization angles of channels 16 and 17 are also rotating with the scan angle. The polarization of the remaining channels is arbitrary in order to facilitate the antenna engineering.

The AMSU-B unit will be about 65 × 64 × 50 cm in size, 30 kg in weight, and will consume 60 watts of power. The AMSU-B will have only one antenna (a reflector) which will have a projected aperture (diameter) of 28 cm.

Table 22. AMSU-B Channel Characteristics

Channel Number	Center Frequency (GHz)	Number of Pass Bands	Maximum Bandwidth (MHz)	Center Frequency Stability (MHz)	Temperature Sensitivity (K)	Absolute Calibration Accuracy (K)
16	89.0	1	6,000	50	0.60	2.0
17	157.0	1	4,000	50	0.60	2.0
18	183.31 ± 1.00	2	1,000	30	0.80	2.0
19	183.31 ± 3.00	2	2,000	30	0.80	2.0
20	183.31 ± 7.00	2	4,000	30	0.80	2.0

VI. RELATIONSHIP TO OTHER INSTRUMENTS

SYNERGISM WITH OTHER Eos INSTRUMENTS

The information provided by the HMMR can in many instances be improved when made in conjunction with other sensors. Some areas in which such complementary information will help improve the measurements planned for HMMR are described below.

Soil Moisture

It would be highly desirable to augment the HMMR soil moisture data with measurements from other instruments likely to be part of the Earth Observing System. Thermal infrared data, for example from MODIS or TIMS (Thermal Infrared Multispectral Scanner), would help estimate surface temperature; and visible and near infrared reflectance data, for example from MODIS or HIRIS, would help estimate shortwave albedo, vegetation type, and possibly photosynthesis rate for vegetated areas. These parameters are necessary for energy and moisture balance models of the surface and upper soil. They will help improve estimates of soil moisture and also augment studies of evaporation and transpiration. Also, an active microwave instrument such as the Synthetic Aperture Radar (SAR) would help to determine the biomass in vegetated areas and would help to identify areas of saturated soil and standing water. The high resolution of the SAR might also make it possible to study the effects of topography, surface roughness, and changes in vegetation cover on remote sensing of soil moisture.

Precipitation

Among the measurements which would complement the passive microwave measurement of precipitation are those which could be provided by a microwave radar (such as an altimeter). A microwave radar could provide the height of the rain column, a necessary parameter in present algorithms for reducing passive microwave measurements to rain rate. Furthermore, a microwave radar specifically designed for meteorological applications (for example, operating at 18 and 35 GHz) is also capable of independently measuring rain rate. In fact, over land, where variations in the emissivity of the surface make measurements of rainfall difficult with a passive microwave device, a microwave radar may eventually prove to be the optimum measuring system. Research to define algorithms involving both dual frequency microwave radiometers and radars to estimate rainfall over land has identified several possibilities (Atlas *et al.*, 1984).

A visible/infrared sensor (HIRIS) would also be a valuable complement to a microwave device for measuring rain. Experience with the AVHRR (Advanced Very High Resolution Radiometer) has shown that it is capable of measuring cloud top temperature and other cloud parameters relevant to rain rates. Such a sensor, with its fine scale horizontal resolution (<1 km), would augment active microwave techniques.

Finally, a polar orbit as proposed for the Earth Observing System presents a particular problem for estimating rain. Rain has a diurnal cycle which cannot be observed from polar orbit and which if not removed will bias estimates made by measuring always at the same location at the same time of day. An ancillary experiment such as the Tropical Rain Measuring Mission (TRMM) (Appendix A) to measure the diurnal cycle is needed so that this bias can be removed.

Snow

The microwave radiation emitted from a snowpack depends on the physical temperature of the snow, the structure of the snow (grain size, density, stratification), the depth and water equivalent of the snow, the amount of liquid water present, and characteristics of the underlying surface such as soil moisture, roughness, and vegetation cover (Foster *et al.*, 1984; Rango and Hartline, 1982). If these parameters were all known, then in principle the microwave brightness temperature of the snow could be calculated and algorithms determined for extracting parameters of the snow of environmental significance from the output of microwave radiometers. Several sensors which are to be part of the Earth Observing System can provide some of this information, and by making measurements concurrently with the HMMR, will improve the information to be obtained about snow.

For example, measurements in the infrared (MODIS, TIMS) can provide surface temperature, and measurements in the visible (MODIS, HIRIS) can help identify vegetated regions which, in the microwave measurements, are confused with bare ground when the snow is melting.

The high resolution available with SAR could help define surface roughness and help determine the effects of rapidly changing topography (e.g., in mountains) on algorithms to extract snow parameters. SAR might also help identify vegetation cover and moisture of the underlying surface.

Finally, multispectral measurements in the visible spectrum (HIRIS, MODIS) are responsive to grain size and may help quantify this parameter for algorithms for extracting the moisture equivalence of snow from the microwave data.

Physical Oceanography

Heat exchange across the air-sea interface consists of the sum of several components: shortwave and longwave radiation, and sensible and latent heat fluxes. Over much of the ocean, shortwave radiation and latent heat flux are the dominant and variable terms. The former is now well-estimated from geostationary imaging sensors such as the Visible Infrared Spin Scanned Radiometer (VISSR) on GOES. But latent heat flux presents a major problem, requiring knowledge of sea surface temperature, scalar wind speed or stress, and atmospheric humidity in the marine boundary layer. The AMSR instrument in HMMR could provide the first two parameters, while AMSU, or elements of such an atmospheric profiling microwave radiometer could provide the third necessary parameter. The accuracy requirements of temperature (0.5°), wind speed (0.5 m/s), and specific humidity (5 to 10 percent) would make the lidar measurements of the LASA an important contributor in this quest. AMSU will not have the vertical resolution required to give moisture at the surface of the ocean; but LASA could be used to tell how thick the boundary layer is, and AMSU can be used to determine how much moisture is in the layer.

The measurements of temperature profiles near the surface, under all weather conditions, will require the combining of data from the microwave radiometer and infrared (4.3 μm) radiometers on HIRIS. The combination results in better measurement accuracies and coverage than either sensor can provide alone.

Runoff

In situ measurements with river gauges and data collection platforms (for example, those collected using the Automated Data Collection and Location System (ADCLS)) will be needed wherever possible to estimate water runoff from land. Also, topographic data obtained with high resolution sensors such as the SAR and LASA will be very helpful to study the structure of water basins. Data on vegetation cover (SAR, HIRIS, MODIS) and soil properties will also be needed, together with information about rainfall and evaporation.

OTHER MICROWAVE INSTRUMENTS

SSM/I

The Special Sensor Microwave/Imager (SSM/I) is a scanning microwave radiometer system to be flown aboard spacecraft of the Defense Meteorological Satellite Program (DMSP). Satellites of the DMSP fly in circular, sun-synchronous, near-polar orbits at an altitude of 833 km with a period of 101 minutes. The SSM/I will be a four-frequency (19.35, 22.235, 37.0, and 85.5 GHz) radiometer system with dual polarization at each frequency except 22 GHz, where only vertical polarization will be recorded. (This channel is primarily to monitor atmospheric water vapor to correct for atmospheric attenuation.) The SSM/I will consist of an offset parabolic reflector approximately 60 × 65 cm in size which will be rotated to effect a conical scan at 45° incidence (see Figure 18). Data will be collected during 102° of this rotation (the remainder will be used for calibration) resulting in a swath of about 1,400 km. The scan rate will be 1.9 seconds per revolution. Data will be collected at 64 positions (every 1.6°) per scan line (128 samples at 85.5 GHz) with an integration time per sample of 7.95 ms (3.89 ms at 85.5 GHz). The performance parameters for the SSM/I radiometers are summarized in Table 23 (Hollinger and Lo, 1983). Notice that because of the large antenna footprint there is substantial overlap between data points.

In comparison to the SMMR, the scanning multifrequency microwave radiometer flown on Seasat and on Nimbus-7, the SSM/I will have one less frequency (four) compared to the five frequencies (6.6, 10.6, 18, 21 and 37 GHz) on the SMMR. The SSM/I will have more frequent global coverage by about a factor of four than the SMMR (about once every 6 days). The spatial resolution of corresponding channels (e.g., 18, 21, and 37 GHz on SMMR versus 19.35, 22.2, and 37 GHz on SSM/I) are very similar, with SSM/I being only slightly worse. The resolution at 85.5 GHz in SSM/I will be substantially better.

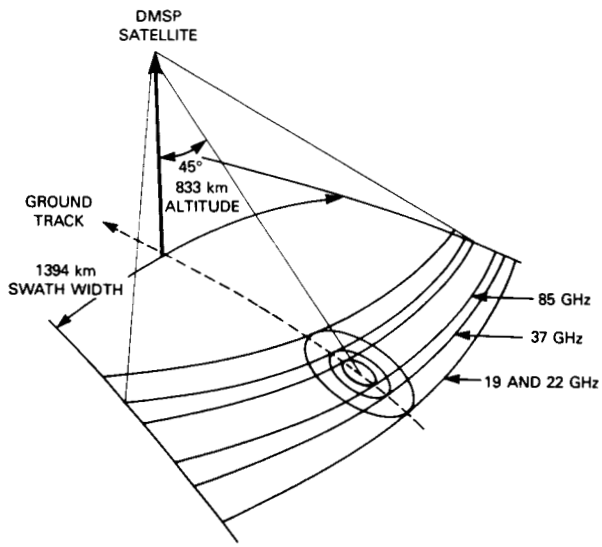

Figure 18. Scan geometry for SSM/I. The rotating antenna system on SSM/I sweeps the observed area on the surface in two alternating modes, one in which all four frequencies are recorded and one in which only the 85 GHz data are recorded. The angle of emission at the surface is a constant across swath. The use of a single antenna for all four frequencies results in a different surface resolution for each frequency, with the highest frequency, 85 GHz, having the finest resolution.

Table 23. SSM/I Performance Characteristics

Parameter	Radiometer Performance			
Center frequency (GHz)	19.35 ± 0.05	22.235 ± 0.05	37.0 ± 0.1	85.5 ± 0.3
Polarization	V and H	V	V and H	V and H
Radiometric accuracy (K)	1.5	1.5	1.5	1.5
Sensitivity (K)	0.8	0.8	0.6	1.1
Dynamic range (K)	375	375	375	375
Effective resolution (km) (3dB antenna beamwidth; includes integration time)	70 × 45	60 × 40	38 × 30	16 × 14
Integration time (ms)	7.95	7.95	7.95	3.89

In comparison to the AMSR proposed for HMMR, the SSM/I is similar in that it is conically scanned (a plus because then the angle of incidence is constant) and in that some of the frequencies (19, 22, 37, and 85.5 GHz) are channels of the AMSR also. However, there are significant differences. An important difference is spatial resolution. The reflector proposed for AMSR is 4 × 7 meters, compared to 0.60 × 0.65 meters for the SSM/I. The difference is nearly a factor of 10 in the size of the spot on the Earth. In addition, the AMSR spot is nearly circular on the Earth (accomplished with the highly asymmetric reflector), whereas the SSM/I spot is elliptical with a high degree of eccentricity at the low frequencies. This difference in resolution is important for remote sensing purposes. The AMSR will have spatial resolution approaching the geophysical scale sizes of phenomena such as sea ice and precipitation cells. This will make new information available to the geophysical community not possible with any present or planned radiometer and of sufficient quality to make significant advances in understanding the fundamental physical processes which drive the environment. The resolution of the SSM/I at 19 and 37 GHz (frequencies used to monitor rain) is far in excess of the cell size of precipitation, making accurate estimates of rain questionable. On the other hand, the resolution cell of the AMSR is sufficiently small (5 km or less) to make sense of statistical techniques for estimating mean monthly rainfall (e.g., see Appendix A). Similarly, in the case of sea ice, the resolution cell for AMSR approaches the resolution needed to understand sea ice properties. With the AMSR, parameters such as ice concentration and ice type, the location of the ice boundary, and surface albedo can be measured with resolutions comparable to the scale of the geophysical processes affecting sea ice.

Figures 19 and 20 illustrate the difference in resolution obtainable with the AMSR and SSM/I and the effect of this difference on the information to be derived about sea ice. Figure 19 shows sea ice concentration across the Bering Sea obtained from a single swath of the Nimbus-7 SMMR using the SMMR radiance data at 37 GHz. The sampling rate of the SMMR at this frequency allows the data to be mapped into a grid of resolution cells 15 km on a side. This resolution is equivalent to that which will be obtained by the SSM/I at its highest frequency (85 GHz) and is better by a factor of two than the SSM/I will obtain at 37 GHz. It is clear from Figure 19 that the data at this resolution locates the extent of the ice pack and variations of concentration within the pack; however, there are many smaller scale features which are not resolved. This is illustrated in Figure 20, which shows ice concentration for a small portion of the same Bering Sea marginal ice zone (the heavy black line in Figure 19) obtained during the MIZEX-West experiment using a scanning microwave radiometer aboard the NASA CV-990 aircraft (Cavalieri *et al.*, 1986). The resolution of the aircraft instrument is approximately 300 m at nadir and is more than sufficient to resolve mesoscale features such as polynyas, ice-edge bands, and streamers (lower left, Figure 20). The resolution which would be obtained with the SSM/I and AMSR (at 37 GHz) is shown for comparison in the lower right-hand corner of Figure 20. The resolution obtainable with the AMSR is clearly sufficient to resolve the mesoscale features apparent in this figure, allowing for the study with data from the AMSR of geophysical processes such as wave-ice interactions, crossfrontal transport, opening and closing of polynyas, and upwelling jets and eddies. The ability of the AMSR to resolve polynyas is of particular importance because much of the

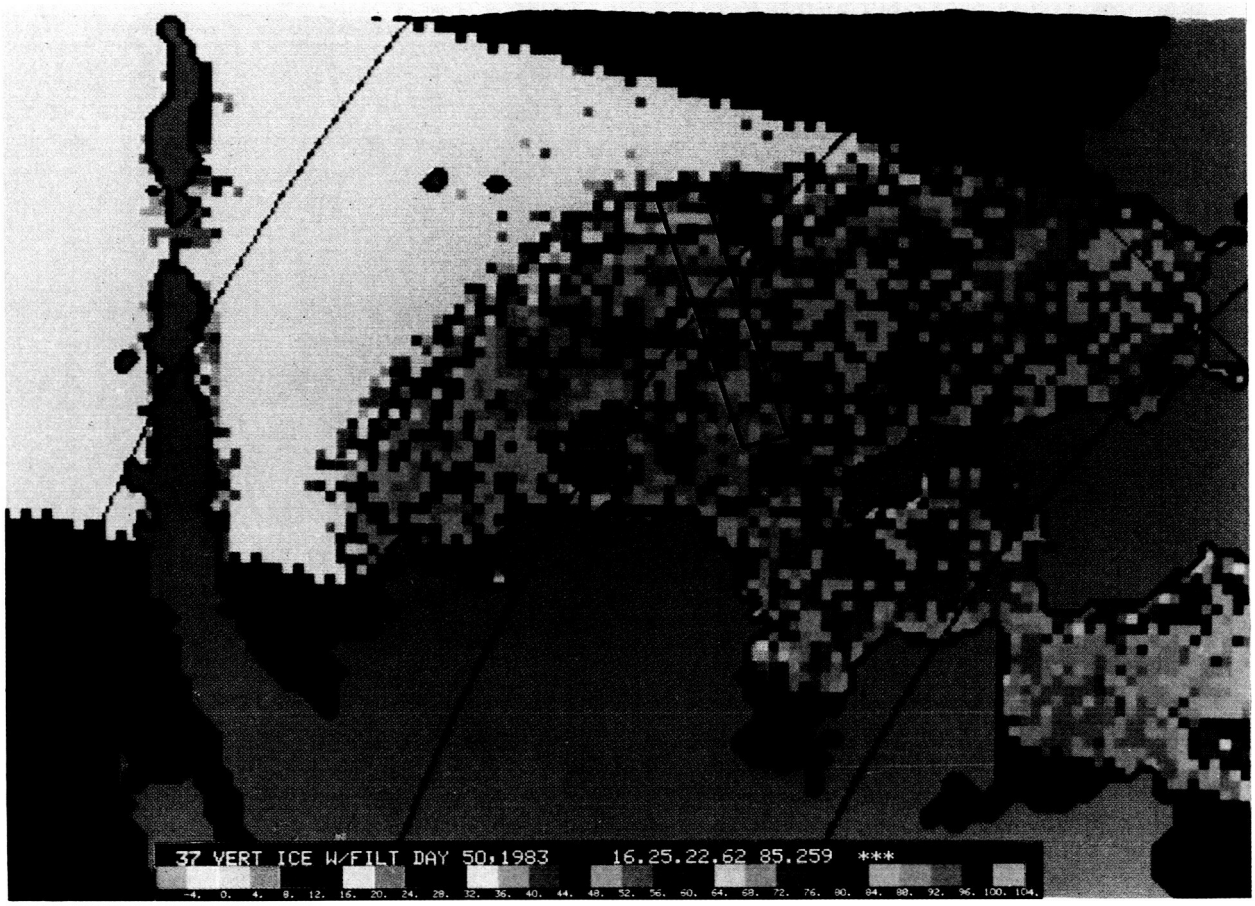

Figure 19. Bering Sea ice concentration derived from the Nimbus-7 SMMR using radiance data at 37 GHz. One swath of SMMR data is shown. The resolution is 15 km × 15 km. The rectangular box is the area of the aircraft data shown in Figure 3.

ice produced in seasonal sea ice zones, such as the Bering Sea and the oceans surrounding Antarctica, are produced in coastal polynyas. These polynyas are often persistent features which result from prevailing winds advecting ice downwind as rapidly as it forms and maintaining an area of open water and thin ice. Furthermore, these recurrent coastal polynyas are also important sources of high salinity shelf water which are believed to be primary sites of bottom water production in both polar regions.

In summary, as a tool for remote sensing, the SSM/I does not represent the step forward in spatial resolution provided by AMSR and needed to achieve understanding at the level of the fundamental geophysical processes controlling the environment. Rather, SSM/I is a well conceived operational tool collecting data on a regular basis of the quality already shown to be useful with such research tools as the SMMR. Certainly, scientific use should be made of SSM/I data; however, it is not the research tool of the future needed to advance measurements of precipitation, sea ice, and snow cover to the stage needed to grasp understanding of the fundamental physical processes controlling the environment.

LFMR

The Low Frequency Microwave Radiometer (LFMR) is a microwave instrument under development for N-ROSS to map sea surface temperature. Specifications, set by requirements for Naval operations, call for a desired resolution of 10 km and accuracy of ± 0.5 K with a resolution of 25 km and ± 1 K being adequate. Present plans (Hollinger and Lo, 1984) call for deployment of a 6 meter wire mesh antenna dish which will scan at 45° with respect to nadir (forming a beam angle of 53° at the surface). The system will be dual polarized and operate at frequencies of 5.2 GHz and 10.4 GHz. The latter is to increase sensitivity to sea surface temperature over warm oceans. The concept of the deployable, wire mesh antenna (an umbrella) was selected to meet the requirements for high spatial resolution and is being studied to determine the effects of the wire mesh on temperature accuracy.

The AMSR, as conceived for Eos, will employ a solid dish of almost the same size (4 × 7 meters). The AMSR will obtain nearly the same spatial resolution and should be able to achieve higher temperature

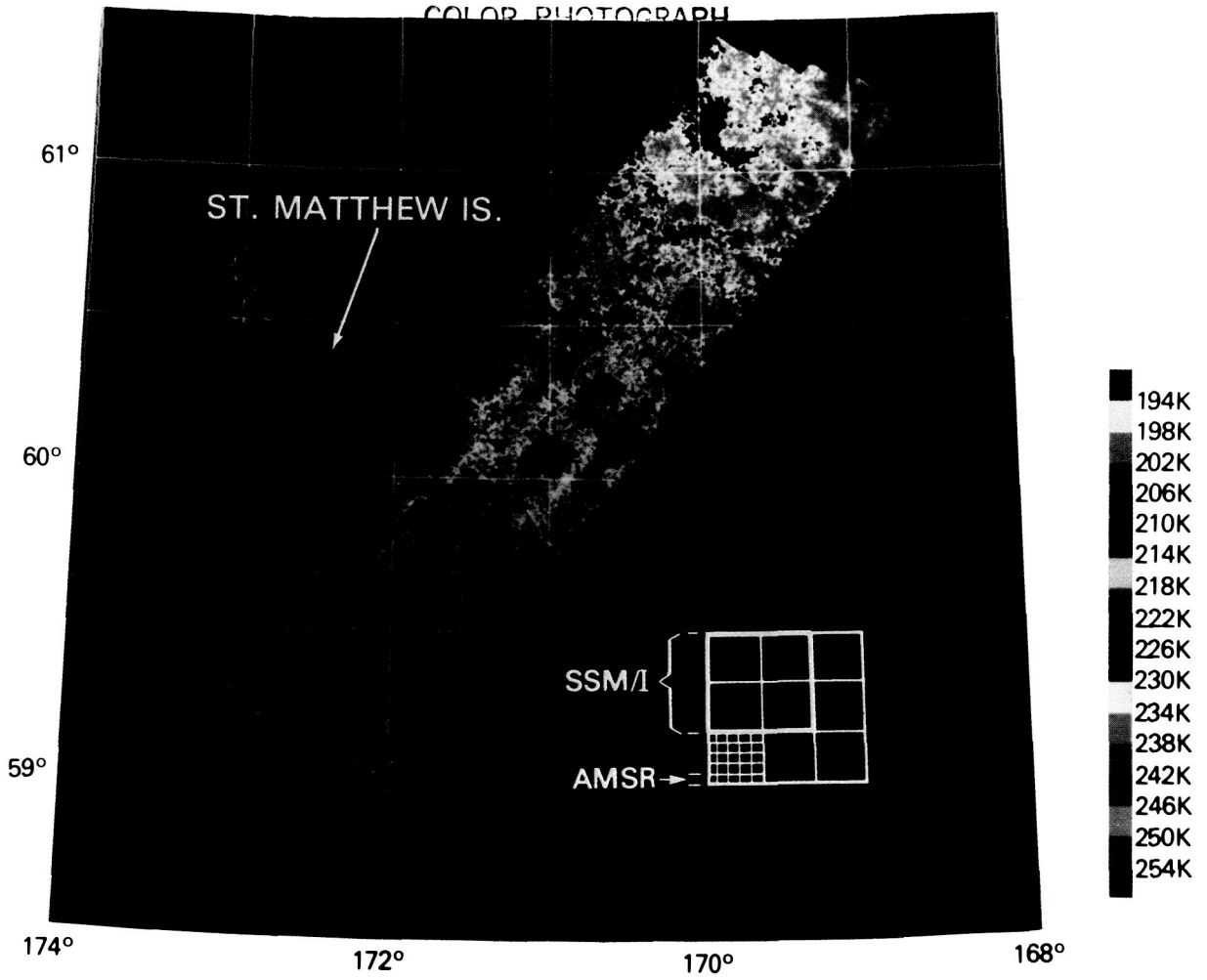

Figure 20. Sea ice concentration for the Bering Sea obtained with an airborne microwave radiometer during the MIZEX-West experiment (1983). The image was obtained from data at 92 GHz and is color coded to show microwave brightness temperature. The resolution is about 300 meters.

sensitivity. The AMSR is a complementary instrument which, by employing a solid reflector, should be more easily calibrated and thereby provide data of the high temperature sensitivity needed for some scientific applications.

SSM/T

The Special Sensor Microwave/Temperature (SSM/T) is a DMSP instrument. It is an atmospheric temperature profiler. Two versions of the SSM/T have flown and other copies are being produced. It is a small, lightweight, low power, passive sensor with 7 channels (50.5, 53.2, 54.35, 54.9, 58.4, 58.825, and 59.4 GHz) in the oxygen spin-rotation band. SSM/T has a 14.4° beam width, weighs 11 kg, and consumes 14 W of power. It has a 200 km footprint at nadir and provides temperatures at 15 levels to 10 mb (about 30 km). The scan is crosstrack through nadir to ±36°.

Plans are being made for a second version of the SSM/T to profile water vapor. This instrument will employ measurements at the 183 GHz water resonance line (3 channels) plus ancillary channels at 19.5 and 150 GHz. It will have a resolution of about 50 km on the surface and have a radiometric sensitivity of 0.5 K and a sensor accuracy of 1 K. Physically this instrument is to be very similar to the temperature profiler and is expected to use the same space on the spacecraft and same antenna as the temperature profiler.

The SSM/T represents an advance in several respects over the MSU flown on TIROS-N. The AMSU-A being developed for NOAA represent further advances in temperature profiling: the AMSU-A will include more channels to profile to higher altitudes, will use improved detector technology, and will have a smaller footprint on the surface.

RAIN MEASURING MISSION

Knowledge of the diurnal cycle of precipitation is deficient over much of the globe, particularly over tropical oceans. Knowledge of this diurnal cycle is important if HMMR is to obtain useful measurements of precipitation. It is needed to correct for the observational bias inherent in the sun-synchronous polar orbit planned for Eos. Among the systems which could obtain this information is the Tropical Rainfall Measuring Mission (TRMM) currently being proposed. TRMM is discussed briefly below (and in more detail in Appendix A) to illustrate how the information needed about the diurnal cycle of rainfall might be obtained.

TRMM has been envisaged as an Explorer-type mission, in a 300 km orbit at 30° inclination to the equator. By choosing a 30° inclination orbit, the sampling rate in the tropics is twice that obtained by polar orbiters and the diurnal cycle is approximately uniformly sampled for each locale in less than 1 month. The TRMM sensors include a dual frequency (16 and 35 GHz) precipitation radar with resolution of 3 km, a microwave radiometer (an existing unused ESMR from Nimbus-5 at 18 GHz could be used) with a resolution of 7 km, and a multichannel visible/infrared sensor (such as a standard AVHRR) with resolution of better than 0.5 km. All three instruments scan across-track and make a very dense sample of measurements. Several hundred thousand readings are taken in a given area over the month, reducing sampling and other random errors. (Additional details are included in Appendix B.)

This non-sun-synchronous satellite would return about one sample for each ground location for each hour of the day in 1 month. The resulting data set should yield vital information on the diurnal cycles of rainfall over the ocean, while also providing rainfall values over land (from the two-frequency radar).

By modifying the orbit (say to 45°) to cover middle latitudes also, important information would be expected from both sea and land areas in middle latitudes, helping to indicate such matters as the diurnal distribution of precipitation (both rain and snow) over mountainous regions, without degrading the frequency of coverage of the tropics by more than about 20 percent.

VII. DATA MANAGEMENT

INTRODUCTION

By satellite instrument standards, the data rates expected from the HMMR are not excessive. The Panel estimates data rates as follows:

Component Instrument	Data Rate
ESTAR	5 kbit/sec
AMSR	50 kbit/sec
AMSU	5 kbit/sec

In the concept of the Earth Observing System, the satellite data is the input to an information system designed to meet the multidisciplinary requirements and interactions necessary for understanding the functioning of the Earth. This information system must effectively store and manage the data generated by the proposed remote sensing instruments and ensure that these data can be extensively exploited in combination with other observables.

Keeping this information goal in mind, the Panel defined several levels of data for the HMMR instruments which reflect an appropriate way in which the data could be processed.

Level 0—Raw data archived permanently

Level 1A—Raw data annotated to include system parameters needed to reduce the data to meaningful measurements. The annotation should include: time, system temperature, calibration coefficients, orbit parameters, and location of each pixel (latitude and longitude).

Level 1B—Radiometric brightness temperatures (i.e., measured values after all instrument calibrations and/or corrections have been made) annotated to include time, orbit parameters, and location and size of each pixel.

Level 2—Geophysical parameters (e.g., sea surface temperature or soil moisture) at each pixel, annotated with time, orbit parameters, and location as in Level 1B.

Level 3—Geophysical parameters referenced to a fixed Earth grid. This would include maps of geophysical parameters with some smoothing to provide uniform space-time sampling.

The Panel felt that Level 0 and Level 1 should both be archived permanently. Level 1 data is the most fundamental, which is practical for use by scientists and instrument specialists; however, it is not reversible to Level 0 data. Therefore, it was felt both Level 0 and Level 1 data should be stored to ensure that proper corrections could be made in the future if necessary. Level 2 data is obtained by applying algorithms to the data. Algorithms currently exist for the major parameters which HMMR is expected to produce. But, clearly one would expect that these will be revised and refined as new information is gathered. The algorithms should be archived and made available to interested researchers.

ALGORITHM DEVELOPMENT AND VALIDATION

The major geophysical parameters to be obtained directly from the passive microwave measurements are soil moisture, sea surface temperature, sea ice concentration, precipitation, total water vapor, and water vapor and temperature profiles in the atmosphere. Algorithms currently exist to extract these parameters from the microwave radiance measurements. Algorithms also exist for several ancillary parameters such as sea ice type, snow cover, and evaporation over the oceans. In several cases (e.g., sea ice concentration and ice type), geophysical parameters are presently being obtained from microwave sensors in orbit. Additional algorithm evolution is to be expected, especially should sensors such as the LFMR and SSM/I and sensor systems such as the TRMM be launched.

Thus, it is to be expected that a repertoire of tested algorithms will accompany launch of HMMR. However, the new high resolution data is certain to stimulate improvement of existing algorithms and development of new algorithms. It is expected that appropriate science teams will be established to select initial algorithms for the major observables and provide a vehicle for revising the algorithms as experience is gained with the data.

Even for the most established algorithms, continued research is needed to further refine the procedure of extracting geophysical parameters from the hierarchy of competing factors. Research is needed in areas such as snow wetness, effects of vegetation on radiation from wet soil, methods for estimating heat and moisture fluxes from the oceans, and evaporation and transpiration from land surfaces. The Panel supports continued research in such areas preceding and during development of HMMR. Research will help improve existing algorithms and help identify additional information which can be obtained from passive microwave measurements.

APPENDIX A: TROPICAL RAINFALL MEASURING MISSION (TRMM)

By
G. R. North, T. T. Wilheit, and O. W. Thiele

This proposal is for a free flying satellite to be launched in the Explorer Program Series for the purpose of measuring rainfall in the tropics. The aim is to collect data which will be useful in the understanding of weather, climate and hydrological dynamic processes. The orbit and sensors have been especially selected to overcome the unique challenges inherent in measuring rainfall. The main data set goal is a 3-year minimum time series of 30-day averages of rainfall rate probabilities taken over rectangles whose area is equivalent to 600 km sided squares with sampling errors of the order of a few percent.

By choosing a 30 degree inclination orbit, the sampling rate in the tropics is doubled over polar orbiters. In addition, the diurnal cycle is approximately uniformly sampled over a month, also impossible from sun-synchronous platforms. The 300 km altitude allows a factor of 1100/300 improvement in resolution for the equivalent instruments over the Nimbus series whose altitudes were 1100 km. The launch and platform are compatible with space shuttle. TRMM may also be revisited by space shuttle or space station associated vehicles. The sensors include a dual-frequency precipitation radar with resolution 3 km, a passive microwave radiometer with resolution 7 km and a multichannel visible/infrared radiometer with resolution better than 0.5 km. All three instruments scan across nadir making a very dense sample of measurements along the track. Several hundred thousand readings are taken in a given measurement area over the month, reducing sampling and other random errors. Strategies are being developed to use all three instruments as well as other satellite data to reduce well known biases in the individual measurements.

The timing of the mission, if not delayed, will coincide with the international project Tropical Ocean Global Atmosphere (TOGA) which runs through 1995. International cooperation via TOGA can benefit mutually because of the possibility of large scale ground truth experiments.

SCIENTIFIC OBJECTIVE

To increase our understanding of the energetic and hydrologic processes in the tropics, especially as they pertain to the general circulation of the atmosphere and oceans. A major advance in our understanding of the general circulation can be achieved by collecting accurate data for rainfall throughout the tropical latitudes, since rainfall rate is the signature of latent heat conversion to buoyant force in the Hadley circulation. In the ocean, rainfall is a source of fresh water which influences the density of water and, therefore, the buoyancy. Over land rainfall is the source of soil moisture which has a strong influence upon the atmospheric circulation. The main purposes of such a data set are climate diagnostics, model validation, and model impact studies. Secondary purposes for the data include the study of tropical rain systems and the collection of a climatology for objective assessment of drought and other climate anomalies.

MISSION OBJECTIVES

To obtain a minimum three-year data set of monthly averaged estimated rainfall rate probabilities averaged over grid boxes of the order of 600 km on a side with sampling errors of a few percent.

To develop new techniques for measuring rainfall by combining the measurements from several instruments to reduce statistical biases and to learn how to combine measurements from other coincident satellite and ground instruments to insure against the undetected occurrence of major storms between visits by the satellite track.

To develop data sets for studies of diabatic initialization of weather forecast models. These impact studies require different data reduction algorithms for selected time segments during the mission.

To develop a comprehensive ground truth program, both before and after launch, through international collaboration by way of the TOGA program.

To develop techniques for studying and removing the diurnal cycle from temporally- and spatially-smoothed rainfall data by using a non-sun-synchronous orbit.

JUSTIFICATION

Anomalous energy sources in the tropics can excite disturbances in the atmospheric general circulation that are felt throughout the tropics and even in the mid-latitude through teleconnections. The dynamic connection between the tropics and mid-latitudes was vividly demonstrated during the last El Niño event in the Tropical Pacific. Numerous documents commissioned by the World Climate Programme and the National Academy of Sciences recommend better rainfall data in the tropics.

A quantitative rainfall data set provides a crucial validation tool for the general circulation models of the 1990s. There is evidence that these models will

be useful operational tools in the near future, and that data sets of this type will be essential to their steady improvement.

Rainfall rates are notoriously difficult to measure even under ideal conditions using surface instrumentation. The problem is compounded in the tropics since most of the region is oceanic and the rainfall type is mostly convective, consisting of many intense small scale features. The station density and reliability are so poor in most tropical countries that, for example, it is not possible to establish objectively whether there was a drought in Ethiopia in 1984.

Sampling from ships of opportunity is inadequate for collecting data for transient response studies with models, since literally hundreds of crossings per month of a grid box would be necessary to achieve the adequate level of sampling density. This limitation is aside from the enormous expense and logistics of equipping and maintaining the hardware.

The diurnal cycle confounds attempts to measure rainfall from sun-synchronous platforms, and it introduces large biases in data taken from small islands. Geosynchronous platforms have shown some modest skill in estimating rainfall rates from infrared imagery. Lack of continuity of these satellites and the inherent limitation of using only the properties of cloud tops as rainfall predictors as well as to recalibrate the regression equations for every climatic type suggest that new methods should be sought.

The mission has the potential to prompt a new international thrust toward understanding the tropical hydrological cycle, not just by the satellite measurements, but by field experiments and advances in modeling rainfall systems and the oceans. The mission is timely because of its overlap with other planned programs and the readiness of the research community to benefit from the data set anticipated.

APPROACH

TRMM proposes to solve the sampling problem by using scanning sensors. For example, the passive microwave radiometer (we suggest an Electronically Scanned Microwave Radiometer (ESMR) which is available now) can measure light to moderate rainfall over ocean. ESMR has a swath width along the satellite track of 600 km with about 80 pixels of size roughly 7 km each. The cross track sweep time is such that contiguous rows of pixels can be achieved along the track. Using these values and the orbit we find that 180,000 readings can be taken in 30 days with ESMR for any given grid box. If the individual pixel readings are all statistically independent, rainfall rate probabilities in the grid box month can be estimated to within a few percent, even for categories as rare as 1 percent probable. Relaxation of the assumptions still leads to acceptable results.

The radar has the capability of estimating the rain column height (200 km) over land and sea at a horizontal resolution of 3 km. The resulting column height climatology is needed in the interpretation of ESMR results and may be a good estimator of rain rate itself. In addition, the radar is capable of estimating rain rate by backscattered power at two frequencies (16 and 35 GHz). Another analysis mode to be explored is the extinction of power as the beam goes through the rain and is reflected back from the surface. The radar is planned to have a swath width of 150 km; hence, the sampling density is less than ESMR by a factor of four, but the number of physically independent measurements of rain drops is significantly augmented. The number of physically independent measurements is very important since the methodology of data interpretation is likely to involve the estimation of several parameters in a multiparameter rain rate probability distribution function.

A visible/infrared radiometer is necessary as a cross check and as yet another independent measure of rain. The experience with AVHRR (Advanced Very High Resolution Radiometer) shows that it is capable of measuring cloud top temperature and other cloud parameters relevant to rain rates. This sensor with its <1 km horizontal resolution will augment active microwave techniques. This instrument provides a transfer standard from previous technology.

The diurnal variation problem is to be solved by assuming uniform statistics through the month over the grid box and by estimating and removing the harmonics by a regression technique. Considering the number of visits per month, this should be a very reliable procedure.

The classic beam filling problem (pixel size comparable to or larger than that of the horizontal scales of rain) will be approached by several methods. First, the microwave pixel sizes contemplated for this mission are smaller by at least a factor of 11/3 than any previously flown satellite microwave sensor. Indeed, the horizontal distance of 7 km may be less than the auto-correlation length of tropical rain. If brute force decrease of pixel size is not enough to solve beam filling, several other strategies are possible using the complementarity of the instrument readings in a parameter estimation algorithm.

Figure A.1 shows how a TRMM satellite might be configured for this experiment, making use of the same shuttle compatible bus as was used on the Earth Radiation Budget Satellite (ERBS), which was launched in 1984.

ORIGINAL PAGE
COLOR PHOTOGRAPH

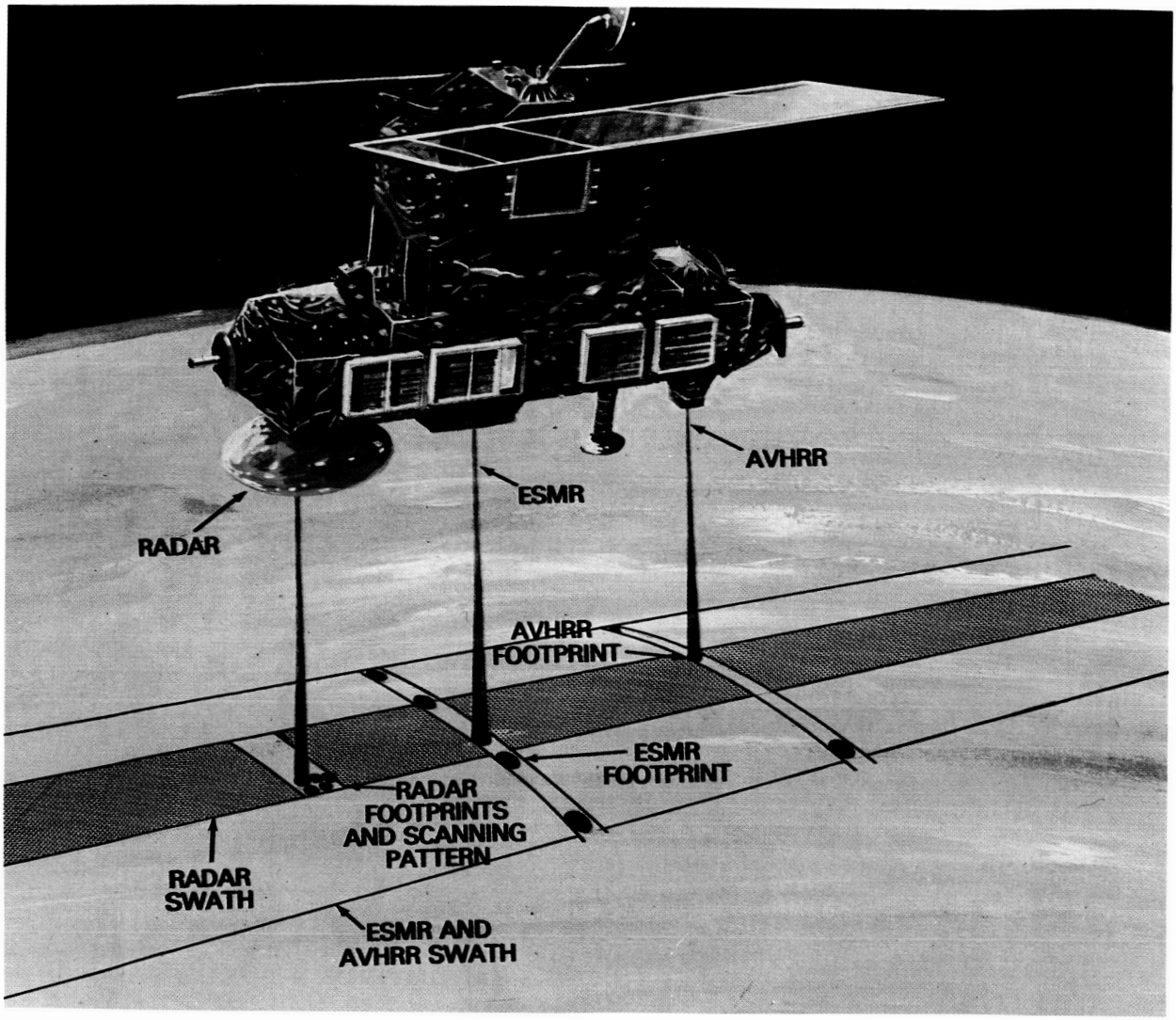

Figure A.1. Tropical Rainfall Measuring Mission

APPENDIX B: RAINFALL SAMPLING

In microwave radiometric measurements of precipitation, rain rate is the parameter being estimated, yet integrated rainfall for some period of time is generally the desired quantity. For radiometers in space, one can only estimate the integral statistically from the observations during the short time when the satellite is overhead. Whether or not this will yield a meaningful estimate depends on the number and distribution of the samples. The highly variable nature of rainfall (variable in both space and time), causes a great deal of difficulty in choosing the samples for any rain measurement scheme. Moreover, there is a large diurnal cycle in rainfall in some circumstances and an unknown, but possibly important, diurnal cycle in most other cases. This causes a large potential for error in any sun-synchronous measurement approach. However, if we ignore, for the moment, the diurnal component of variability, we can arrive at some estimates of the statistical component of error in the rainfall estimates made from measurements with sun-synchronous systems such as SSM/I or HMMR. The swath width of either instrument will be about 1,400 km and either satellite will have a ground speed of about 7 km per second. This will provide an imaged area of 3×10^{10} km^2 per month. The correlation length of rain varies geographically and according to rain type, but 10 km is a typical value. The correlation length provides an estimate of the spacing needed for sample independence. Thus, the imaged area can be considered as 3×10^8 samples per month. The probability of any cell containing precipitation is similarly variable, but 1 percent is typical, leaving about 3×10^6 rain samples per month globally. On a monthly basis, a square 2,000 km on a side would include the 100 independent samples required to obtain an estimate of integrated rainfall with less than 10 percent measurement error. Clearly, this sort of sampling is only adequate for problems on climatological space and time scales; it is grossly inadequate for flood forecasting and other problems of short space and time scales. The diurnal cycle has been ignored but any satellite-based system which is sun-synchronous will always measure at the same (two) local times at any given location, making any determination of a diurnal cycle impossible. On the other hand, if the strength and phase of any diurnal cycles are known on a statistical basis by any other means, the sun-synchronous data may be corrected. A separate experiment on a non-sun-synchronous satellite represents an obvious way of obtaining these data.

REFERENCES

Adler, R.F., and E.B. Rodgers, Satellite observed latent heat release in a tropical cyclone, *Mon. Wea. Rev., 105,* 956, 1977.

Aerojet Electrosystems Co., LAMMR Definition Study, Report #6069, 1980.

Arya, L.M., J.C. Richter, and J.F. Paris, Estimating profile water storage from surface zone soil moisture measurements under bare field conditions, *Water Resour. Res., 19,* 403, 1983.

Atlas, D., J. Eckerman, R. Meneghini, and R.K. Moore, The outlook for precipitation measurements from space, *Atmos. Ocean, 20,* 50, 1982.

Atlas, D., and O.W. Thiele, Precipitation measurements from space, Workshop Report, GSFC, Greenbelt, MD, 1981.

Atlas, D., C.W. Ulbrich, and R. Meneghini, The multiparameter remote measurement of rainfall, *Radio Sci., 19,* 3, 1984.

Barrett, E.C., and D.W. Martin, *The Use of Satellite Data in Rainfall Monitoring,* Academic Press, 1981.

Barry, R.G., Arctic ocean ice and climate: Perspectives on a century of polar research, *Ann. Assoc. Amer. Geograph., 73,* 1983.

Bernstein, R.L., Sea surface temperature mapping with the Seasat microwave radiometer, *J. Geophys. Res., 87(C10),* 7865, 1982.

Blanchard, B.J., and P.F. O'Neill, *Estimation of the hydrolic character of soils with passive microwave systems,* Proc. Conf. on Advances in Infiltration, Amer. Soc. Agricul. Eng. (ASAE) Chicago, IL, 215, 1983.

Brouw, W.N., Aperture synthesis, in *Methods in Computational Physics, 14,* Edited by B. Adler, p. 131, Academic Press, 1975.

Butler *et al.,* Earth Observing System, *NASA TM 86129,* Vol. I, GSFC, Greenbelt, MD, 1984.

Cavalieri, D.J., P. Gloersen, and W.J. Campbell, Determination of sea ice parameters with the Nimbus-7 SMMR, *J. Geophys, Res., 89,* 5355, 1984.

Cavalieri, D.J., P. Gloersen, and T.T. Wilheit, Aircraft and passive microwave observations of the Bering Sea ice cover during MIZEX-West, *IEEE Trans. Geosci. Remote Sens., GE-24,* 368, 1986.

Cavalieri, D.J., and H.J. Zwally, Satellite observations of sea ice, XXVth COSPAR, *Advances in Space Research, 5,* 247, 1985.

Chang, A.T.C., J.L. Foster, and D.K. Hall, Nimbus-7 derived global snow cover parameters in *Proceedings of the Glaciological Society Symposium on Remote Sensing,* Cambridge, England, 1986.

Charney, J., W.J. Quirk, S. Chow, and J. Kornfield, A comparative study of the efforts of albedo change in drought in semi-arid regions, *J. Atmos. Sci., 34,* 1366, 1977.

Choudhury, B.J., T.J. Schmugge, A. Chang, and R.W. Newton, Effect of surface roughness on the microwave emission from soils, *J. Geophys, Res., 84,* 5699, 1979.

Cihlar J., and F.T. Ulaby, Dielective properties of soils as a function of moisture contents, *RSL TR 177-47,* University of Kansas Center for Research, 1974.

Colbeck, S.C., A simulation of the enrichment of atmospheric pollutants in snow cover runoff, *Water Resour. Res., 17,* 1383, 1981.

Comiso, J.C., Characteristics of arctic winter sea ice from satellite multispectral microwave observations, *J. Geophys. Res., 91,* 975, 1986.

Cosby, B.J., G.M. Hornberger, R.B. Clapp, and T.R. Gunn, A statistical exploration of the relationships of soil moisture characteristics to the physical properties of soil, *Water Resour. Res., 20,* 682, 1984.

Crane, R.G., and M.R. Anderson, Satellite discrimination of snow surfaces, *Int. J. Remote Sens., 5,* 213, 1984.

Crist, E.P., and R.C. Cicone, Physically based transformation of thematic mapper data: VTM Tasseled Cap, *IEEE Trans. Geosci. Remote Sens., GE-22,* 256, 1984.

Department of Energy, Glaciers, ice sheets and sea level: Effect of a CO_2 induced climatic change, Workshop Report, 330 pp., Seattle, WA, 1984.

Dooge, J.C.I., The nature and components of the hydrologic cycle, in *Man's Influence on the Hydrological Cycle,* Irrigation and Drainage Paper, No. 17, 1, FAO, Rome, 1973.

Dozier, J., Snow reflectance from Landsat-4 thematic mapper, *IEEE Trans. Geosci. Remote Sens., GE-22,* 323, 1984.

Dozier, J., S.R., Schneider, and D.F. McGinnis, Jr., Effect of grain size and snow pack water equivalent on visible and near-infrared satellite observations of snow, *Water Resour. Res., 17,* 1213, 1981.

Foster, J.L., D.K. Hall, A.T.C. Chang, and A. Rango, An overview of passive microwave snow research and results, *Rev. Geophys. Space Phys., 22,* 195, 1984.

General Electric Space Division, LAMMR Definition Study, Final Review, 1980.

Gloersen, P., and D.J. Cavalieri, Reductions of weather effects in the calculation of sea ice concentrations from microwave radiances, *J. Geophys. Res., 91(C3),* 3913, 1986.

Gloersen, P., T.T. Wilheit, A.T.C. Chang, and W.J. Campbell, Microwave maps of the polar ice of the Earth, *Bull. Amer. Meteor. Soc., 55,* 1442, 1974.

Grody, N.C., Remote sensing of atmospheric water content from satellites using microwave radiometry, *IEEE Trans. Antennas Propag., AP-24,* 155, 1976.

Herman, G.F., and W.T. Johnson, The sensitivity of general circulation to arctic sea ice boundaries: A numerical experiment, *Mon. Wea. Rev., 106,* 1649, 1978.

Hewish, A., The synthesis of giant radio telecopes, *Science Progress, 53,* 355, 1965.

Hibler, W.D., Modeling a variable thickness sea ice cover, *Mon. Wea. Rev., 108,* 1943, 1980.

Hollinger, J.P., and R.C. Lo, SSM/I project summary report, *NRL MR 5055,* Naval Research Laboratory, 106 pp., Washington, D.C., 1983.

Hollinger, J.P., and R.C. Lo, Observation of sea surface temperature with N-ROSS, *NRL MR 5375,* Naval Research Laboratory, 59 pp., Washington, D.C., 1984.

Kraus, F.D., *Radio Astronomy,* McGraw-Hill Book Company, New York, NY, 481 pp., 1966.

Lang, R.H., Electromagnetic backscattering from a sparse distribution of lossy dielectric scatterers, *Radio Sci., 16,* 15, 1981.

Lang, R.H., and J.S. Sidhu, Electromagnetic backscattering from a layer of vegetation: A discrete approach, *IEEE Trans. Geosci. Remote Sens., GE-21,* 62, 1983.

Leech, J., On the representation of 1,2,. . ., n by difference, *J. London Math. Soc., 31,* 160, 1956.

Le Vine, D.M., and J.C. Good, Aperture synthesis for microwave radiometers in space, *NASA TM 85033,* 1983.

Liu, W.T., Assessing the capability of Eos sensors in measuring ocean-atmosphere moisture exchange, JPL Publ., 85, 1985.

Lvovitch, M.I., The water balance of the continents of the world and the method of studying it, International Association for Scientific Hydrology, General Assembly of Moscow, 1971.

Manabe, S., Climate and the ocean circulation. I. The atmospheric circulation and the hydrology of the Earth's surface, *Mon. Wea. Rev., 97,* 739, 1969.

Manabe, S., Simulation of climate by general circulation models with hydrologic cycles, in *Land Surface Processes in Atmospheric General Circulation Models,* edited by P.S. Eagleson, p. 19, Cambridge University Press, New York, NY, 1982.

Manabe, S., and J.L. Holloway, Jr., Seasonal variation of the hydrologic cycle as simulated by a global model of the atmosphere,*J. Geophys. Res., 80,* 1617, 1975.

Marshall-Palmer, T.S., and W.M. Palmer, The distribution of rain drops with size, *J. Meteor., 5,* 165, 1948.

Maykut, G.A., Energy exchange over young ice in the central arctic, *J. Geophys. Res., 83,* 3646, 1978.

Maykut, G.A., Large-scale heat exchange and ice production in the central arctic, *J. Geophys. Res., 87,* 7971, 1982.

McGinnis, D.F., Jr., J.A. Pritchard, and D.R. Wiesnet, Determination of snow depth and snow extent from NOAA-2 satellite very high resolution radiometer, *Water Resour. Res., 11,* 897, 1975.

Meeks, M.L., and A.E. Lilley, The microwave spectrum of oxygen in the Earth's atmosphere, *J. Geophys. Res., 68,* 1683, 1963.

Mintz, Y., Very long-term global integration of the primitive equations of atmospheric motion: An experiment in climate simulation, *Meteorological Monograph, 8,* p. 20, American Meteorological Society, Boston, MA, 1968.

Mintz, Y., The sensitivity of numerically simulated climate to land surface conditions, in *The Global Climate,* edited by J.T. Houghton, P. 79, Press Syndicate of the University of Cambridge, New York, N.Y., 1984.

Moffet, A.T., Minimum redundancy linear arrays, *IEEE Trans. Antennas Propag., AP-16,* 172, 1968.

Monteith, J.L., Evaporation and the environment, *Symp. Soc. Exp. Biol., 19,* 205, 1965.

Mosely-Thompson, E., A.J. Gow, M. Herron, K. Jezek, M. Kahlil, and B. Kamb, *GISPII Science Plan,* prepared for Division of Polar Programs, National Science Foundation, 1985.

Nace, R.L., The present state and future prospects of global hydrology, in *Proceedings of Symposium on the World Water Balance,* Reading, England, UNESCO, WMO, 1970.

Napier, P.J., A.R. Thompson, and R.D. Ekers, The very large array: Design and performance of a modern synthesis radio telescope, in *Proceedings of the IEEE, 71,* 1295, 1983.

National Research Council (NRC), a Strategy for Earth Science from Space in the 1980s and 1990s, Part II: Atmosphere and Interactions with the Solid Earth, Oceans, and Biota, National Academy Press, 1985.

Njoku, E.G., Passive microwave remote sensing of the Earth from space-A review, in *Proceedings of the IEEE, 70,* 728, 1982.

Norsex Group, Norwegian remote sensing experiment in a marginal ice zone, *Science, 220,* 781, 1983.

Parkinson, C.L., J.C. Comiso, H.J. Zwally, D.J. Cavalieri, P. Gloersen, and W.J. Campbell, Arctic sea ice, 1973-76: Satellite passive microwave observations, NASA, Washington, D.C., in press, 1986.

Phillips, N.A., The general circulation of the atmosphere: A numerical experiement, *Quart. J. Roy. Meteor. Soc., 82,* 123, 1956.

Prevot, L., R. Bernard, D. Taconet, and D. Vadal-Madjar, Evaporation from bare soil evaluated using a soil water transfer model and remotely sensed surface soil moisture data, *Water Resour. Res., 20,* 311, 1984.

Rango, A., and J. Martinec, Application of a run-off model using Landsat data, *Nordic Hydrol., 10,* 225, 1979.

Rango, A., and B. Hartline, *et al.,* Plan of research for snowpack properties remote sensing-(PRS)^2, Recommendations of the Snowpack Properties Working Group, GSFC, Greenbelt, MD, 40, 1982.

Rango, A. *et al.,* Plan of research for integrated soil moisture studies, Recommendations of the soil moisture working group (A. Rango, Chairman), NASA, 70 pp., Washington, D.C., 1980.

Rao, M.S.V., W.V., Abbott, III, and J.S. Theon, Satellite derived global oceanic rainfall atlas (1973 and 1974) *NASA X-911-76-116,* GSFC, Greenbelt, MD, 1976.

Rind, D., The influence of ground moisture conditions in North America as modelled in the GISS GCM, *Mon. Wea. Rev., 110,* 1487, 1982.

Rowntree, P.R., and J.A. Bolton, Experiments with soil moisture anomalies over Europe, The GARP Programme on Numerical Experiementation. *Research Activities in Atmospheric and Oceanic Modelling,* edited by R. Asselin, *18,* 63, 1978.

Rowntree, P.R., and J.A. Bolton, Simulations of the atmospheric response to soil moisture anomolies over Europe, *Quart. J. Roy. Meteor. Soc., 109,* 502, 1983.

Schaerer, G., and T.t. Wilheit, A passive microwave technique for profiling of atmospheric water vapor, *Radio Sci., 14,* 371, 1979.

Schanda, E., Multiple wavelength aperture synthesis for passive sensing of the Earth's surface, *International Symposium Digest,* IEEE/Antennas and Propagation Society, 762, Seattle, WA, 1979.

Schmugge, T., Remote sensing of surface soil moisture, *J. Appl. Meteor., 17,* 1551, 1978.

Schmugge, T.J., Microwave remote sensing of soil moisture, in *Proceedings XIII International Symposium on Remote Sensing of the Environments,* 859, Paris, France, 1984.

Schmugge, T.J., P.E. O'Neill, and J. Wang, Passive microwave soil moisture research, *IEEE Trans. Geosci. Remote Sens., GE-24,* 12, 1986.

Shukla, J., and Y. Mintz, Influence of land surface evapotranspiration of the Earth's climate, *Science, 215,* 1498, 1982.

Shuttleworth, W.J., Evaporation models in the global budget, in *Variations in the Global Water Budget,* edited by A. Street-Perrott *et al.,* Reidel, Dordrecht, 173, 1983.

Smagorinsky, J., General circulation experiment with the primitive equations, I. The basic experiment, *Mon. Wea. Rev. 93,* 99, 1963.

Smagorinsky, J., Large scale climate modeling and small scale physical processes, in *Land Surface Processes in, Atmospheric General Circulation Models,* edited by P.S. Eagleson, p. 19, Cambridge University Press, New York, N.Y., 1982.

Spencer, R.W., D.W. Martin, B.B. Hinton, and J.A. Weinman, Satellite microwave radiances correlated with radar rain rates over land, *Nature, 304,* 141, 1983.

Staelin, D.H., Inversion of passive microwave remote sensing data from satellites, in *Inversion Methods in Atmospheric Remote Sounding,* edited by A. Deepak, p. 361, New York, N.Y., 1977.

Staelin, D.H., Passive microwave techniques for geophysical sensing of the Earth from satellites, *IEEE Trans. Antennas Propag, AP-29,* 683, 1981.

Staelin, D.H., and P.W. Rosenkranz, High resolution passive microwave satellites, Research Laboratory of Electronics, Mass. Inst. of Technology, Cambridge, Mass., Report of NASA Applications Review Panel, NAS5-23677, 1978.

Svenden, E., K. Kloster, B. Farrelly, O.M. Johannessen, J.A. Johannessen, W.J. Campbell, P. Gloersen, D.J. Cavelieri, and C. Matzler, Norwegian remote sensing experiment: Evaluation of the Nimbus-7 scanning multichannel microwave radiometer for sea ice research, *J. Geophys. Res., 88,* 2781, 1983.

Swenson, G.W., and N.C. Mathur, The interferometer in radio astronomy, in *Proceedings of the IEEE, 56,* 2114, 1968.

Swift, C.T., and D.J. Cavalieri, Passive microwave remote sensing for sea ice research, Eos, *Am. Geophys. Union, 66,* 1210, 1985.

Swift, C.T., *et al.,* airborne microwave measurements of the southern Greenland ice sheet, *J. Geophys. Res., 90,* 1983, 1985.

Swift, C.T., L.S. Fedor, and R.O. Ramseier, An algorithm to measure sea ice concentration with microwave radiometers, *J. Geophys. Res., 90(C1),* 1087, 1985.

Tarpley, J.D., Estimating incident solar radiation at the surface from geostationary satellite data, *J. Appl. Meteor., 18,* 1172, 1979.

Ulaby, F.T., Passive microwave remote sensing of the Earth's surface, *IEEE Trans. antennas Propag., AP-24,* 112, 1976.

United Nations Educational, Scientific and Cultural Organization, Scientific framework of the world water balance, *technical papers in Hydrology, #7,* 27 pp., Paris, France, 1971.

United Nations Educational, Scientific and Cultural Organization, World water balance and the water resources of the Earth, *Studies and Reports in Hydrology, #25,* 663 pp., 1978.

Untersteiner, N., *et al.,* Passive microwave remote sensing for sea ice research, Science Working Group for the Special Sensor Microwave Imager (SSM/I), 55 pp., NASA, Washington, D.C., 1984.

Valovcin, F.R., Snow/cloud discrimination, *AFGL-TR-76-0174,* Hanscom AFB, MA, 1976.

van Bavel, C.H.M., and D. Hillel, Calculation potential of actual evaporation from a bare soil surface, *Agricul. meteor., 17,* 453, 1976.

van de Griend, P.J., P.J., Camillo, and R.J. Gurney, Discrimination of soil physical parameters, thermal inertia and soil moisture from diurnal surface temperature fluctuations, *Water Resour. Res., 21,* 997, 1985.

Vernadskii, V.I., Izbrannye sochineniya (selected works), Vol. 4, Book 2, Moskva, AN SSSR, 651 pp., 1960.

Walker, J., and P.R. Rowntree, The effect of soil moisture on circulation and rainfall in a tropical model. *Quart. J. Roy. Meteor. Soc., 103,* 29, 1977.

Walsh, J.E., D.R. Tucek, and M.R. Peterson, Seasonal snow cover and short-term climatic fluctuation over the United States, *Mon. Wea. Rev., 110,* 1474, 1982.

Warren, S.G., Optical properties of snow, *Rev. Geophys. Space Phys., 20,* 67, 1982.

Warren, S.G., Optical constants of ice from the ultraviolet to the microwave, *Appl. Opt., 23,* 1206, 1984.

Warren, S.G., and W.J. Wiscombe, A model for the spectral albedo of snow, 2, snow containing atmospheric aerosols, *J. Atmos. Sci., 37,* 2734, 1980.

Wetzel P.J., D. Atlas, R.H. Woodward, Determining soil moisture from geosychronous satellite infrared data: A feasibility study, *J. Climate and Appl. Meteor., 23,* 375, 1984.

Wilheit, T.T., Radiative transfer in a plane stratified dielectric, *IEEE Trans. Geosci. Electron., GE-16,* 138, 1978.

Wilheit, T.T. Passive microwave measurement of precipitation, to appear in *Bull. Am. Meteor. Soc.,* 1986.

Wilheit, t.T., A.T.C. Chang, J.L. King, E.B. Rodger, R.A. Nieman, B.M. Krupp, a.S. Milman, J.S. Stratigos, and H. Siddalingaiah, Microwave radiometric observations near 19.35, 92 and 183 GHz of precipitation in tropical storm cora, *J. appl. Meteor., Z1,* 1137, 1982.

Wilheit, T.T., A.T.C. Chang, M.S.V. Rao, E.B. Rodger, and J.S. Theon, A satellite technique for quantitatively mapping rainfall water over oceans, *J. Appl. Meteor., 16(s),* 551, 1977.

Wiscombe, W.J., and S.G. Warren, A model for the spectral albedo of snow, 1, pure snow, *J. Atmos. Sci., 37,* 2712, 1980.

Zwally, H.J., J.C. Comiso, and C.L. Parkinson, Antarctic sea ice, 1973-76: Satellite passive microwave observations, *NASA SP-459,* NASA, 206, Washington, D.C., 1983.